# Real-time monitoring of sweat of Cystic Fibrosis patients

T.D. Bakker

Cl⁻

Na⁺

TUDelft

UMC Utrecht

# Real-time monitoring of sweat of Cystic Fibrosis patients

by

## T.D. Bakker

to obtain the degree of Master of Science
at the Delft University of Technology,
to be defended publicly on Tuesday November 5, 2019 at 9:00 AM.

*This thesis is confidential and cannot be made public until November 6, 2021.*

An electronic version of this thesis is available at `http://repository.tudelft.nl/`.

**TU**Delft    UMC Utrecht

# Preface

This thesis is written as part of my master graduation project to obtain a master's degree in BioMedical Engineering at the Delft Universtity of Technology. This project interested me since it required to use both theoretical as practical skills and contributes to a serious health and society problem. The topic was diverse, which required a multidisciplinary approach. The multidisciplinarity is also visible in the cooperations of multiple groups and universities during this project, among which Electronic Instrumentation Laboratory and Industrial Design at the TU Delft, University Medical Center (UMC) Utrecht and Wilhelmina Kinderziekenhuis (WKZ) Utrecht. During the project, I learned a lot, from the medical background of CF to the production of sensors using screen-printing. Furthermore, I developed myself in conducting individual research.

*T.D. Bakker*
*Rijswijk, October 2019*

# Abstract

This research provide a proof of principle to use a sweat sensor system for real-time monitoring of medicine effectiveness in Cystic Fibrosis (CF) patients. Cystic Fibrosis (CF) is an autosomal recessive genetic disorder affecting mostly the respiratory, digestive and perspiration system. Patients with CF have dysfunctional chloride channels in their cells, due to mutations in both copies of the gene for the Cystic Fibrosis transmembrane conductance regulator (CFTR) protein. The CFTR proteins are necessary for the production of mucus, a malfunction of the CFTR protein will result in tough mucus.

In CF, a lack of functional CFTR prevents normal sodium and chloride absorption in sweat and leads to excessive salt loss. Due to increased sodium and chloride concentration in sweat from CF patients, sweat makes a good clinical body fluid to indicate the medicines' effectiveness. By measuring the chloride or sodium concentration before treatment with the medicine and after treatment, an indication of the medicines' effectiveness can be obtained.

In this study, a potentiometric screen-printed sweat sensor has been developed to monitor the medicine effectiveness in CF patients. The sensor consists of a reference electrode and ion-selective electrodes for measurements of chloride and sodium concentrations. Multiple prototypes of the sensor have been developed and evaluated on their performance. Furthermore, a read-out circuit with low leakage/bias currents and 8 channels is designed to increase the read-out accuracy and speed.

Since the sweat volume during rest appeared to be too low for real-time measurements, a sweat collector was implemented with the sensor to increase the sweat sample volume during real-time measurements. Furthermore, a pilocarpine sweat stimulator has been designed and tested to artificially increase the sweat rate.

The developed system proofed to be a functional concept for real-time patient monitoring. In future research, the chemical structure of the membranes is the most important topic to be improved. Improvements in this field could extend the life-time of the sensor and would minimise the sensitivity differences between the sensors. Finally, the sweat sensor, collector and stimulator have to be integrated and minimised in one design to make a wearable device out of it.

# Contents

# List of Figures

# List of Tables

# Abbreviations

| | |
|---|---|
| **ABC** | ATP-binding Cassette |
| **Ag/AgCl** | Silver/Silver-Chloride |
| **AMPs** | Antimicrobial Peptides |
| **BME** | BioMedical Engineering |
| **CDC** | Constant Direct Current |
| **CF** | Cystic Fibrosis |
| **CFTR** | Cystic Fibrosis transmembrane conductance regulator |
| **DC** | Direct Current |
| **EMF** | Electromotive Force |
| **ENaC** | Epithelial Sodium Channel |
| **FEV$_1$** | First Forced Expiratory Volume |
| **FFC** | Fexible Printed Circuit |
| **HREC** | Human Research Ethics Committee |
| **ISE** | Ion Selective Electrode |
| **ITO** | Indium Tin Oxide |
| **NTC** | Negative Temperature Coefficient |
| **PDC** | Pulsed Direct Current |
| **PET** | Polyethylene Terephthalate |
| **PVB** | Polyvinyl Butyral |
| **QNS** | Quantity Not Sufficient |
| **SCE** | Saturated Calomel electrode |
| **SHE** | Standard Hydrogen electrode |
| **THF** | Tetrahydrofuran |

# 1

# Introduction

This report is written as part of the BioMedical Engineering (BME) master graduation project. The research is carried out by Thomas D. Bakker, BME master student with specialization in BioElectronics. The research topic has been proposed by Prof. dr. J.M. Beekman from UMC Utrecht, and is supervised by Prof. dr. P.J. French from TU Delft. The project is hosted by UMC Utrecht and TU Delft. Furthermore, the Nederlandse Cystic Fibrosis Stichting (NCFS) is also involved in this project. The student carried out his research in the Electronic Instrumentation group which is focusing on sweat analysis and which is supervised by Prof. dr. P.J. French, Dr. ir. A. Bossche and ing. J. Bastemeijer.

This report will first focus on the clinical background of the project to provide a good understanding of the project.

## 1.1. Cystic Fibrosis

Cystic Fibrosis (CF) is an autosomal recessive genetic disorder that affects mostly the respiratory, digestive and perspiration system. CF has an incidence of about 45 new-borns yearly and a prevalence of about 1500 patients in the Netherlands [1]. Due to the improvement in treatments, the quality of life and life expectancy has significantly improved in the last decades [2]. In the United States, life expectancy was 33.9 years observed in 2001, while life expectancy in 2016 was 47.7 years [3]. However, both quality of life as life expectancy will further increase with the use of personalised medicine [4]. In this section, the clinical background, symptoms and treatment of CF will be discussed.

### 1.1.1. General background

Patients with CF have dis-functional chloride channels in their cells, due to mutations in both copies of the gene for the Cystic Fibrosis transmembrane conductance regulator (CFTR) protein. Over 2000 variants of mutations are described to date [4]. The function of the CFTR protein is to create channels on the cell surface to allow the movement of chloride ($Cl^-$) in and out of the cell.

When only mutations in one of the genes is present, it will not seriously influence the health of that person. However, that person will be a carrier of the mutation. The carrier rate in the Netherlands is on average 1:30 [3]. When both parent's are carrier of a CF mutation, the chance of having a child with CF is 1:4 and having a child who is (only) carrier of the mutation is 1:2. It is not possible to have a child with CF if only one parent is carrier of a mutation. This is illustrated in figure 1.1.
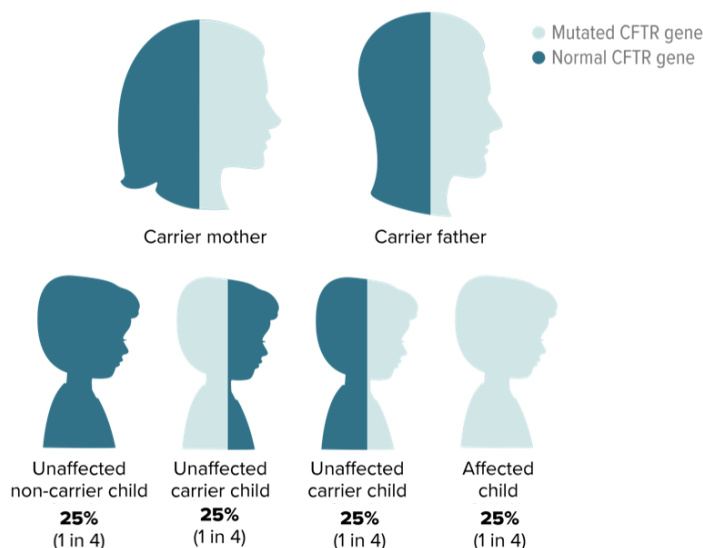
Figure 1.1: Autosomal recessive inheritance pattern [5].

The CFTR protein is constructed out of 1480 amino acids. When the CFTR protein is build in the right order with the correct amno acids, it forms a stable 3D shape, which is important to transport the chloride ions. In case of a misfolding, the cell will probably detect this and will dispose of the CFTR protein.

CFTR mutations can be categorised into five distinct classes based on the resulting damaging effect on the protein due to abnormalities in CFTR synthesis, structure and functionality [6]. These mutation classes are illustrated in figure E.1 from appendix E. Patients with class IV and V mutations have some residual function of CFTR protein, the outcome of the disease is therefore less severe. Mutations of classes I, II, and III are associated with no residual CFTR function, resulting in a severe phenotype [3].

The CFTR protein is part of a group of pumps called ATP-binding Cassette (ABC) transporters. For the functionality of the ABC transporters, two cytoplasmic nucleotide-binding domains (NBDs) are essential. In most ABC transporters, the NBDs bind and hydrolyze ATP to actively pump a substrate across the membrane of the cell. However, in the CFTR channel, the NBDs open and close a transmembrane pore through which $Cl^-$ can passively flow down its electrochemical gradient [7]. This makes them unique in the group of ABC transporters.

### 1.1.2. Symptoms
As a consequence of the double mutation, the genetic disorder CF affects processes in the human body that are depending on the functionality of the chloride channels, such as osmosis. Osmosis plays a crucial role in the production of mucus. The dis-functionality of chloride channels in patients with CF, result into mucus that is not getting fluid and will become though. In the lungs, this often causes pneumonia, while in the pancreas, the tough mucus results in poor transport of enzymes to the intestine which are crucial for the functionality of the digestive system [5]. As a consequence, severe loss-of-function mutations in CFTR, will lead to a multi-organ disease.

Lungs
Mucus plays a critical role in protecting the lungs from unwanted materials that are inhaled such as germs and pollutants. The mucus in the lungs traps these germs and pollutants. Tiny hairs called cilia, propel the mucus out of the lungs and into the throat where the mucus can be swallowed or coughed out [8]. However, in people with CF, the hydration of the mucus is dis-functional. The hydration of the mucus is dependent on the transport of salts from the inner to the outer cells, which will be followed by water flow from the inner cell to the outer cell due to osmosis. When the CFTR protein is missing or dis-functional, the transport of salts is disturbed and therefore also the water flow. As a consequence, the following problems occur [9] [3]:

- The cilia are unable to propel mucus out of the lungs
- Mucus clogs the airways, which make breathing difficult
- Tough mucus is less able to kill germs and creates a fertile breeding ground for infections

These lung problems affect the quality of life dramatically of CF patients, they experience a lack of energy, severe tightness, persistent coughing and pain in the lungs. These symptoms are also the best visible for outsiders, therefore, CF is often qualified as a lung disease. When the quality of the lungs is becoming too low, a lung transplantation will be considered [10][11].

On average, the lung functionality of CF patients is decreasing every year till the age of 27 years, when it becomes stable around 60% [1], as illustrated in figure 1.2. However, patients who die with decreased lung functionality are not taken into account in this figure. Therefore it should be noted that the 60% lung functionality in figure 1.2 disguises the disastrous consequences of CF for the lung functionality.
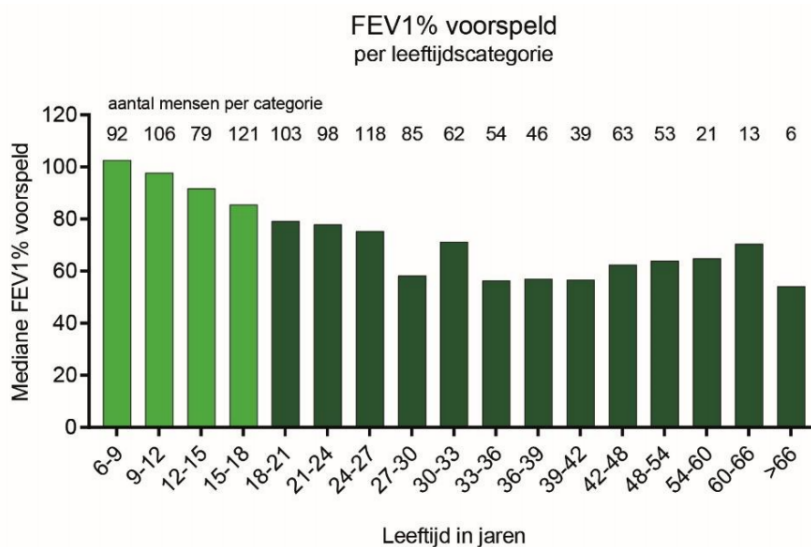


Figure 1.2: Predictad First Forced Expiratory Volume (FEV$_1$) per age category in 2017 [1].

Digestive system
Complications in the gastrointestinal tract can have significant influence in the daily life of CF patients [12]. The pancreas contains exocrine and endocrine glands, which are responsible for 2 liters of isotonic fluid secretion every day [8]. However, in patients with CF this fluid production is dis-functional, comparable with the dis-functional mucus production in the lungs. The fluid production has an essential role in the functioning of the pancreas, one of the main functions of the fluid is to transport enzymes to the small intestine. Due to the dis-functional fluid production, enzymes do not sufficient reach the small intestine causing all kind of digestive problems. Furthermore, the CFTR protein is involved in the $HCO_3^-$ transport, which has an important role in pH regulation [8]. Typical problems that occur in CF patients are ductal luminal obstruction, pancreatic damage, atrophy, and CF-related diabetes mellitus [3].

Sweat
The effect of CF is also visible in the composition of sweat. Sweat, produced by the sweat glands, flows to the skin surface through narrow ducts. During the production phase, the sweat has high salt concentrations. To regulate the right salt concentration in the organism, salt will normally get reabsorbed. However, this re-absorption process depends on the functionality of the chloride channel. Since the protein necessary for the functionality of the chloride channel is defective in CF patients, the salt re-absorption is blocked and therefore the salt is accumulating on the skin surface [2].

Under normal conditions, this will not result in major clinical problems. However, during more extreme conditions, such as hot or humid conditions, people with CF are likely to lose excessive salt and fluid. This can cause dehydration and heat prostration [8].

### 1.1.3. Treatment

Treatment for CF patients is focused on both the principle defect of the CFTR protein as on the symptoms of the defect, which is mainly in the respiratory system and digestive system. Besides these treatments, CF patients also have high rates of outpatient visits and hospitalisations due to diseases induced by CF during [1], The amount of therapy and medicines needed is increasing with the age of the patients, mainly due to the decreasing lung functionality and therefore lower vitality.

The treatments have a major impact in the daily life of CF patients and their families, and therefore also limits the quality of life. Medicinal treatments which do not treat the symptoms but the real cause of the disease would bring a solution and reduce suffering of CF patients.

### 1.1.4. CFTR-modulating therapies

Recently developed medicines are focused on repairing the CFTR-protein instead of treating the symptom-based therapies. These are called CFTR-modulating therapies, these CFTR-modulating therapies result in an enormous progress for patients having the specific gene mutation for which the medicine is effective. However, the efficacy of these new drugs that target the mutant CFTR protein are associated with significant inter-subject variability, and people with rare mutations that may benefit from these treatments remain unidentified [12].

The first CFTR-modulating therapy which came to the market was Kalydeco, which was released in the Netherlands in 2014. This therapy was only effective for a small group of patients, as can be seen in table 1.1. Since 2015, another CFTR modulator, Orkambi, reached the market, which was effective for more patients. Orkambi works by enabling CFTR protein with an F508del mutation to fold in a more correct shape, and then activates the protein to allow more chloride to pass through. Although this drug combination is not a perfect fix, it helps the mutant CFTR protein to move some chloride. This movement of chloride reduces the symptoms of CF [6] [13].

Table 1.1: Indication of patients treated with CFTR-modulating therapy 2014 - 2017 [1].

| CFTR-modulating therapy | 2014 | 2015 | 2016 | 2017 |
|---|---|---|---|---|
| Kalydeco (on children) | 5 | 14 | 17 | 15 |
| Kalydeco (on adults) | 8 | 18 | 31 | 35 |
| Orkambi (on children) | - | 5 | 10 | 120 |
| Orkambi (on adults) | - | 15 | 80 | 310 |

## 1.2. Personalised medicine

As described in table 1.1, two types of CFTR-modulating therapies are used for treatment at the moment. However, with two medicines only, there are still mutation variants which can not be treated. In the nearby future, it is expected that more medicines are coming to the market which are useful for other types of mutations. Furthermore, a combination of medicines could be even more effective. The best treatment could be composed by making an optimum combination of medicines for each patient, called personalised medicine. However, composing a personalised medicine by trial and error on patients is not ideal, since it will take long to find an optimum, can result in discomfort for the patients and can be very costly. Therefore, an approach to test medicines on cultured stem cells from CF patients is developed by the research group of Prof. dr. J.M. Beekman from UMC Utrecht. Intestinal organoids provide a highly precise and sensitive measurement of CFTR function in vitro, reflective of the CFTR genotype and other individual genetic factors that modify CFTR function and response to therapy. By using the cultured stem cells from individuals with CF as small intestinal organoids and applying the forskolin-induced swelling (FIS) assay, an individual therapy program could be compiled [4][12].

## 1.3. Patient monitoring

The approach of compiling an individual therapy program by using cultured stem cells is the state of the art. However, the approach has to be proofed on the patients themselves. Therefore, it is necessary to monitor medicine effectiveness before and during treatment with the individual therapy program.

Real-time monitoring of effectiveness can be beneficial for:

- Improving patient treatment

- Validating the use of intestinal stem cell cultures for selecting and composing personalised medicines treatment

- Obtaining reimbursement for CF medicines from health insurers

- Obtaining insight for physicians in the patient's health

Since CF affects mostly the respiratory system, the digestive system and the perspiration system, it is rational to look to conditions related to these systems. However, monitoring the digestive system is currently not a standard monitoring measurement and comes along with all kind of unpractical situations. Therefore, monitoring the digestive system is not taken into account in this research. For monitoring the respiratory system in CF patients, a lung functionality test is used, which is described in section 1.3.1. For monitoring the perspiration system in CF patients, a sweat test is currently used, which is also the golden standard for the diagnosis of CF, this is described in section 1.3.2.

### 1.3.1. Lung functionality

Since CF is affecting the respiratory system, it is usefully to measure the lung functionality. To have an indication of the progress of the lung functionality, it is necessary to measure the lung functionality of the patient multiple times per year. On average, the lung capacity is measured four times a year in 70-75% of all the CF patients in the Netherlands [1]. However, using the lung functionality as standard for monitoring medicine effectiveness in CF patients has the following disadvantages:

- The measurement causes hassle for the patient to visit often the hospital

- The measurement offers just a snapshot of the patient's condition

- The long functionality can be dominated by other diseases, for example pneumonia

- The estimation needed of expected lung functionality introduces errors

- The measurement cannot be made wearable

- The measurement is not implementable in real-time monitoring

- Long functionality has a slow response on the medicine since repairing of CFTR protein is not directly related to lung functionality

The last point means that an increase of CFTR protein functionality does not directly result in a better lung functionality. The lung functionality will go up due to more watery mucus. However, the process of making more watery mucus and repairing the lungs which will result in an increase in $FEV_1$ will have some delay. Therefore and combined with the other points, using lung functionality as indicator for medicine effectiveness is not very appropriate. In conclusion, lung functionality is a predictive pharmacodynamic biomarker on a population basis but is unsuitable for the prediction of treatment benefits for individuals [13].

### 1.3.2. Sweat test

As will be described in detail in section 2.1 and 2.2, ion concentrations in sweat of CF patients differ from those of healthy persons. The largest difference is in the chloride and sodium concentration. Furthermore, the concentration of $HCO_3^-$ is elevated compared to healthy persons. Since the increase in chloride concentration in sweat is directly linked to the non-functionality of the CFTR protein, it can be used as a biomarker for CF [13]. Using sweat for the diagnosis of CF started in 1970's and has become the golden standard [3]. An illustration of how the diagnosis works is presented in figure 1.3.
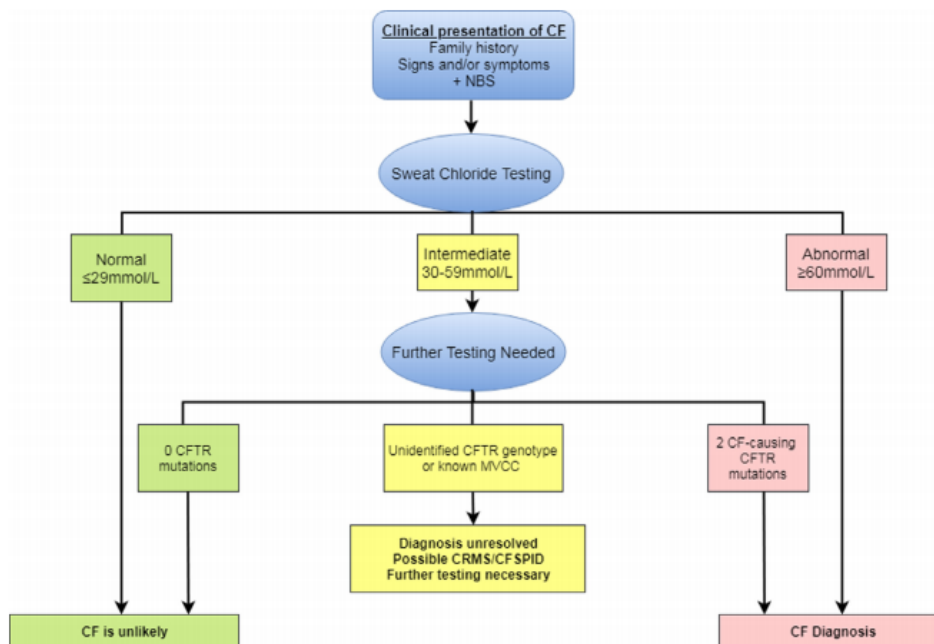
Figure 1.3: Sweat testing algorithm. [CFTR-related metabolic syndrome (CRMS), Cystic fibrosis screen positive inconclusive diagnosis (CFSPID), mutation of varying clinical consequence (MVCC), newborn screening (NBS).] [3].

For clinical use in CF, the standard methods for sweat testing are the Wescor Macroduct® Sweat Test system or the Gibson-Cooke Pilocarpine Iontophoresis (GCQPIT) [14][15]. These tests consist of 3 steps, firstly stimulation of perspiration, secondly sweat sample collection, and finally chemical analysis for chloride and sodium concentrations [2].

Sweat testing is the golden standard in diagnosis of CF patients, due to the excellent sensitivity and specificity. However, the results are sometimes ambiguous and confusing [16]. In hospitals the aim is to collect $60\mu$l of sweat for proper analysis. The minimal amount of sweat needed for proper executing the GCQPIT and Macroduct tests is 15 $\mu$l, which is often not obtained during the sweat collection phase. This will mean that the test will result in a "Quantity Not Sufficient (QNS)", requiring to redo the test and resulting in a delay in the diagnosis of the patient. Especially in infants, QNS occurs, often due to the quality of the skin. Since the skin is not fully developed yet and affected by the amniotic fluid during pregnancy (oral explanation by *Prof. dr. C.K. van der Ent, WKZ Utrecht, The Netherlands*).

Medicines such as Kalydeco and Orkambi influence the CFTR proteins in and around the sweat glands, the re-absorption of chloride, and indirectly sodium, will increase if the medicines are effective [13]. Therefore, the sweat test can be used as prediction method. By measuring the chloride or sodium concentration before treatment with the medicine and after treatment, an indication of the medicines' effectiveness can be obtained. However, the current sweat test is not optimal for monitoring the effectiveness of these medicines, due to the following three points.

- The sweat test will only provide the chloride concentration at the moment of the test, which is not a reliable indication for the concentration of chloride during the hours or even days before and after the test.

- The sweat test can only be conducted in the hospital, which forms a hassle for the patients.

- The test is not reliable if the amount of sweat collected is too low, as described before [17].

If the sweat test is optimised to avoid these problems, it could become a useful tool for monitoring medicine effectiveness.

### 1.3.3. Conclusion

At the moment, there is not a real-time monitoring system for CF patients. All of the monitoring systems used are based on a measurements in the hospital on a specific moment and will therefore only tell something

about the patient on that exact moment instead of during the whole period of usage of the medicine. However, by developing a system that can measure sodium and chloride levels in sweat continuously, medicine effectiveness can be monitored. Therefore, this research focuses on making a real-time medicine effectiveness monitoring device by optimising the sweat test.

## 1.4. Project objectives and thesis outline

This thesis provides a design for real-time monitoring of medicine effectiveness in CF patients through sweat measurements. It is part of the start of making sweat sensors for the Electronic Instrumentation group of the TU Delft, which focused on making wearable sensors used for athletes.

The research goal of this thesis is:

**Perform research into the development of a sweat sensor for measuring chloride and sodium concentration and provide a proof of principle to use it for real-time monitoring of medicine effectiveness in CF patients.**

This document is written to show how the project objective is achieved and were future research should be focused on. This report showcases all the work that went into the development process. It discusses and evaluates the results and explains the reasoning behind decisions that were made in subsequent parts of the research.

### 1.4.1. Development orientation

The first two chapters lay the groundwork for starting the development progress. The relevance of developing an sweat sensor system is discussed in chapter 2, this is done by looking into detail in biomedical background of sweat and the relation with CF and by investigating related research. The design considerations and requirements discussed in chapter 3, which is about the functionality of the sweat sensor system and the factors that should be considered in the design phase.

### 1.4.2. Design of the sensor system

The design of the sensor system can be divided into four parts, the sweat sensor, the sensor read-out circuit, the sweat stimulator and the sweat collector, described in chapter 4 to 6 respectively. In these chapters, the design choices are illustrated, motivated and validated. By validation is meant that the sub-part is tested if it meets the requirements necessary before testing it in a experimental setup.

### 1.4.3. Proof of concept

The sub-parts of the sensor system are tested and evaluated on several aspects. This was done by testing the sensor in artificial sweat conditions, testing the sweat stimulator in an experimental setup on a participant and finally testing the sweat sensor combined with the sweat collector on artificial sweat conditions.The results obtained are shown in chapter 9. The results are discussed in chapter 10.

### 1.4.4. Conclusions and recommendations

The conclusions from the proof of concept are drawn in the last part of the report, chapter 11. Since this thesis takes place in the start of two projects, the recommendations are important to decide what should be done in future work.

$2$

# Relevance of real-time sweat monitoring

In this chapter, the relevance of real-time sweat monitoring is discussed by firstly explaining in detail how sweat is a useful biomarker for the medical condition of CF patients. Secondly, the composition of sweat is discussed to explain what the region of interest is for the sweat measurements. To use sweat as a biomarker in a real-time measurement, it is necessary to have a continuous flow of sweat to avoid the accumulation of sweat on the sensor. Therefore, it can be necessary to artificially stimulate the sweat production at moments the patient does not sweat enough on him or themselves. How sweat can be artificially stimulated is discussed in section 2.3. In section 2.5, research related to real-time sweat monitoring is discussed. Furthermore, in section 2.6, it is concluded what is missing in previous research and what the main focus points of this research are.

## 2.1. Sweat production

Sweat is a clear hypotonic biofluid. Sweat is produced by eccrine and apocrine glands located in the epidermis. Although sweat can be a useful indicator for routine clinical analyses, it is not often used as clinical sample [18]. In literature, clinical diagnosis with sweat is almost only seen in Cystic Fibrosis (CF) research. Due to the increased sodium and chloride concentration in sweat from CF patients, sweat makes a good clinical body fluid to diagnose CF [19]. However, if well monitored, sweat could also be a useful indicator for other health conditions, as mentioned in table 2.2 [20].

Sweat has an essential role in body heat loss. Due to the secretion of sweat onto the skin surface, body heat gets lost by the latent heat of sweat fluid evaporation. The ability to lose heat is influenced by the prevailing outside temperature and humidity. Besides the role in heat loss, sweat has a number of other essential roles which include an essential role in the immune system by producing and secreting of a multiple Antimicrobial Peptides (AMPs) such as LL-37, lactoferrin and dermcidin, AMPs unique to the skin, as well as compounds that maintain skin barrier function and skin lubricants [8][21].

Sweat glands are small, coiled, tubular glands that produce sweat. Sweat glands are also called sudoriferous or sudoriparous glands. These names are derived from the Latin word 'sudor' which means 'sweat' [22]. There are three types of sweat glands in humans: apocrine, apoeccrine and eccrine glands. Eccrine sweat glands are involved in the thermoregulation. These glands are located in the dermis of the skin throughout the body, except for a few areas such as lips and external auditory canals [23]. Apocrine and apoeccrine glands are mainly found in armpits and perianal area, the sweat produced in these glands is more abundant in proteins, fats and salts compared to sweat from eccrine glands. Therefore this sweat evaporates slower than sweat from eccrine glands, and consequently, it has less impact in thermoregulation [24].

The sweat glands are composed of two structurally and functionally different units, the secretory coil and the reabsorptive duct [22], as illustrated in figure 2.1.
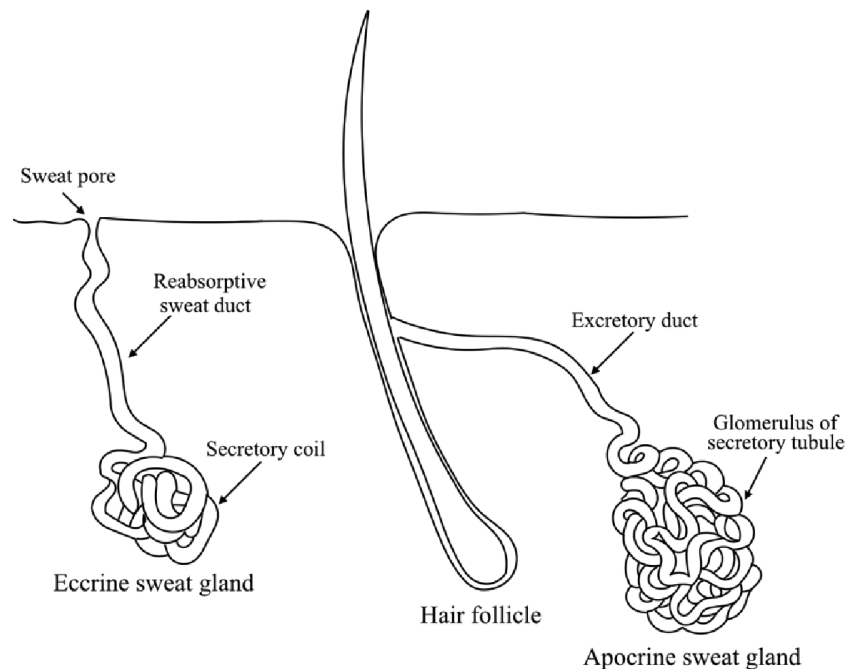
Figure 2.1: Anatomy of the eccrine and apocrine sweat gland [25].

According to the two-step theory of exocrine fluid formation as described by Taylor, Hardcastle, and Southern, fluids are firstly secreted as an iso-osmotic fluid by the secretory compartment of the gland. Secondly, secretions are modified by reabsorption of electrolytes as they pass through the duct or tubular network before being excreted [20], as is illustrated in figure 2.2. The structure and functionality of both the secretory coil and the reabsorptive duct is explained below.
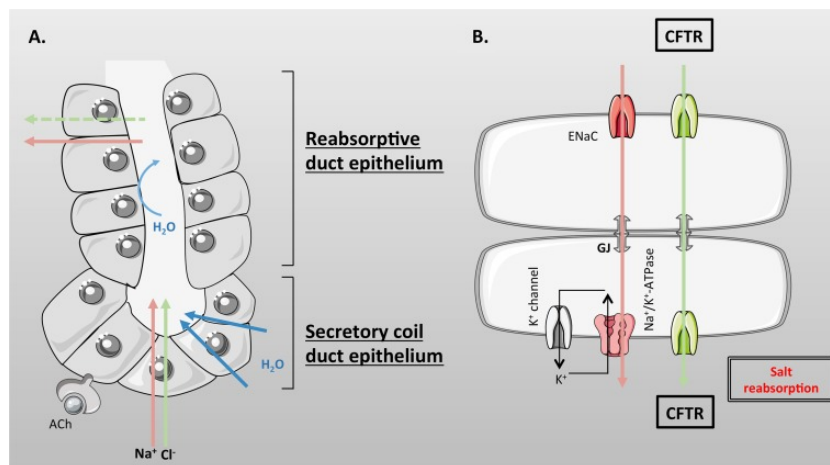


Figure 2.2: Ion transport in the sweat gland [8].

**Secretory coil**
The secretory coil of the sweat gland consists of three types of cells called dark, clear and myoepithelial cells [24]. There is a single layer of epithelial cells, which consists of equal proportions of clear and dark cells. These cells are responsible for producing the primary sweat secretion [8]. The secretion of sweat is based on the transport of electrolytes and fluid through ion channels and the membrane, respectively. The transport is controlled by cholinergic and alpha- and beta-adrenergic neurotransmitters which attach to the receptors of the clear cells. The ion channels are activated by chemicals produced by activated neurotransmitters. The excretion of electrolytes (actively and passively) by ion channels in the cell membrane, causes the excretion

of fluid due to osmosis.

Clear cells contain multiple ion pumps, as can be seen in table 2.1. The clear cells also contain CFTR chloride channels in their cell membrane, which play a role in the sweat secretion in response to beta-adrenergic stimulation. However, their role is not dominant in the secretion. The major physiological stimulus for secretion is acetylcholine. Acetylcholine is a cholinergic neurotransmitter which is released from post-ganglionic sympathetic cholinergic fibres. Acetylcholine stimulates fluid transport through a non-CFTR dependent pathway, mostly resulting in $Cl^-$ excretion via the TMEM16A $Cl^-$ channel. The TMEM16A $Cl^-$ channel is functioning normal in CF patients. Therefore, the excretion of sweat electrolytes is only limitedly influenced by CF in the secretory coil [8]. The sweat excretion can also be artificially increased by using a cholinergic agonist, such as pilocarpine. Cholinergic agonists mimic cholinergic neurotransmitters and will bind to the neurotransmitter receptors of clear cells, stimulating sweat excretion.

The function of the dark cells is not clear yet. Some literature suggests that these cells also contribute to sweat secretion and could have an additional role in sweat fluid and pH regulation [8].

Myoepithelial cells are modified by smooth muscle cells that contract during sweat secretion. The function of the myoepithelial cells is to provide mechanical support to the secretory coil wall against the increase in luminal hydrostatic pressure during sweating to protect the coil from damage [24].

**Reabsorptive duct**
The reabsorptive duct, also called excretory duct, forms the pathway from the secretory coil to the skin surface or in case of apocrine sweat glands into hair follicles [22]. The reabsorptive duct absorbs sodium and chloride but does not absorb water. The result after the absorption of electrolytes is hypotonic sweat, which is secreted out to the skin. The reabsorption of salt helps to minimise salt loss from the body [8]. The reabsorptive duct consists of two layers of cells, the basal ductal (peripheral) cells and the luminal cells [24].

The basal ductal cells contain many mitochondria for the production of ATP, used for actively transporting ions. The membrane of the basal ductal cells contains many ion pumps, as described in table 2.1. Active transport is used to reabsorb ions actively. The primary transported ions are sodium and chloride. Sodium is actively transported via mainly the Epithelial Sodium Channel (ENaC), which uses ATP as the energy source to transport sodium against its electrochemical gradient. Chloride is actively transported via mainly the CFTR channel. However, chloride is not transported against its electrochemical gradient; it uses the ATP just for opening the channel as already explained in section 1.1.1 [7][20].

Table 2.1: Cellular constituents and known key regulators of human eccrine sweat glands [23].

| Anatomical structures | Cellular constituents | Key proteins |
|---|---|---|
| Sweat duct | Basal cells | CFTR, ENaC, Na+ -K+ -ATPase, NKCC1 (weak), NHE1, K1, K10, K5, K14 |
| | Luminal cells C | CFTR, NHE1, K1b, K10, K19, K77 |
| Secretory portion | Dark cells | NKCC1, Na+ -K+ -ATPase, NHE1, CFTR, AQP5, CGRP, K8, K18 |
| | Clear cells | NKCC1, Na+ -K+ -ATPase, NHE1, CFTR, AQP5, S100, CA II, K8, K18 |
| | Myoepithelial cells | K5, K14 |

In contrast to the CFTR channels in the excretory cells, CFTR channels have a dominant role in the transport of chloride in the basal duct. As a consequence, chloride is not or barely absorbed in patients with CF due to their dis-functional CFTR channels. The absorption of sodium is also dependent on the functionality of the CFTR channel since the activation of ENaC also depends on the functioning of the CFTR channel. Sodium will not or barely be absorbed from sweat in the reabsorptive duct in CF patients [26]. As a consequence, sweat at the skin surface from CF patients contains elevated concentrations of both chloride and sodium compared to the sweat of healthy persons. This is illustrated in figure 2.3.

Besides its influence on chloride and sodium transport, the CFTR channel is also influencing the reabsorption of $HCO_3^-$. However, the concentration of $HCO_3^-$ in sweat is much lower compared to chloride and sodium, as is explained in section 2.2.

Compared to the basal duct cells, the luminal cells have fewer ion pumps. The primary function of the luminal cells is to provide mechanical support for the reabsorptive duct [24].
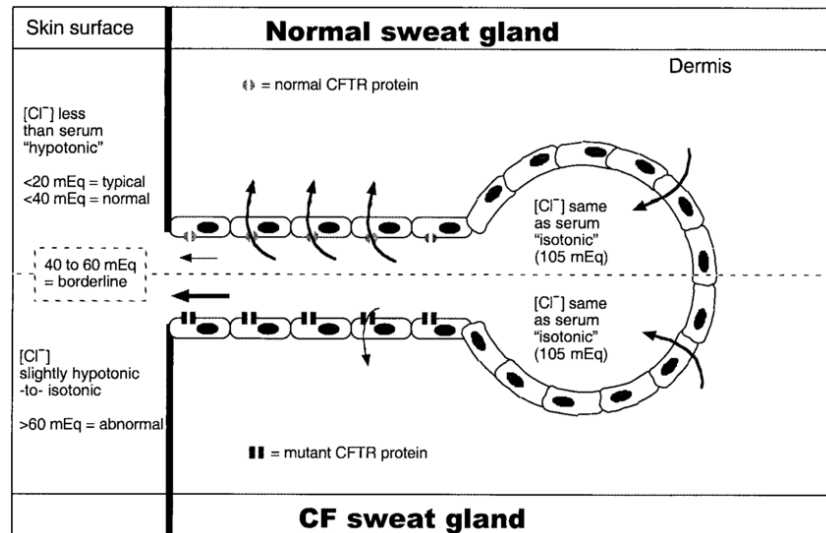
Figure 2.3: Diagram of a sweat gland, showing paths taken by chloride ions (arrows) during secretion [9]

## 2.2. Sweat composition

As can be seen in table 2.2, sweat consists primarily of water and salt. However, it is hypotonic with respect to the interstitium of the skin cells [8]. As mentioned before, multiple disorders involving defects in electrolyte and fluid production can be detected in sweat. Several of these disorders are mentioned in table 2.2.

Table 2.2: Electrolyte concentrations sweat.

| Ion | Range/mM | Sweat-rate dependence | Biomarker for physiology | Biomarker for medical condition | Ref. |
|---|---|---|---|---|---|
| $Cl^-$ | 10-100 | Yes | Dehydration, indirect sweat-rate | Cystic Fibrosis, Type 1 fucosidosis, Vasopressin-resistant diabetes insipidus, Ectodermal dysplasia, Panhypopituitarism, Familial cholestasis, Familial hypoparathyroidism, Atopic dermatitis, Iatrogenic causes (infusion of prostaglandin E1), Anorexia Nervosa | [27] [28] [20] [29] |
| $Na^+$ | 10-100 | Yes | Dehydration, indirect sweat-rate | Cystic Fibrosis Pseudohypoaldosteronism (PHA) | [27] [28] [20] [8] [29] |
| $NH_4^+$ | 0.5-8 | No | Exercise intensity | Liver dysfunction | [29] |
| $K^+$ | 4-24 | No, proportional to blood | Muscle activity | Hypo- or hyperkalemia | [20] [29] |
| $HCO_3^-$ | 0.2-2.5 | Various | Acid-base equilibria | Cystic Fibrosis, Acid-alkali balance | [29] |
| $Ca^{2+}$ | 0.5-3 | No | Homeostasis, stress fractures | Hyperparathyroidism and kidney-stone | [20] [29] |
| $Mg^{2+}$ | 0.04-0.7 | Various | Muscle strength, aerobic performance | Hypomagnesemia, cardiac arrhythmias | [29] |
| pH | 4-7 | Dependence from other species | Acid-base equilibria | Acid-alkali balance disorder, kidney-stone | [29] |

At high sweat rates, both $Na^+$ and $Cl^-$ concentrations are elevated. The proportion between $Na^+$ and $Cl^-$ is the same during all sweat rates. In most instances, chloride concentrations are 20 - 25 $mM$ less than sodium concentrations due to the contribution of other anions present in sweat such as bicarbonate ($HCO_3^-$) [28][16]. It should be noted that sweat electrolyte concentrations can be very high in newborns during the first 48 hours. After two to three weeks, the electrolyte levels are decreased in healthy persons [20]. The typical electrolyte levels for diagnosis are presented in table 2.3.

Table 2.3: CF diagnosis based on chloride concentrations in sweat [19].

| Diagnosis | Chloride (mmol/l) infants | Chloride (mmol/l) elders |
|---|---|---|
| Typical CF | $\geq 60$ | $\geq 60$ |
| Atypical CF | 30 - 59 | 40 - 59 |
| Not CF | < 30 | < 40 |

## 2.3. Sweat stimulation

During the sweat tests for CF patients described in section 1.3.2, it is unwanted to stimulate the sweat production by exercising, partly due to the physical state of the patients and partly due to differences in concentrations of chloride during exercising [30] which will not result in a good reference of the chloride concentration. Furthermore, to have a continuous flow of sweat for continuous monitoring, it can be necessary to artificially stimulate the sweat production at moments the patient does not sweat enough on themselves.

The method used in the sweat test to locally stimulate sweat production is called pilocarpine iontophoresis. Pilocarpine gel is a cholinergic agonist hydrogel. Other hydrogels that can be used for sweat stimulation are acetylcholine gel and methacholine gel [31]. The hydrogel is applied to the region of interest of the patient, mostly the forearms due to practical considerations. Iontophoresis is a technique used to increase the penetration of ions through the skin layers. By applying a controlled current through a cholinergic agonist hydrogel, the cholinergic agonist is pushed into the skin where it stimulates the sweat production [32].

The author of this report underwent the sweat test, which was conducted according to the following protocols:

- **Step 1.** Clean skin with alcohol and dry afterwards

- **Step 2.** Place the pilocarpine gels in the electrodes

- **Step 3.** Place the positive electrode at the underarm close to the flat of the hand, place the negative electrode at 10 cm distance typically

- **Step 4.** Stimulate with 1mA typically for 5 minutes

- **Step 5.** Remove electrodes and gels, dry the skin

- **Step 6.** Place collector at the location where the positive electrode was placed, connect it tight to the skin surface by using the straps

- **Step 7.** Collect sweat till collector is full enough, typically the collection time is between 30 to 60 minutes

- **Step 8.** Store the collector in a sealed bag en analyse it in a suitable coulometric analyser

The principle of iontophoresis is to use a small current to push a chemical agent through the skin [17], as illustrated in figure 2.4. By applying iontophoresis trough pilocarpine, typically on the forearm of the patient, the pilocarpine is imbibed into the sweat glands as illustrated in figure 2.5 and 2.6. Pilocarpine nitrate is a cholinergic agent that binds to muscarinic receptors of eccrine sweat glands and induces sweat production [33]. Since the sweat attracts to the surface of the skin, this process is also called reverse iontophoresis, meaning that it aims to attract substances out of the skin [34].
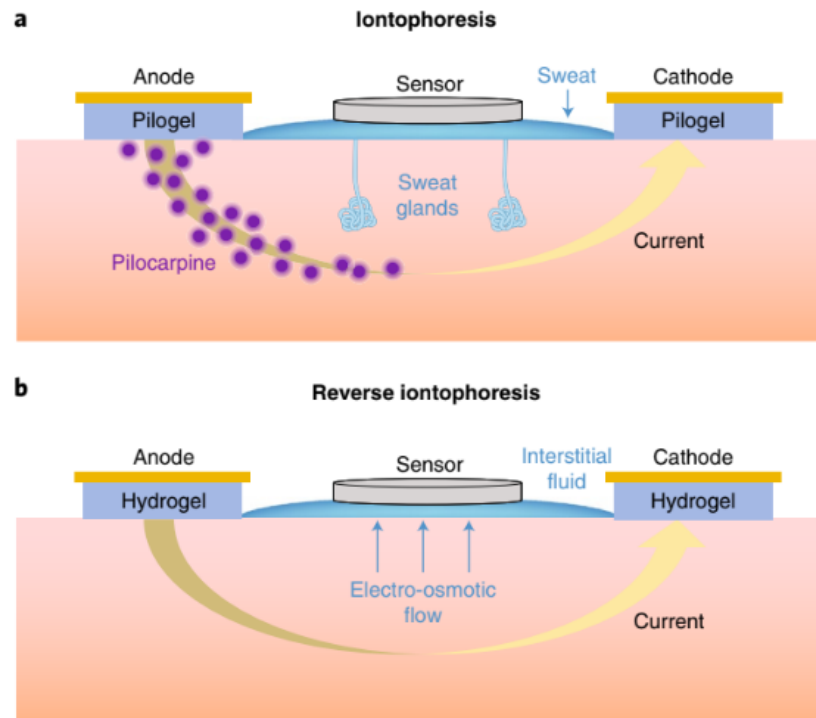
Figure 2.4: Working principle of pilocarpine iontophoresis a) start of iontophoresis, b) reverse iontophoresis, artificial stimulated sweat reaches the skin surface [35].



Figure 2.5: Placement of electrodes for pilocarpine iontophoresis [17].
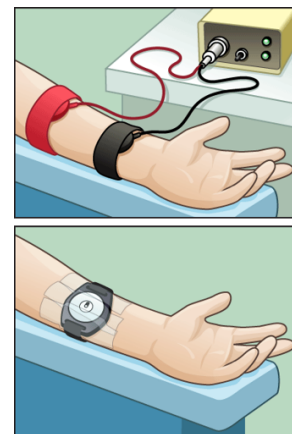


Figure 2.6: Placement of electrodes and collector for pilocarpine iontophoresis [36].

## 2.4. Sweat measuring methods

The interconversion of chemical energy and electric energy is the area of chemistry called Electrochemistry. With the use of the known relations between the chemical energy and electrical energy, it is possible to characterise a sample. This can be used for elemental and molecular analysis, but also for acquiring information about equilibria, kinetics and reaction mechanisms [37]. The techniques described in table 2.4 are the general techniques used in electrochemistry and is explained in more detail in the subsections below, figure 2.8 shows a more elaborated overview of the electrochemical techniques.

All these techniques are based on reduction and oxidation reactions, known as redox reactions in which electrons are transferred from one reactant to another. A chemical species that gains electrons in the redox reaction are *reduced* and a species that loses electrons is *oxidized*. An example of this principle is shown below:

Table 2.4: Electroanalytical Techniques [38].

| Technique | Controlled parameter | Parameter measured |
|---|---|---|
| Potentiometry | Current $i$ (fixed at $i$=0) | Potential $E$ |
| Voltammetry | Potential $E$ | Current $i$ vs. Potential $E$ |
| Amperometry | Potential $E$ (fixed) | Current $i$ |
| Coulometry | Potential $E$ or Current $i$ | Charge $q$ (integrated current) |
| Conductometry | Voltage $V$ (AC) | Conductance $G = 1/R$ |

$$\text{Reduction}: Cl_2(g) + 2e^- \rightarrow 2Cl^- \tag{2.1}$$

$$\text{Oxidation}: Cu(s) \rightarrow Cu^{2+} + 2e^- \tag{2.2}$$
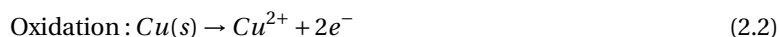
The side where the reduction takes place is called the *cathode* and the side where the oxidation takes place is called the *anodee*. An electrical circuit is realised with the use of an electrochemical cell in which Redox reactions are carried out. This makes it possible to measure the electrons transferred, the current, and the voltage. To correlate these electrical properties to chemical properties, some important relationships are shown below. The total charge transferred in the redox reaction is the multiplication between the number of moles ($n$) involved in the reaction and the Faraday constant 2.5.

$$\text{Charge of one electron}: 1.602 \cdot 10^{-19} C \tag{2.3}$$

$$\text{Number of electrons in one mol}: 6.022 \cdot 10^{23} e^- / mol \tag{2.4}$$

$$\text{Faraday constant (F)}: 1.602 \cdot 10^{-19} \cdot 6.022 \cdot 10^{23} = 96.485 C / mol \tag{2.5}$$

$$\text{Total charge transferred in redox reaction}: q = n \cdot F \tag{2.6}$$

The electrochemical cell consists of two half-cells. In each half-cell, a metal strip (electrode) is placed in an ionic solution (electrolyte). The reaction between the electrode and the electrolyte can be represented as shown in equation 2.7 and 2.8. Each half-cell has its characteristic electrode potential, which represents the ability of the half-cell to do work, or the driving force for the half-cell reaction. Measuring the potential differences between the half-cells is not immediately possible since for an electrical circuit it is necessary to have a complete loop. Without a complete loop, no reaction between the cells takes place and no current will flow through the electrodes. The circuit of the electrochemical cell can be completed by adding a salt-bridge. The two half-cells are still physically separated; however, from an electric point of view, the circuit is completed and balance the charge in the cells. The charge balance in the cell is possible due to the ionic motion in the salt bridge [37], [38]. In many commercially available and in-house-prepared reference electrodes, nanoporous glass frits contain the electrolyte solution that forms a salt bridge between the sample and the reference solution [39]. A schematic overview of an electrochemical cell with a porous frit is illustrated in figure 2.7.

The measured potential, between the half-cells can be described by equation 2.9 in which both half-cell reactions are written as reduction reactions. This cell potential is called the Electromotive Force (EMF).

$$\text{Anode (oxidation)}: M^0 \rightarrow M^{n+} + ne^- \tag{2.7}$$

$$\text{Cathode (reduction)}: M^{n+} + ne^- \rightarrow M^0 \tag{2.8}$$
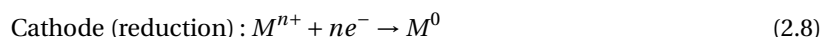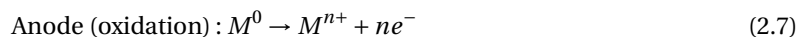
$$E_{cell} = E_{cathode} - E_{anode} \tag{2.9}$$

However, in practice, another potential influence the cell potential; this is the junction potential. If there is a difference in the concentration or types of ions of the two half-cells, a small potential is created at the junction of the membrane or salt bridge and the solution. This can cause an error in the measurement since the exact junction potential is often unknown. The junction potential can be minimised by working with
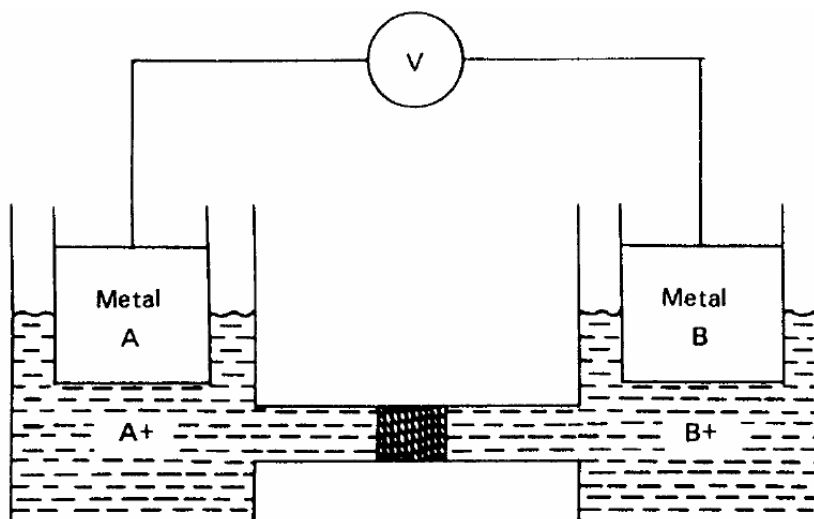
Figure 2.7: A schematic complete cell with a porous frit separating the half-cells [38].

sample solutions with a high ionic strength background, for example, Potassium Chloride (KCl). In a cell with a porous fit, the junction potential can be decreased by increasing the pore sizes. However, solution flow through the frits increases as the pore sizes increase, which in long-term measurements can cause significant contamination of test solutions by the inner filling solution of the reference electrodes [39]. The effect of the junction potential on the cell potential is described in equation 2.10.

$$E_{cell} = E_{cathode} - E_{anode} + E_{junction} \tag{2.10}$$

By making one half-cell the reference, it is possible to calculate the potential of the other half-cell. By convention, the reference electrode is the anode. The reference half-cell has to provide a known and stable potential which can not be affected by the indicator electrode, by convention the cathode. Therefore, a proper combination of an electrode and analyte is necessary. In general, there are 3 common reference electrodes, listed in table 2.5.

Table 2.5: Common reference electrodes.

| Name | Electrode | Analytic | Reaction | Standard-state potential |
|------|-----------|----------|----------|--------------------------|
| Standard Hydrogen electrode (SHE) | Pt | $H_2$ | $2H^+(aq) + 2e^- \rightleftharpoons H_2(g)$ | $E = 0.00V$ at all temperatures |
| Saturated Calomel electrode (SCE) | Hg | KCl | $Hg_2Cl_2(s) + 2e^- \rightleftharpoons 2Hg(l) + 2Cl^-(sat'd)$ | $E = 0.28V$ with 1.00M KCl 25 °C |
| Silver/Silver Chloride electrode (Ag/AgCl electrode) | Ag | KCl | $AgCl(s) + e^- \rightleftharpoons Ag(s) + Cl^-(sat'd)$ | $E = 0.197V$ with saturated KCl 25 °C |

The SHE is the standard reference electrode it is used to establish standard-state potentials for other half-reactions. As can be seen in table 2.5, the standard-state potential E $0.00V$ for all temperatures. Although the SHE is the standard for all the analytical work, it is rarely used since it is hard to prepare and inconvenient to use.

A disadvantage of the SCE and the Ag/AgCl electrode is the temperature dependence, due to the solubility of KCl is sensitive to a change in temperature. At higher temperatures, the solubility of KCl increases, causing a potential decrease at the electrode. For example, the potential of the SCE is +0.2444$V$ at 25°C and +0.2376$V$ at 35°C vs the SHE. When prepared using a saturated solution of KCl, the potential of an Ag/AgCl electrode is +0.197$V$ at 25°C. Another common Ag/AgCl electrode uses a solution of 3.5 M KCl and has a potential of

+0.205$V$ at 25°C. The potential for a Ag/AgCl electrode with a saturated NaCl has a potential of +0.197$V$ at 25°, which is comparable with the KCl saturated.
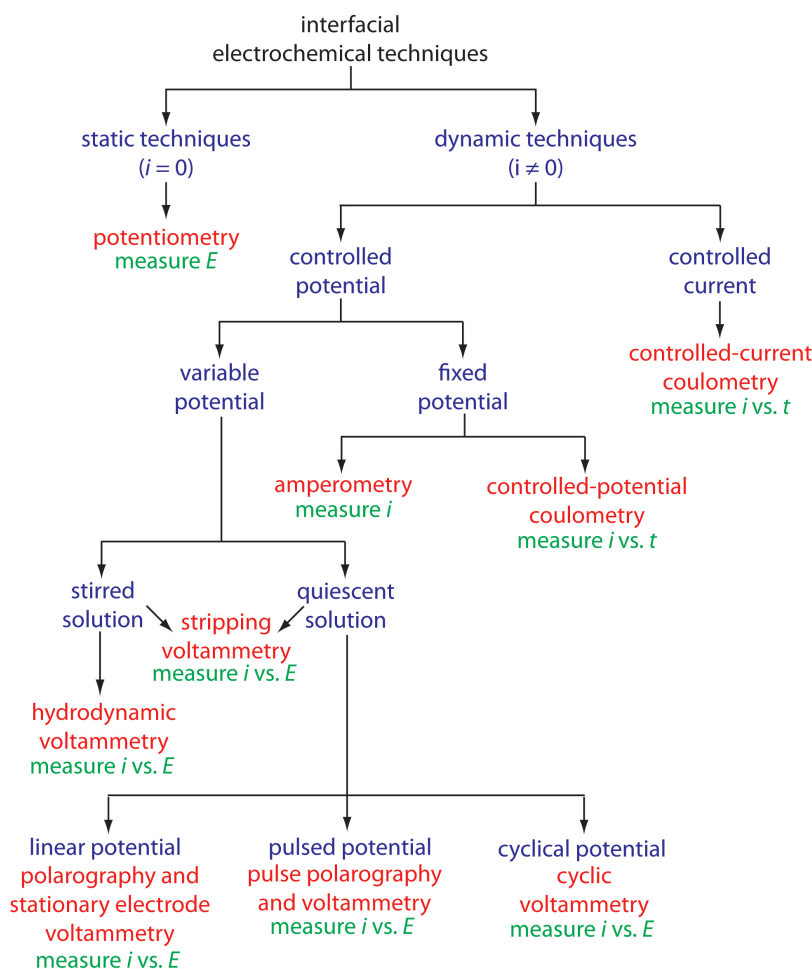


Figure 2.8: Family tree highlighting a number of interfacial electrochemical techniques. The specific techniques are shown in red, the experimental conditions are shown in blue, and the analytical signals are shown in green [37].

### 2.4.1. Potentiomtery

The difference in the developed potential by an electrochemical cell is measured in potentiometry. The electrochemical cell consists of a reference electrode and a sensing electrode. The potential difference is measured under static conditions, meaning that there is non or only a very limited current, as can be seen in figure 2.8. As illustrated in figure 2.9, the development of potentiometry originates from the beginning of 1900. The relation between an electrochemical cell's potential and the concentration of electroactive species in the cell is described by the Nernst equation, which was formulated in 1889 [37], [38]. The Nernst equation is described in equation 2.11.

$$E = E^0 - \frac{RT}{nF} ln \frac{[C]^c \, [D]^d}{[A]^a \, [B]^b} \tag{2.11}$$
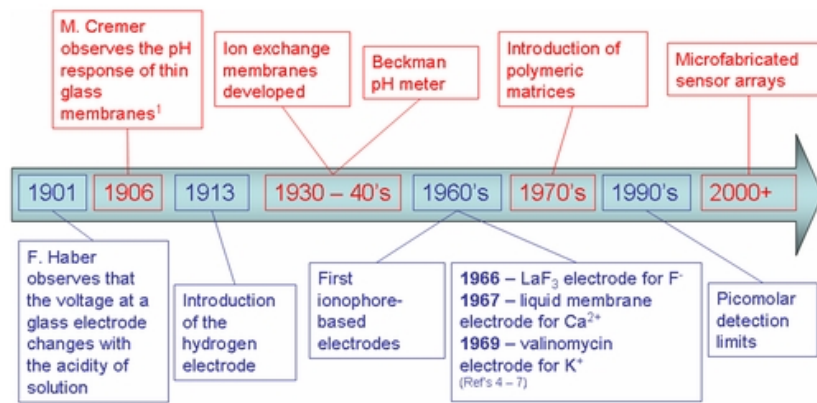
Figure 2.9: Milestones in the development of potentiometry [37].

Both the Ag/AgCl electrode standard potential $E^0_{Ag/AgCl}$ and the RT/F term in Eq. 2.11 depend on temperature. Concerning $E^0_{Ag/AgCl}$ temperature coefficients between -0.6 and -0.65 $mV\,°C^{-1}$ have been reported [40]. For example, a decrease in temperature by 10°C would thus lead to a decrease of ca. 6 mV in $E^0_{Ag/AgCl}$ and of ca. 3 $mV$ in the RT/F term. Nevertheless, these errors can be corrected by taking into account the temperature when applying the sensors under temperature fluctuating conditions. In addition, temperature effects can be reduced by using silver/silver chloride based reference electrodes (e.g. Ag/AgCl/sat. NaCl) since in this case, the reference electrode and the Ion Selective Electrode (ISE) have the same standard potential, $E^0_{Ag/AgCl}$ and thus temperature only affects the RT/F term in Eq. 2.11.

As mentioned before, potentiometry is a zero-current technique that measures the potential difference between the working electrode and the reference electrode in an electrochemical cell. The selectivity for ions is dependent on the electrode type. A very common material used for electrodes is Ag/AgCl. Electrodes made from Ag/AgCl are selective for chloride. Therefore it can be used as a reference electrode as can be seen in table 2.5. However, for other ions such as sodium, it is not possible to measure it directly with an electrode. To make an electrode selective to other ions, an ionophore can be used [37]. For example, sodium ionophore X can be used to measure sodium and valinomycin can be used to measure potassium. The ionophore acts as a membrane for the electrode. The membrane can only bind to a selective ion, in this case, sodium. The potential causes a difference in the composition of the membrane which makes it possible to release or obtain an ion or an electron from the electrode, which causes a potential change [41]. The potential change can be measured against the potential from the reference electrode. The measured voltage can be translated to the concentration of sodium with the use of the Nernst equation. For sodium or potassium sensing at room temperature, theoretically, an ion-selective sensor should have a sensitivity of 59.16 $mV$ per decade of concentration [42]. This concept is illustrated in figures 2.10 and 2.11.
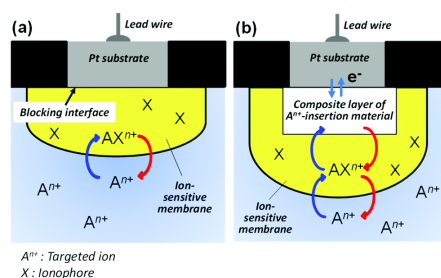


Figure 2.10: Working principle of an ionophore [41].
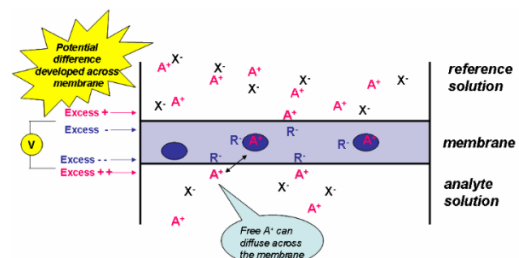


Figure 2.11: Interaction of an ionophore with reference solution [37].

## 2.4.2. Other electrochemical techniques

An overview of the electrochemical methods applied before in measurements of chloride and sodium concentrations in sweat is given in table 2.6. The different methods are described in more in the comming section.

**Voltammetry**

Voltammetry is a commonly used electroanalytical method for measuring concentrations in solutions. The method is based on a transduction principle for deriving information about one or multiple analytes dynamically by measuring the current as a function of the varied potential. There are multiple types of voltammetry, as can be seen in figure 2.8. An example is stripping voltammetry; this technique is suitable for monitoring heavy metals in body fluids [42]. Compared to potentiometry, this method is less suitable for measurements of chloride and sweat since it needs a supporting chemical. This is not a problem when samples are taken from sweat. However, in the application as a real-time monitoring device, it is not allowed to take samples.

**Amperometry**

Amperometric sensors measure the current generated from the oxidation or reduction of an electroactive analyte in a chemical reaction. Enzymatic amperometric sensors have been used for continuous monitoring of glucose, lactate, ethanol and uric acid, where chemical reactions of the target metabolite catalysed by a specific enzyme (e.g. glucose oxidase, lactate oxidase and urate oxidase) generate an electrical current proportional to the target concentration [42] [43]. Compared to potentiometry, this method is less suitable for measurements of chloride and sweat for the same reason as voltammetry, since it will need a supporting chemical [44].

**Colorimetry**

Colourimetry refers to sensing elements undergoing a colour change in the presence of a target analyte through a chemical reaction. With an absorbance measurement, the colour change can be quantified and translated to a concentration of the ion. Specificity and sensitivity are typically dictated by the modified substrates or colourimetric chemical reactions. Colourimetry is used for measuring all kind of body fluid properties, such as glucose, lactic acid, sodium and chloride [42]. Since it is based on a chemical reaction with the support of a chemical, it is possible to take multiple samples to measure differences over time. However, it is not possible to have real-time measurements.

**Conductometry**

Conductometry is based on the principle that the conductance of sweat is related to chloride concentration [45]. Values for sweat conductivity are different from those of sweat chloride concentration because of the presence of unmeasured anions such as lactate and bicarbonate when sweat conductivity is analysed. Although, the test does reflect the concentration of sodium chloride since these are the primary components in sweat, as shown in table 2.2. However, there are two problems with this technique. Firstly, since the concentration of chloride nor sodium is measured directly, any contamination or increase of other ions in sweat can influence the test. Secondly, it is necessary to take samples of sweat since directly measured on the skin is not possible due to the influences of skin conductance on the measurement. As a consequence, it is not possible to have real-time measurements suitable for monitoring medicine effectiveness.

It is concluded that using potentiometry as the electrochemical technique is the best suitable for the real-time monitoring application since it complies with all the requirements for measurements of chloride and sodium concentrations in sweat. Therefore, this method is researched in more detail.

Table 2.6: Electrochemical techniques for chloride and sodium measurements in sweat applications.

| Electrochemical technique | Used in real-time $Cl^-$ $Na^+$ sweat measurements | Commercially | Need for supporting chemical | Small | Flexible | Reliable results | Reference |
|---|---|---|---|---|---|---|---|
| Potentiometry | ✓ | ✗ | ✗ | ✓ | ✓ | ✓ | [29] [31] [46] [47] [48] [49] [50] |
| Voltammetry | ✗ | ✓ | ✓ | ✓ | ✓ | ✓ | [51] |
| Amperometry | ✗ | ✓ | ✓ | ✓ | ✓ | ✓ | [43] [52] [53] [51] |
| Colorimetry | ✗ | ✓ | ✓ | ✗ | ✗ | ✓ | [42] |
| Conductometry | ✓ | ✓ | ✗ | ✓ | ✓ | ✗ | [45] [53] [54] |

Blue highlighted is used in this study

## 2.5. Related research

Sweat sensor systems consisting of a reference electrode and a sensing electrode found in literature with the best properties will be elaborated in more detail below.

**Ag/AgCl reference and sensing electrode with pHEMA reference membrane patch** [46]

This epidermal sensor patch is unique in its detailed explanation of the sensor production by the authors Dam, Zevenbergen, and Schaijk. One of the authors is contacted to retrieve inside information. During the conversation, it is mentioned that the application of this sensor was not to monitor medicines effectiveness in CF patients. However, the author expects that this application is suitable for this sensor if the sweat collector and the reference electrode is optimised. The pro's and con's of this sensor are elaborated below:



+ Detailed explanation of sensor production

+ Sensitivity and drift mentioned

+ Different implementations described

− Reference electrode not stable in application for at least 24 hours

− pHEMA membrane costly

− Not integrated and tested with Pilocarpine Iontophoresis
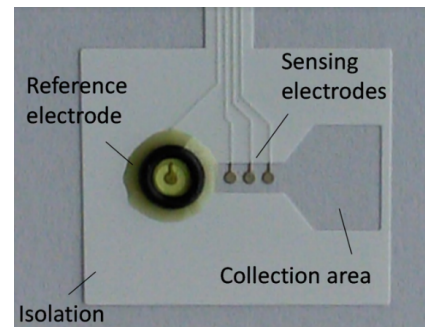
**Ag/AgCl reference and sensing electrode with Polyvinyl Butyral (PVB) reference membrane with integrated iontophoresis electrodes in a patch** [31]

This epidermal sensor patch is integrated with electrodes for iontophoresis. Furthermore, the effect of applying iontophoresis with pilocarpine, acetylcholine, methacholine are studied. The stability of the reference electrode was also long enough for the application of monitoring medicines effectiveness in CF patients. Therefore, this sensor patch comes closest with the end goal of the thesis project. The pro's and con's of this sensor are elaborated below:



+ Detailed explanation of effect of iontophoresis

+ Reference electrode stable for 2 weeks

+ Integration of sensor and stimulator in patch

+ Both $Cl^-$ as $Na^+$ sensing electrodes

+ Electrical circuit explained in paper

+ Less costly reference membrane due to the use of PVB

− Drift not clearly mentioned

− Not integrated with an sweat collector

− Not tested in application form for multiple hours
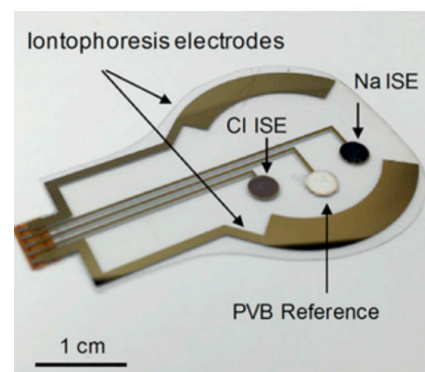
**Ag/AgCl reference with PVB reference membrane and carbon sensing electrode with $NH_4^+$ ionophore, integrated in a tattoo [47]**

This sensor is screen-printed on temporary-transferred tattoo paper. Therefore, the sensor is easy and comfortable for the patient. This sensor is implemented $NH_4^+$ sensing electrode, in an additional implementation a sodium sensing electrode is used. This is the only paper from which a separate and detailed paper of the reference electrode is published. The pro's and con's of this sensor are elaborated below:

+ Temporary-transferred tattoo paper for comfort and easy to use

+ Separate paper with additional information concerning the reference electrode

+ Longest stability of the reference electrode

+ Implemented as $NH_4^+$ and as $Na^+$ sensor

+ Less costly reference membrane due to the use of PVB

− Not integrated with a sweat collector

− Not tested in the application for multiple hours

− Not integrated and tested with Pilocarpine Iontophoresis
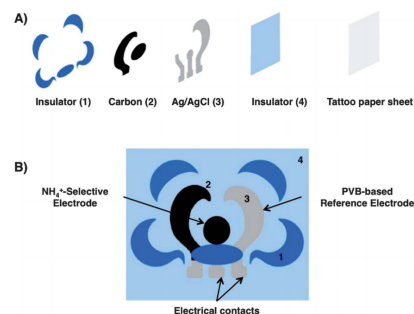


**Ag/AgCl reference with PVB reference membrane and Ag/AgCl sensing electrode with Sodium ionophore X, integrated in a RFID patch [50]**

This sensor patch is not outstanding in its performance as a sensor. However, the integration in an RFID patch can be very useful in the future to The pro's and con's of this sensor are elaborated below:

+ Integrated with RFID patch

+ Integrated with sweat collector

− Sensor performance is low

− Not tested in application form

− Stability only tested for 45 minutes in reference solution
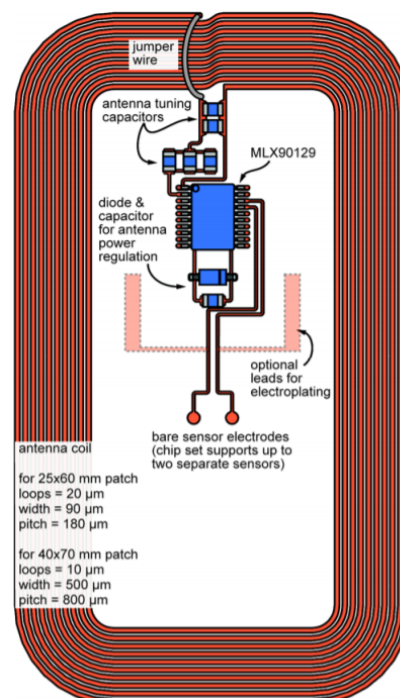


## 2.6. Conclusion

Chloride and sodium are the main ions in sweat, in which the CFTR protein has an important role. The secretion of sweat is based on the transport of electrolytes and fluid through ion channels and the membrane, respectively. The sweat glands consist of a secretory coil and a reabsorptive duct. Sweat excreted by the secretory coil contains high concentrations of chloride and sodium. However, the transport of the chloride ions is dominated via non-CFTR depend pathways. Therefore, the sweat excreted by the secretory coil is normal

in CF patients. The primary function of the reabsorptive duct is to reabsorb ions to prevent the body from excessive salt loss. However, this reabsorption of ions is dependent on a CFTR pathway. Since that pathway is dis-functional in CF patients, the reabsorption is insufficient, causing sweat with high chloride and sodium concentrations at the skin surface. These elevated levels for chloride and sodium are measured in the sweat test.

Research is in progress on wearable real-time sweat monitoring systems. Most of the studies used potentiometry as chemical sensing technique. Studies which took samples also used voltammetry, amperometry or colourimetry. However, these techniques are less suitable for real-time measurements. Another technique, conductometry, could be used in real-time measurements but has less promising results compared to potentiometry. Potentiometry is based on the potential difference between a reference electrode and a sensing electrode. At both electrodes, a potential is developed due to the redox reaction between the electrode (AgCl) and the analyte ($Cl^-$). The sensing electrode can be made selective for other ions by using an ionophore.

To measure real-time chloride and sodium concentrations, it is necessary to collect enough sweat to flow over the sensor. During sweat tests in hospitals, a sweat stimulator and collector is used for this purpose. The final sweat sensor system should also have a comparable system. In conclusion, a sweat sensor and electronic circuit for the read-out have to be developed. In addition, a sweat collector and sweat stimulator have to be developed.

# 3

# Design considerations and requirements

As described in chapter 2, to create a fully functional sensor system, four parts have to be developed as illustrated in figure 3.1:

- A sweat sensor to measure chloride an sodium concentration in sweat

- A electric circuit for the read-out of the sweat sensor

- A sweat collector to increase the sweat collection volume by enlarging the sample surface

- A sweat stimulator to increase the sweat collection volume by artifically increasing the sweat rate
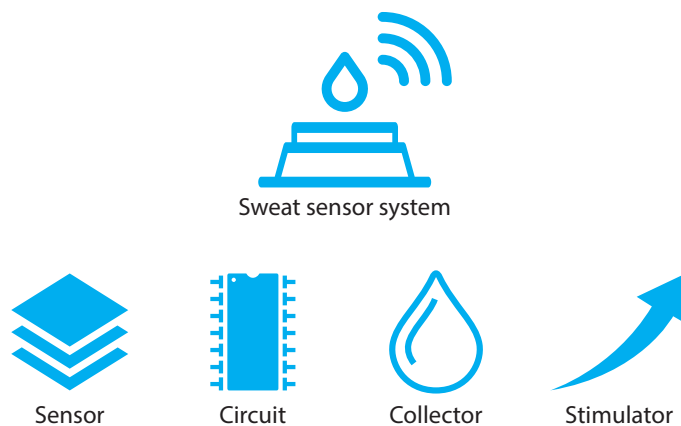


Figure 3.1: Overview of research topics.

In this chapter, the design considerations and requirements for these four parts of the sensor system are discussed.

For the proof of principle of a sweat sensor system, multiple issues have to be taken into account requiring a multidisciplinary approach:

- R1. The system should be capable of reliably monitoring a patient for 24 hours.

    - The region of interest for the measurements of the system in sweat are in the concentration range of $30\,mmol/l$ to $60\ mmol/l$ sodium and chloride.

    - The measurements should have an accuracy of $\pm\,3mmol/l$.

- R2. The materials and techniques used for the system should enable the end product to become a wearable device.

    - The complete system should fit in a single wearable package.

- The system should survive without user interactions for at least 24 hours of measurements.

- R3. The system should be safe for the operator and patient.

    - The electronics should be electrically isolated from the operator and patient.

    - Any energy transmission into the patient (for example, electrical current, heat, sound waves) should be based on techniques that have been medically approved. The usage of these proven techniques instead of new techniques is to enhance the medical approval process since obtaining the required clinical evidence for a new technique can take a long time.

Since this project is the start of a long term project, it is also advisable to take already the following considerations and requirements in mind, although these are not a priority in this phase of the project.

- The system should be easy to be used by the patient.

    - The system should be usable without medical or technical background.

    - The sensor should be easily replaceable for a new one if it is expired.

- The materials used have to be medically graded materials or should be proven of minimal risk if they come into contact with the patient.

## 3.1. Sweat sensor

The sweat sensor itself is the main item of the sensor system. For medical reasons, it should be able to measure both the chloride and the sodium concentration in sweat. Furthermore, the values of both sodium and chloride sweat concentrations should be close to each other as explained in section 2.2. Deviated values between the chloride ans sodium sweat sensor output could be an indication of a measurement error.

Some of the requirements were already defined before the start of the research; these requirements are discussed in this section. Other requirements, for example, exact size and material, were defined after exploration of the sensor type, production technique and practical usage. These requirements are discussed in chapter 4.

Based on the literature study, it was defined that the sensor should meet the following requirements next to the requirements listed in the previous section:

- The substrate should be flexible to be used comfortably on the skin.

- The production technique should allow for making multiple prototypes during this project.

- The materials should be delivered in 5 weeks maximum, to start in time with the production.

- The materials for the prototypes have to be affordable, the aim is to keep the total costs below €1000.

- If chemicals are used, it should be possible to meet the safety rules of the lab.

In the literature study, multiple production techniques were investigated, resulting in a selection of promising sensor types and production techniques, mentioned in table 3.1.

Table 3.1: Sensor types and production techniques with promising results in sweat sensing applications.

| Type | Technique | Wearable | Real-time | Stability | Prototype | #Ref. |
|---|---|---|---|---|---|---|
| Potentiometry | Screen-printing | ✓ | ✓ | 4 months | ✓ | 25 |
| Potentiometry | Glass tube | ✗ | ✓ | 12 months | ✓ | N/A |
| ISE-FET | Silicon | ✓ | ✓ | Unknown | ✗ | 3 |
| Amperometry/voltametry | Screen-printing | ✓ | ✓ | 4 months | ✓ | 2 |
| Coulometry | Plastic collector | ✗ | ✗ | N/A | ✓ | N/A |
| CF Quantum sweat test | Patch | ✓ | ✗ | N/A | ✗ | 2 |

Blue highlighted was used in this study

The combination of potentiometry as sensor type and screen-printing as the production method is chosen for their best fit in this project:

- Screen-printing as production technique allows for fast prototyping.

- The materials needed are affordable and can be delivered in time.

- The chemicals needed are allowed in the lab (provided the correct usage of the protection measures).

- Literature shows promising results for the usage of potentiometry and screen-printing in sweat sensor applications.

    – The research best related to this project used potentiometry and screen-printing.

    – Results described in literature proves the possibility for 24 hours of stable measuring.

    – This production and sensor technique is used in a wearable prototype tested on human subjects, while most other techniques are only tested in lab settings.

- The read-out circuit can be build from commercially available components. This allows for combining the design and production of both a sensor and a read-out circuit in the limited period of time of this project.

- Potentiometry combined with screen-printing can be miniaturised allowing for the production of small sensors.

- Screen-printing can be applied on a flexible substrate allowing for the production of flexible sensors.

## 3.2. Read-out circuit

The accuracy of the read-out circuit in combination with the sensor should meet the measurement specification of $\pm 3mmol/l$. Since the accuracy of the read-out circuit also depends on the accuracy of the sensor the desired accuracy of the read-out circuit is defined after the development of the sensor.

The read-out circuit should be capable of reading both the chloride and the sodium sensor in the same setup. The sample frequency should be high enough to distinguish interfering signals from the sensor signal. This requires a sample frequency above 100Hz, to distinguish 50Hz interference from the local power-line.

## 3.3. Sweat collector

In two papers, it was mentioned that sweat sensors without a collector were used and that instead of that, sensors were directly applied on the skin [55][31]. This approach limits the sweat flow and will, therefore, result in the accumulation of sweat on the sensor. As a consequence, the measurements will not be real-time any more since the sweat measured will also contain old sweat. To avoid this accumulation, a continuous flow of sweat over the sensor is required [56].

Currently, the sweat collector in the golden standard sweat test for clinical usage is only effective when it is applied tightly to the skin. Since this is uncomfortable for the patient, it is not possible to wear it for multiple hours. The collector for the real-time monitoring application should, therefore, be based on a different technique to limit the sweat leakage.

After the sweat has passed the sensors, the sweat should be transported to a buffer reservoir to maintain a continuous flow of fresh sweat. This buffer can be realised by using cotton wool as absorbing material. This reservoir should be large enough to collect sweat for multiple hours. If this is too small, the reservoir may get full in a short time, which may result in an accumulation of sweat on the sensor.

In conclusion, to have a reliable real-time sweat measurement, the following points concerning the sweat collector should be taken into account:

- There has to be a continuous flow of sweat over the sensors

- It should be possible to wear the collector for 24 hours at least

- The buffer for collecting old sweat should have sufficient capacity for 24 hours

## 3.4. Sweat stimulator

A sweat sensor system can handle only reliable work real-time if there is a sweat flow. For continuous monitoring, stimulation of a natural sweat flow by exercising is not feasible requiring another approach for stimulating sweat flow. A sweat stimulator, which eventually can become a wearable device, has to be added to the sweat sensor system. To speed up the process of medical acceptance, this system should be preferably based on the already proved pilocarpine iontophoresis stimulator currently used in the hospital.

The stimulator used in the hospital (Macroduct Sweat collection system Model 37700-SYS), is also commercially available. However, the costs are high compared to the components needed for the stimulation and the system is too large to have a comfortable wearable device. Taking this into consideration, a new stimulator based on the clinically accepted principle of the Macroduct Sweat collection had to be designed for this research. The aim for the sweat collection is to collect at least $60\mu l$ of sweat after stimulation, which is based on the aim of sweat collection in hospitals for proper analysis.

The stimulating signal in the Macroduct Sweat collection stimulator is a constant current which can ramp up in the first minutes. This is also required for the stimulator in this project. In addition, it is desired to have a Pulsed Direct Current (PDC) since this has promising results in literature, as will be explained in more detail in 7.2. It is required to change easily the maximum voltage, the maximum current and the shape of the signal (e.g. CDC or PDC), for example with a potmeter or a switch.

In this project, it is not wanted to test the stimulator on patients, only on healthy volunteers to prove the basic working principles. The stimulator should be approved by the Human Research Ethics Committee (HREC) from the TU Delft before it will be used on participants. In order to avoid medical risks, the stimulation should be applied following the same protocol for sweat stimulation as used in the hospital.

The basic safety requirements from this protocol are listed below. A more detailed explanation of the safety measures are described in section 7.

- The maximum applied constant current per squared area should be below the value in which unacceptable skin irritation occurs

  - $0.5mA/cm^2$ [15][57]
  - Maximum of 5 minutes in case of stimulation with maximum constant current

- Maximum of $28V$

- The operator and participant should be protected from direct contact with the circuit

- The system should be easily switched off by the operator

## 3.5. Validation

The validation of the sweat sensor system is devided in four steps:

1. The four sub-parts are validated on itself in a laboratory setting.

2. The sweat sensor and read-out circuit are integrated together and validated in a laboratory setting.

3. The sensor and read-out circuit are integrated into the sweat collector and validated in a laboratory setting.

4. The sweat stimulator is validated on a human volunteer.

Due to strict medical ethical regulation, it is not possible to obtain medical acceptance for running a test with the complete system on human subjects in this phase of the research.

$4$

# Sweat sensor

This chapter highlights the design choices, working principle and production method of the sweat sensor. Three prototype versions, V1, V2 and V3, of the sensor have been designed, built and tested during this study. Figure 4.1 shows the final designs of these prototypes.
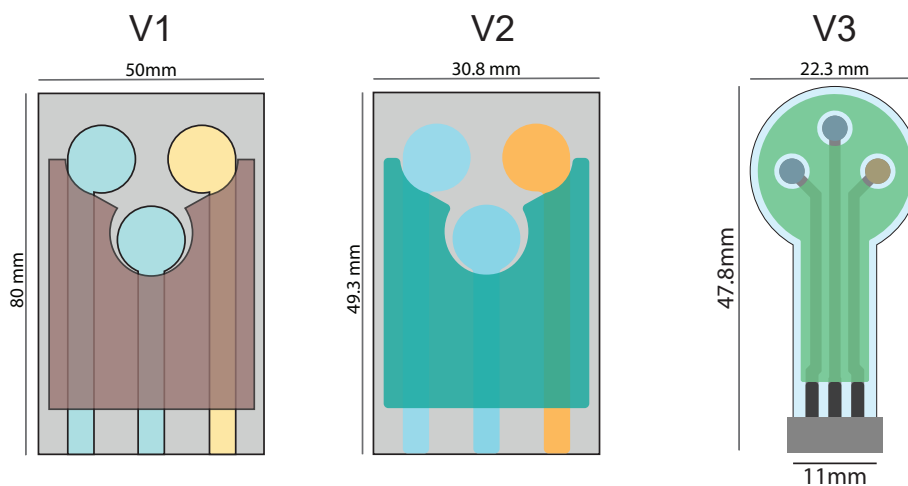


Figure 4.1: Screen-printing design of sensor prototype V1, V2 and V3.

## 4.1. Design

The working principle is basically in all the sensor types the same, while the design and materials are different. The sensors consist in basic out of four layers:

- The substrate

- The conducting layer

- The sensing electrodes

- The insulation layer

These layers are built using screen-printing, in which the patterns are deposited layer by layer. Screen-printing was chosen as method for the production of the sensor because it allows flexibility in prototyping, can be built small and flexible and due to the availability of the equipment. The basic principle of screen-printing is a controlled deposition of ink on a substrate by pressing ink through a mesh [58]. This technique can also be used for manufacturing of electrical circuits. Screen-printing is interesting due to the low investment, the opportunity for mass customisation and the compatibility with variation in material, size and complexity. The production method is explained in more detail in section 4.1.1 and 4.2.

Figure 4.2 depicts the layers of Sensor V3. The use of a vinyl stencil on top of the screens makes it possible to create layers with the desired patterns, as will be explained in more detail in section 4.1.2. The vinyl stencil can be modified to obtain the right patterns using a vinyl plotter. Adobe Illustrator is used for the designs of the vinyl.

During the design, the following considerations were taken into mind:

- The conducting paths have to be wide enough to obtain good conduction.

- The conducting paths have to be isolated with a water-resistant insulation layer, to isolate the paths from each other when placed under water.

- It should be possible to connect wires to the conducting paths by using a clip or connector.

- Sharp corners are not allowed since this result in more printing errors.
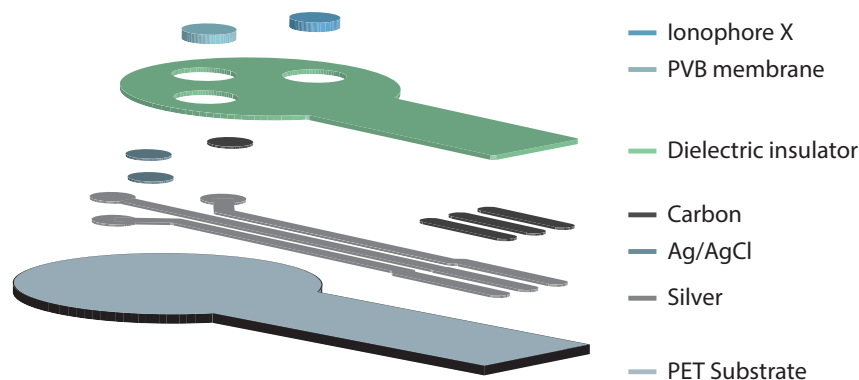


Figure 4.2: Layers by layer design of sensor V3.

## 4.1.1. Production method

The method used in this project is based on the methods described by Claus (2016). As described in his report and illustrated in figure 4.3, the process of screen-printing consists out of 3 steps:

Step 1:  Place the screen with the vinyl stencil on top of the substrate. Put a portion of ink on top of the cover.

Step 2:  Push the squeegee down right behind the ink and execute a smearing motion to cover the entire image. High pressure should be used to force the ink through the holes of the mesh.

Step 3:  Lift the frame, the screen printed image remains.
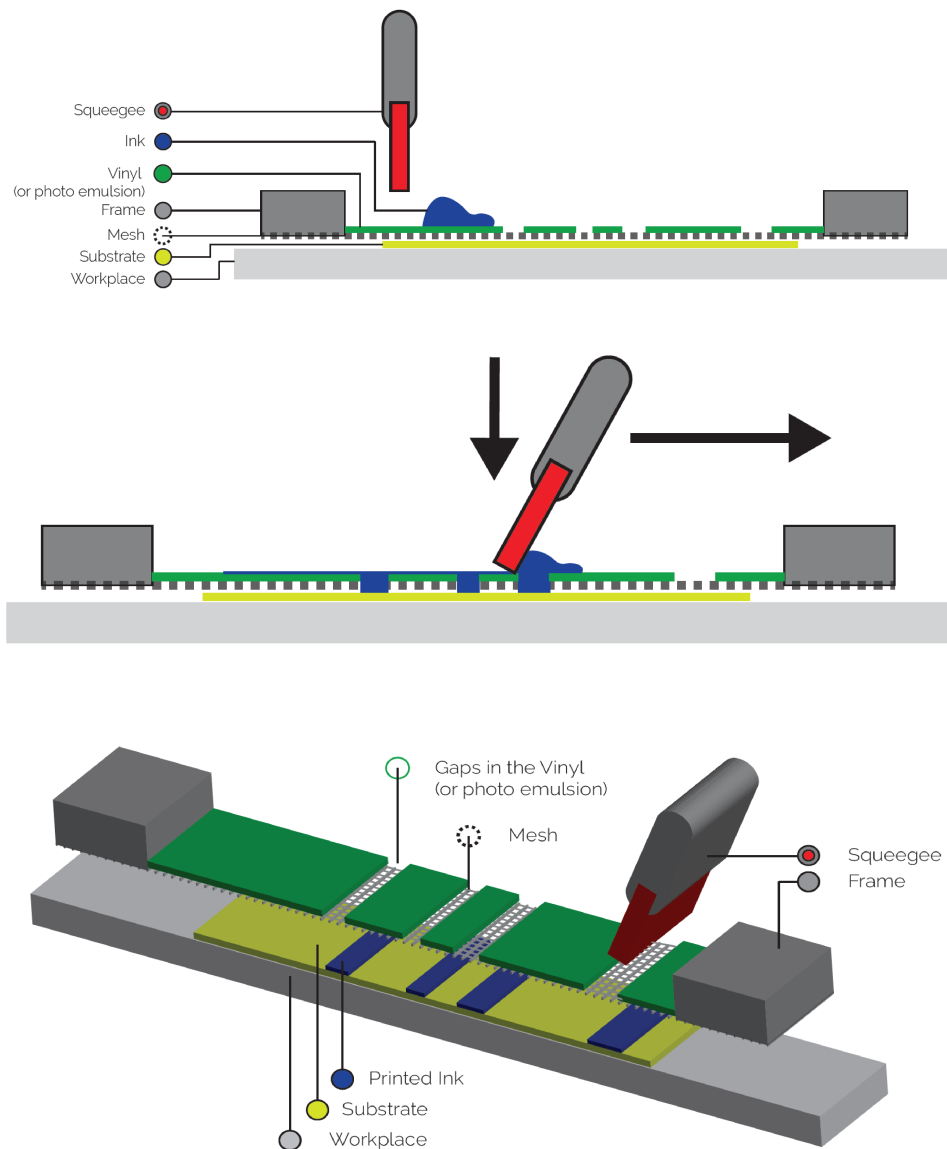
Figure 4.3: Production steps of screen-printing [58].

## 4.1.2. Stencil

The stencil is created from vinyl, and the shapes are created using a vinyl plotter. An example of the different layers is illustrated in figures 4.4 - 4.7. The vinyl stencil in version V2 and V3 is designed to have the patterns of multiple sensors next to each other, to make multiple sensors at the same time. It is important to clean the screen in time before the ink is dried in the screen, making the screen unusable. Since some inks can dry in a few minutes, it is the best to make only one squeegee smearing motion and cleaning directly afterwards. Therefore, not more than five sensors are placed in a row since this is the maximum with which can be covered with a single squeegee smearing motion.
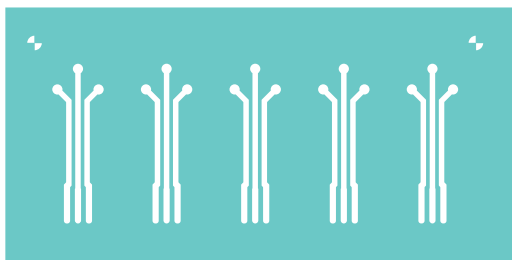
Figure 4.4: Screen-printing layer 1 of sensor design V3.

Figure 4.6: Screen-printing layer 2 of sensor design V3.

Figure 4.5: Screen-printing layer 3 of sensor design V3.

Figure 4.7: Screen-printing layer 4 of sensor design V3.

### 4.1.3. Substrate

In the datasheets of the inks, the following substrates are advised: Polyester, PVC, Polycarbonate or ceramic. In literature, Polyethylene Terephthalate (PET) is also used multiple times. Furthermore, a company specialised in screen-printing of electronic circuits, Metafas, advised using a modified PET sheet (personal communication). The modified PET and in addition, PVC, ITO coated PET and Polypropylene sheets were tested. The quality of the substrate was tested on the following items:

- Flexibility

- Box-oven heat resistance

- Adhesion of ink on the substrate

The flexibility was in all the materials good enough for the application in a sweat sensor where it should be possible to slightly bend it to shape it to fit for example better on the arm of the patient. The heat resistance in the box-oven was only insufficient for the PVC substrate. The results of the adhesion differed between the substrates. The adhesion was tested by placing and removing tape on the screen-printed samples with Silver/Silver-Chloride (Ag/AgCl) (60:40) ink. The residue of the ink on the substrate is an indicator for the adhesion level. Furthermore, the screen-printed samples were tested in water and on scratching with a thick needle. The results are summarised in table 4.1.

Table 4.1: Substrate flexibility, heat resistance and adhesion test results.

| Substrate | Flexibility | Box-oven 60 °C | Box-oven 80 °C | Box-oven 100 °C | Tape-test after 80 °C box-oven | Scratching-test | Water resistance |
|---|---|---|---|---|---|---|---|
| PVC | ✓ | Little deformation | Deformation | Deformation | ++ | + | ++ |
| ITO coated PET | ✓ | ✓ | ✓ | ✓ | - | + | ++ |
| Polypropylene | ✓ | ✓ | ✓ | Little deformation | − | − | - |
| Polypropylene with adhesion promoter | ✓ | ✓ | ✓ | Little deformation | + | - | + |
| Modified PET (Metafas) | ✓ | ✓ | ✓ | ✓ | + | + | ++ |
| PEEK | ✗ | ✓ | ✓ | ✓ | ++ | + | ++ |

### 4.1.4. Screen-printing ink

A drawback of using screen-printed electronics is related to the limited availability of suitable materials. Traditionally, enabling the functionality of printing inks requires thermal curing at high temperatures, which limits the usage of temperature-sensitive materials, such as polymers [59]. However, much more inks are becoming commercially available in the last years. The inks needed for this research are also available commercially. However, the exact qualities and costs of the inks differ a lot from each other.

Typical indicators used to determine the quality of the screen-printing inks are:

- Conductivity, in ohm per square ($\Omega/\square$)

- Adhesion strength

- Ink coverage

In this research, the adhesion strength and paint coverage are considered most important. The conductivity is less relevant for this study since the sensor is based on a voltage measurement in which the current is very low, as will be explained in chapter 5. Since the sensor is used in a watery environment, the inks should be water-resistant, and water should not influence the adhesion as mentioned in section 4.1.3. In screen-printing, it is possible to add multiple ink layers on top of each other in case the coverage is not good enough. However, time and quality-wise it is requested to have a good ink coverage.

The inks described in table 4.2 are commercially available. From all the inks, the cost, information- and or datasheet were requested. Furthermore, M.A.G. Zevenbergen author of [46] and researcher at imec, has been asked to advise on the Ag/AgCl ink based on his experience. Zevenbergen advised using Ag/AgCl ink with high concentration for AgCl. The ink from SunChemical (Gwent group) with 40:60 ratio and 60:40 was selected based on the Ag/AgCl ratio, the availability and costs.

Table 4.2: Overview commercially available inks useful in this research.

| Ink | Manufacturer | Package | Costs | Delivery time | Comment |
|---|---|---|---|---|---|
| Ag/AgCl 32/68 | Dupont | 100 g | €514 | 8 weeks | Advised by M.A.G. Zevenbergen, author of [46] |
| Ag/AgCl 65/35 | Dupont | 100 g | €433 | 8 weeks | |
| Ag/AgCl 40/60 | SunChemical | 200 g | €355 | 4 weeks | |
| Ag/AgCl 60/40 | SunChemical | 200 g | €355 | 4 weeks | |
| Ag/AgCl | Ercon | ? | ? | ? | Was not possible to get in contact |
| Ag/AgCl 50/50 | Applied Ink Solution | 100 g | €262.80 | 4 weeks | |
| Ag/AgCl 3/2 | Henkel | 400 g | €653.80 | 8 weeks | |
| Ag | Dupont | 100 g | N/A | N/A | Available at TU Delft |
| Ag | SunChemical | 200 g | €355 | 4 weeks | |
| Carbon | Dycotec Materials | 100 | €255 | 4 weeks | |
| Carbon | SunChemical | 200 g | €355 | 4 weeks | |
| Carbon | Ercon | ? | ? | ? | Was not possible to get in contact |
| Dielectric | SunChemical | 400 g | N/A | N/A | Available at TU Delft |

Blue highlighted was used in this study

The inks were tested for their qualities. The results are shown in table 4.3. Especially, the ink coverage showed significant differences between the different inks. The dielectric ink did need overall at least three layers to make a complete coverage. Furthermore, after applying the ink and removing the screen from the substrate, small bubbles between the substrate and the ink formed. The bubbles were mainly caused due to the stickiness of the ink, possibly due to the expired shelf life of these inks. The ink stuck to the screen when the screen was lifted, making it possible for air to get under the ink. The stickiness of the ink was partly solved by adding solvent to the ink to make it less sticky and by using a new, less contaminated screen.

Table 4.3: Overview inks used and tested.

| Ink | Manufacturer | Product code | Production year | Conductivity (datasheet) | Adhesion | Ink coverage, min. layers | Hazard |
|---|---|---|---|---|---|---|---|
| Ag | Dupont | LuxPrint 9145 | 2015 | ≤50 mΩ/□ | ++ | 1 | |
| Ag/AgCl 40:60 | SunChemical | C2040308P2 | 2018 | ≤5 Ω/□ @ 25$\mu$m | + | 2 | ✖ |
| Ag/AgCl 60:40 | SunChemical | C2040308P3 | 2018 | ≤5 Ω/□ @ 25$\mu$m | + | 2 | ✖ |
| Carbon | SunChemcial | C2030519P4 | 2018 | ≤75 Ω/□ @ 25$\mu$m | + | 2 | ◇ ◈ ✖ |
| Dielectric | SunChemical | D2080121P12 | 2016 | | + | 3 | |
| Dielectric | SunChemical | D2080121P12 | 2018 | | – | 3 | |



Figure 4.8: Bubble formation in dielectric ink.

## 4.2. Chemical modification

After screen-printing, the sensor is not functional yet. To make the sensor functional, the membrane for the reference electrode and the sodium selective electrode have to be placed. Both membranes have a gel-like structure. The reference membrane holds a high salt concentration. The sodium selective membrane holds Sodium Ionophore X. In the following sections, a more detailed explanation of the chemicals and production steps will be discussed.

### 4.2.1. Reference electrode

As described in section 2.4, the standard reference electrode is built with a reference electrode placed in a known electrolyte solution, for example, a saturated NaCl or KCl solution. The membrane holds a high salt concentration to create a redox reaction at the electrode with saturated salt conditions. This is causing a potential, as can be seen in equation 4.1 - 4.3. The potential of the electrode will be stable as long as the electrode is covered with the saturated salt solution.

$$Ag^+_{(aq)} + e^- \rightleftharpoons Ag_{(s)} \tag{4.1}$$

$$Ag^+_{(aq)} + Cl^-_{(aq)} \rightleftharpoons Ag_{(s)} \tag{4.2}$$

The electrode potential is defined by the Nernst equation, which is modified for this specific electrode for moderate chloride concentrations as eq. 4.3 [60].

$$E = E^0 - 2.303 \frac{RT}{nF} log([Cl^-]) \tag{4.3}$$

The term 2.303(RT/nF) is temperature dependent and thus the Ag/AgCl electrode in theory, exhibits a typical susceptibility of -59.16$mV/pCl$ at a temperature of 25°C.

A commercially available reference electrode is illustrated in figure 4.9. However, in screen-printing, it is hard to place the electrode in an aqueous salt solution due to size and flexibility. A better implementation

is the usage of a gel saturated with salt. In literature, multiple methods are described. However, only a few papers explain in detail how their reference electrode is performing, see table 4.4 for an overview. It should be remarked that in the different papers also different techniques and qualifications tests are used for indicating the performance of the sensors, which makes it hard to compare. This is explained in more detail in chapter 10.



Figure 4.9: Commercially available reference electrode for use on all electrochemical cells filled with a electrolyte solution [61].

Table 4.4: Reported screen-printed reference electrode techniques in sweat applications.

| Electrode ink | Substrate | Reference membrane composition | Cl$^-$ response (mV (log a$_{cl}$)$^{-1}$ | Stability (mV h$^{-1}$) | Stability time tested | Application time tested | Conditioning | Reconditioning | Application | Ref. |
|---|---|---|---|---|---|---|---|---|---|---|
| Ag/AgCl | PET | pHEMA hydrogel, 3M KCl | 2 | 0.001 | 1 week | 1 hour | 24 hours | - | Patch | [46] |
| Ag/AgCl | Adhesive film | Agarose hydrogel, 0.5M NaCl, PVC film | -1.7 ± 1.2 | 4 | 1 h | - | - | - | Patch | [62] |
| Ag/AgCl | PET, textile, tattoo paper | PVB, NaCl | 0.2 ± 1 | 0.09 ± 0.03 | 3 weeks, 4 months (shelf life) | 1 h | 12 h | 10-30 min | Patch, sweatband, textile, tattoo paper | [48] [49] [47] |
| Carbon | PET | HMIM-FAP, PMMA-co-BMA, DEHP | - | 0.2-0.4 | - | 1 h | 2 h | - | Patch, sweatband | [63] |
| Ag/AgCl | PET | PVB, NaCl | - | <5% in 2 weeks | 2 weeks | 1 h | 1 h | 1 h | Patch | [31] |
| Ag/AgCl | PDMS | Agarose hydrogel, 1M KCl | - | 2.92 | 24 h | 1 h | - | - | Patch | [64] |

Stability = stability in test solution, also called *static system stability*; PET = Polyethylene Terephthalate; pHEMA = 2-hydroxyethyl methacrylate (HEMA), 2 g polyvinylpyrolidone K-90 (PVP K-90), 0.8 g 2,2-dimethoxy-2-phenylacetophenone (DMPAP) and 0.1 g ethyleneglycol dimethacrylate; CNTs = Carbon nanotubes; PMMA-co-BMA = poly(methylmethacrylate-co-butylmethacrylate; PVB = polyvinyl butyral.
Blue highlighted was used in this study

From table 4.4, it can be concluded that for the first and third reference electrode method, based on a pHEMA and PVB membrane respectively, most details are known. Furthermore, the results concerning the stability and application are promising. The other described options are less stable or were not performing as good as the first and third option. Therefore, only the pHEMA and PVB reference gels were researched in more detail concerning production and cost. The production of both membranes consists of the mixing of the chemicals mentioned in table 4.5.

The material cost for both membrane types are illustrated in table 4.5 and are based on prices from Sigma Aldrich in February 2019. Since PVB scores better on costs, production steps and stability over time, it was decided to use this membrane during this project.

Table 4.5: pHEMA and PVB membrane material costs at Sigma Aldrich.

| Membrane | Material | Amount needed | Package |
|---|---|---|---|
| pHEMA | 2-Hydroxyethyl methacrylate | 20 mg | 500 g |
| | Polyvinylpyrolidone K-90 (PVP K-90) | 2 mg | 250 g |
| | 2,2-Dimethoxy-2-phenylacetophenone | 0.m8 g | 50 g |
| | Ethylene glycol dimethacrylate | 0.1 mg | 100 ml |
| | O-ring | 1 | 1 |
| | 3M Scotch Weld Epoxy DP460 | - | 50 g |
| | KCl 3M | - | 250 ml |
| | **Total costs** | | **€230.00** |
| | | | |
| PVB | Polyvinyl butyral resin BUTVARs B-98 (PVB) | 78.1 mg | 100 g |
| | Methanol | 5 ml | 1 l |
| | NaCl | | 500 g |
| | **Total** | | **€81.30** |

## 4.2.2. Production of PVB reference membrane

The production steps for the PVB membrane are described below [48] [49]:

Step 1: A 10 wt.% of stock solution of PVB is prepared by dissolving $78.1 mg$ of PVB and $50 mg$ NaCl in 5 ml of methanol to create the reference cocktail

Step 2: An ultrasonic bath is used to achieve a homogenous solution

Step 3: The stock solution is stored at 7 °C in order to prevent the evaporation of the solvent.

Step 4: Drop-cast $4 \mu l$ of the reference cocktail on top of of the Ag/AgCl reference electrode

Step 5: Dry overnight before use

As can be seen in table 4.6, the usage of methanol has some hazards. Therefore, the following measures are taken during the production:

• Working in a fumehood

• Using a AXBEK respirator in case of failure of fumehood without flow alarm

• Using gloves from butyl rubber with a thickness of minimal $0.3 mm$

• Wearing safety glasses

• Wearing a laboratory suit

In the first experiments, the chemicals were mixed with a spoon. However, the material did cloth to the spoon, making it hard to dissolve in the solution. To optimise the stirring, an ultrasonic bath was used. This resulted in a more homogenous solution. As solvent, both methanol and ethanol is used for solving the PVB and sodium chloride salt (NaCl). The PVB did not dissolve completely in the ethanol, but was forming a more solid gel structure making it hard to drop-cast. Furthermore, after drop-casting the membrane, multiple bubbles were formed, as illustrated in figure 4.10. With the usage of methanol, PVB and NaCl dissolved better, making it also easier to drop-cast on the electrode with less bubbles. To decrease the bubble formation, the particle size of the NaCl was decreased by using a mortar and pestle. The smaller particle size resulted in a better mix of PVB and NaCl and fewer bubbles, this technique is used in sensor prototype V3.

Figure 4.10: Bubbles formed in PVB reference membrane.

Table 4.6: Chemical materials used to adjust screen-printed electrodes for potentiometry.

| Material | Manufacturer | Product code Sigma Aldrich | Internal available | Package | Costs | Hazards |
|---|---|---|---|---|---|---|
| Polyvinyl Butyral (PVB) | Sigma Aldrich | P110010 | ✕ | 100 g | €25.50 | - |
| Methanol | Sigma Aldrich | 34860 | ✕ | 1L | €30.30 | ◇ ◇ ◇ |
| Sodium chloride (NaCl) | Sigma Aldrich | 746398 | ✕ | 500 g | €25.50 | - |

### 4.2.3. Ion-selective electrodes

As explained before, the sensing electrode has to be placed in the solution under test, in this case, sweat. In literature, multiple types of sensing electrode techniques with screen-printing are described. Some are tested already in detail in sweat applications, while from others almost all of the needed information is missing. The most promising studies related to the application and information available are described in table 4.8. This table also contains studies which are not based on screen-printing. However, sensing electrodes mentioned in table 4.8 can be manufactured by screen-printing techniques.

All sensing electrodes described in table 4.8 have been tested in real-time applications, except two. As can be seen, most sensors are only tested in a period between 30 and 60 minutes in their application as a sweat sensor. The period of 30 to 60 minutes is typical for exercise tests, such as cycling activities. Sweat production is high during exercise tests, which makes it measurable. However, stimulation of sweat production by exercise is not realistic for the application of patient monitoring for 24 hours. Therefore, ion-selective electrodes should work with small amount of sweat samples, for example obtained via artificially sweat stimulation. Unfortunately, most papers did not provide information about the minimum sweat volume for reliable measurements, which make it not doable to compare between ion-selective electrodes on this specification.

As described in section 2.4.1, ionophores are used to make electrodes selective to some ions. For the measurements of chloride concentration an ionophore is not needed since Ag/AgCl ink is already selective to chloride ions. For the measurements of sodium concentration the mostly used ionophore is *Sodium Ionophore X*, as can be seen in 4.8. The principle of the ionophore is based on the charge separations between the organic phase (membrane) and the aqueous phase (sample) [49].

In this project, Sodium Ionophore X, also known as 4-tert-Butylcalix[4]arene-tetraacetic acid tetraethyl ester, was used as ionophore for the sodium selective electrode. Since it has the best stability, selectivity and best explanations of the production steps compared to the other options described in literature. The costs of the ionophore and exact composition can differ a lot between brands as can be seen in table 4.7. In this table, the first part is based on the chemical composition described in most papers ([31][43][49][50]) while the second part was described in 2 papers ([65], [66]). In the second part, a cheaper version of the Sodium Ionophore X is used. The cheaper one is from Sigma Aldrich itself, while the official Sodium Ionophore X is from Supelco, a subsidiary company from Sigma Aldrich. The composition and results of the Sigma Aldrich version are comparable with the Supelco version [65]. However, in literature, the Sigma Aldrich version was not used in the composition described in the first part of the table. Nevertheless, it was decided to use the Sigma Aldrich version based on the costs. Furthermore, it was decided to use the composition described in the second part of table 4.7 since this would make it possible to compare the obtained results with the results in literature were the same chemical composition is used.

Table 4.7: Chemical materials used to create the sodium-selective membrane.

| Material | Manufacturer | Product code Sigma Aldrich | Purpose | Package | Hazards |
|---|---|---|---|---|---|
| Selectrophore Ionophore X | Supelco | 71747 | Ionophore | 50 mg | - |
| Bis(2-ethylhexyl) sebacate (DOS) | Supelco | 84818 | Plasticizer | 5 mL | - |
| Na-TFPB | Sigma Aldrich | 692360 | Catalyzer | 250 mg | - |
| Polyvinyl chloride (PVC) | Supelco | 81392 | Structure | 1 g | - |
| Tetrahydrofuran (THF) | Supelco | 87369 | Solvent | 10 ml | ⚠️ ⚠️ ⚠️ |
| **Total** | | | | **€356.60** | |
| | | | | | |
| 4-tert-Butylcalix[4]arenetetraacetic acid tetraethyl ester | Sigma Aldrich | 420484 | Ionophore | 250 mg | - |
| Potassium tetrakis(4-chlorophenyl)borate (KtCB) | Supelco | 60591 | Fluorescent optode | 100 mg | ⚠️ |
| 2-Nitrophenyl octyl ether (NPOE) | Supelco | 73732 | Solvent | 5 ml | - |
| Polyvinyl chloride (PVC) | Supelco | 81392 | Structure | 1 g | - |
| Tetrahydrofuran (THF) | Supelco | 87369 | Solvent | 10 ml | ⚠️ ⚠️ ⚠️ |
| **Total** | | | | **€240.70** | |

Table 4.8: Reported sensing electrode techniques in sweat applications.

| Application | Ion Analyte | ISE Membrane | Working range (mM l$^{-1}$) | Sensitivity (mV (log a$_i$)$^{-1}$) | Drift (mV h$^{-1}$) | Stability tested | Application time tested (h) | Response time (s) | Ref. |
|---|---|---|---|---|---|---|---|---|---|
| Epidermal patch | Cl$^-$ | | 10-150 | 52.8 ± 0.7 | 0.3mM h$^{-1}$ | 12h | 60 min | 2 | [67] [68] [64] |
| Epidermal patch | Cl$^-$ | | 1-3000 | 58.5 ± 0.5 | 0.001 h$^{-1}$ | 17h | 60 min | 3 | [46] [69] [70] [71] |
| Epidermal patch | Cl$^-$ Na$^+$ | Sodium ionophore X | 10-160 | 63.2, 55.1 | - | 2 weeks | 60 min | - | [31] |
| Epidermal patch | Na$^+$ K$^+$ | Sodium ionophore X, valinomycin | 10-160, 1-32 | 64.2 (RSD = 1%)/61.3 (RSD = 1%) | 2-3 h$^{-1}$ | 4 weeks | 23 min | - | [43] |
| Epidermal patch | Cl$^-$ | | 10-100 | 65 ± 4 | 6.3 ± 0.9 | 200 min | 5 min | - | [72] |
| Epidermal patch | K$^+$ NH$_4^+$ Cu$^{2+}$ Ag$^+$ | Valinomycin, nonactin, Cu$_2$S Ag$_2$S | - | - | - | - | - | - | [73] |
| Epidermal patch | Na$^+$ | 2-Nitrophenyl octylether | - | 56 ± 1 | - | 5 weeks | 100 min | - | [65] |
| Epidermal patch | Na$^+$ | Sodium ionophore X | 10-90 | 57 ± 3 | - | 45 min | - | 30 | [50] |
| Epidermal patch | Na$^+$ | 2-Nitrophenyl octyl ether | 20-100 | 50 | - | 3 h | 55 min | - | [74] |
| Tattoo | Na$^+$ | Sodium ionophore X | 0.1-100 | 63.75 mV ± 5.77% | 2.8 | 36 min | 3 weeks | 10 | [49] |
| Tattoo | NH$_4^+$ | Nonactin | 0.1-100 | 57.5 ± 1.4 | - | - | 36 min | 5 | [47] |

Blue highlighted was used in this study

### 4.2.4. Production of sodium selective membrane
The production steps for the sodium selective membrane with the materials mentioned in table 4.7 are described below [65][46][49][66]:

Step 1: Mix $1mg$ of the sodium ionophore with $0.3mg$ KtCB, $95mg$ NPOE, $47mg$ PVC, and $1mL$ THF

Step 2: An ultrasonic bath is used to achieve a homogeneous solution

Step 3: Drop-cast the sodium selective membrane on top of of the carbon electrode

Step 4: Dry overnight before use

As can be seen in table 4.7, the usage of Tetrahydrofuran (THF) has some hazards. Therefore, the following measures are taken during the production:

- Working in a fumehood

- using a AXBEK respirator in case of failure of fumehood without flow alarm

- Using gloves from butyl rubber with a thickness of minimal $0.3mm$

- Wearing safety glasses

- Wearing a laboratory suit

The mixing of the chemicals and drop-casting was easier compared to the PVB membrane since the chemicals dissolved better. However, the weighing error was more significant due to the small amount of Sodium Ionophore X and KtCB. Compared to the PVB membrane, this membrane structure is more like a gel with a thin protecting layer, where the PVB membrane is a more solid structure. Drop-casting the membrane with too much of THF could result in the dissolving of the carbon ink. Therefore, only the minimal required amount of THF was used to dissolve the materials.

## 4.3. Prototypes

During this study, three prototypes have been developed. The design of each prototype is explained in the following sections.

### 4.3.1. Sensor V1

The first prototype of the sensor, Sensor V1, was built at the start of the thesis research. This was useful to practice and understand the principles and tricks of screen-printing and working with the chemicals. Furthermore, this design is used in the first tests to see if it is possible to obtain results comparable to those from literature.

Sensor design V1 consists out of 3 electrodes, the reference sensor in the middle, the chloride selective electrode left and the sodium selective electrode right, as can be seen in figure 4.11.

The substrate used was a PVC sheet. The choice to start with the usage of PVC was based on the recommendations in the datasheet of the used inks. Also, the box-oven temperature used was based on the advised temperatures mentioned in the datasheets of the used inks. However, the first prototype bended due to the box-oven temperature of 80 °C. To avoid bending of the PVC, it is necessary to use lower temperatures than advised in the datasheet.
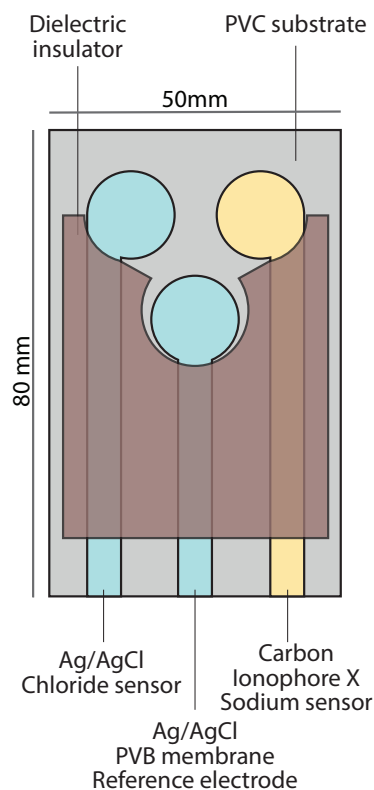


Figure 4.11: Sensor prototype V1.

The size of sensor V1 is, with a size of 8 $cm$ by 5 $cm$, relatively large. The reason to start with a large size prototype of the sensor was to make the alignment and visual check easier.

Due to the distance between the tracks and the width of the tracks, it is possible to use a regular (toothless) alligator clip as the connector. The connectors are wired to the read-out circuit which is discussed in chapter 5.

From the first prototype, it was concluded that design-wise the following items had to be changed:

- Sharp edges in the vinyl design had to be removed.

- Smaller electrode to improve coverage of electrode with the PVB membrane had to be used.

- Substrate that can handle higher temperatures in the box-oven, at least 80 °C had to be used.

- Alignment indicators had to be defined.

### 4.3.2. Sensor V2

Whereas version V1 was used for comparing results with literature, version V2 was designed to improve version V1 and to avoid the practical problems from the first version for obtaining more reliable results.

The main design differences can be found in size and rounding of the edges. The usage of sensors of the size $8cm$ by $5cm$ appeared to be impractical in the measurement setup in which the sensor is immersed in beakers with different salt concentrations. Therefore, the size was decreased to 60% of the size of V1. The round edges improved the cutting precision.

Indium Tin Oxide (ITO) coated PET was used instead of the PVC substrate to avoid the bending problem. The ITO layer (conducting layer) was not used since this would require a significant design change. To increase the ink coverage, multiple layers of ink where screen-printed on top of each-other. To avoid offsets between the screen-printing layers, it is required to have a precise placement of the screen related to the substrate. The alignment indicators shown in figure 4.13 were successfully implemented.
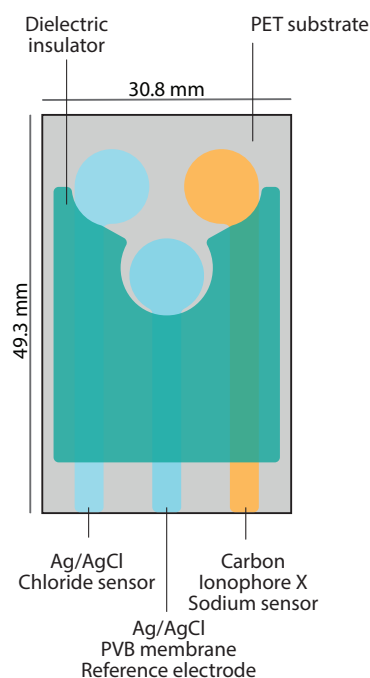
Figure 4.12: Sensor prototype V2.

Problems faced with the design were mainly in the connection with the read-out circuit. In this design toothless alligator clips were used. Nevertheless, the clips were not strong enough to hold the sensor in place. As a consequence, the sensor could get detached from the read-out circuit during the measurements.

From the second prototype, it is concluded that design-wise the following items had to be changed:

- Smaller design to reduce the screen-printing surface

- An option to connect the sensor with a stronger connector instead of alligator clips
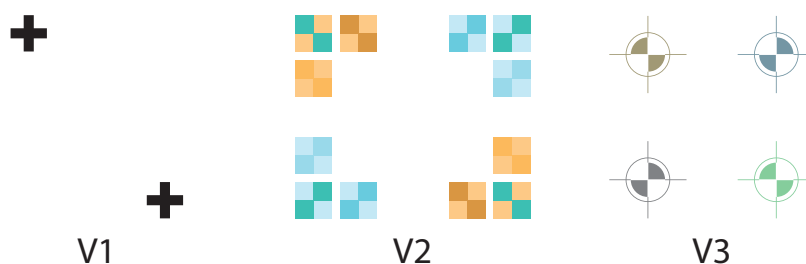
Figure 4.13: Layer alignment indicators used in the prototypes.

### 4.3.3. Sensor V3

For sweat sensor prototype V3 a smaller and more curved design was used. This enables placement in the sample beakers and reduces the screen-printing surface. The modified PET substrate described in section 4.1.3 was used instead of the ITO coated PET, for better adhesion.

The alligator clips were replaced by a Fexible Printed Circuit (FFC) 8-pin connector to connect the sensor to the read-out circuit. The sensor design was adjusted to fit perfectly in the sensor, which resulted in a robust connection. The redesign for the connector is shown in figures 4.15 and 4.16. As can be seen in these figure, pin 3 and 6 are removed from the connector and serve as an isolation barrier. Figure 4.17 presents a picture of the sensor connected in the FFC connector.

To increase the conduction of the conducting tracks, a silver ink layer is used instead of a track from Ag/AgCl ink. To improve the durability of the connector, a carbon layer is added on top of the silver ink around the connector. Without this layer, the silver ink could be scratched of by reconnecting the sensor multiple times.
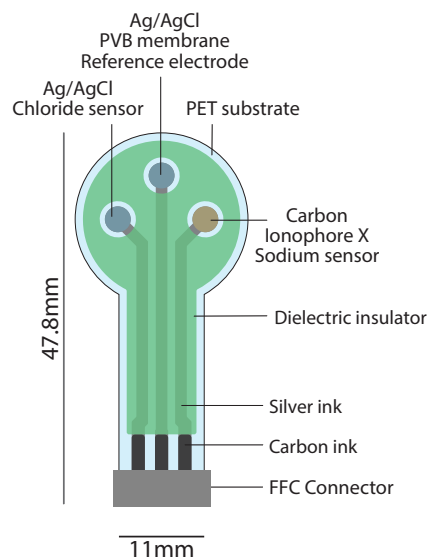
Figure 4.14: Sensor prototype V3.
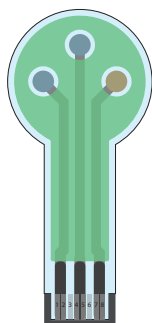
Figure 4.15: FFC 8 pin connector, JST - 08FMN-SMT-A-TF(LF)(SN).
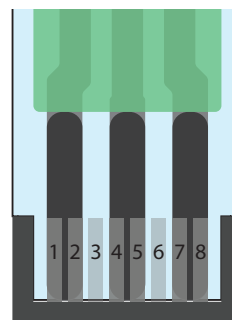
Figure 4.16: Sensor FFC connector, pin 3 and 6 removed for isolation.
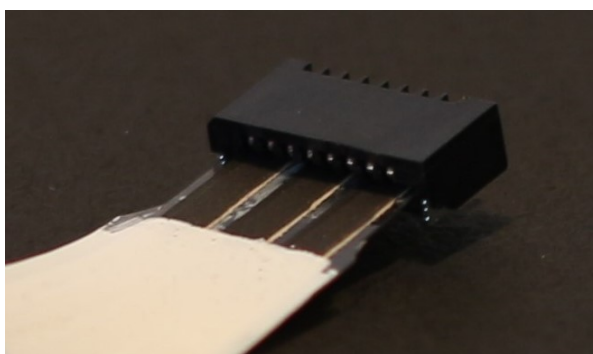
Figure 4.17: Sensor connected in the FFC connector.

In section 4.1.4 it is mentioned that the dielectric was forming air bubbles and required 3 layers ink before proper coverage and thus isolation. Therefore, an other dielectric ink was used in prototype V3. Although the coverage was improved, it started forming cracks after immersing into water. Probably, this is caused due to bending of the sensor after exposing the dielectric ink to water as illustrated in figure 4.18. The tear down in the dielectric caused shorts between the conducting layers once applied to water. Pictures of the

formed cracks are illustrated in figure 4.19. The sensors were heavily damaged due to the cracks. However, the damage was stopped after applying a layer of dielectric ink used in prototype V2, as shown in figure 4.20.
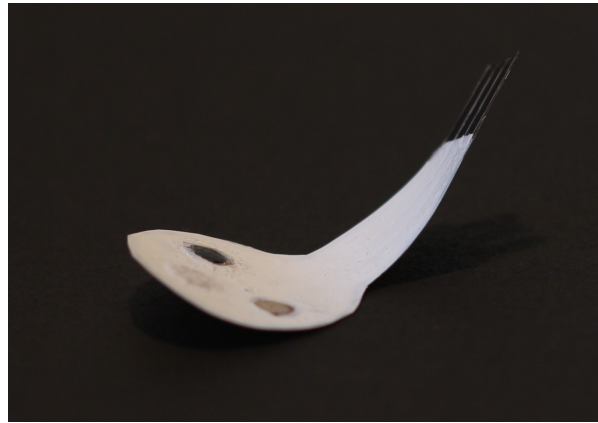


Figure 4.18: Bending of the sensor.
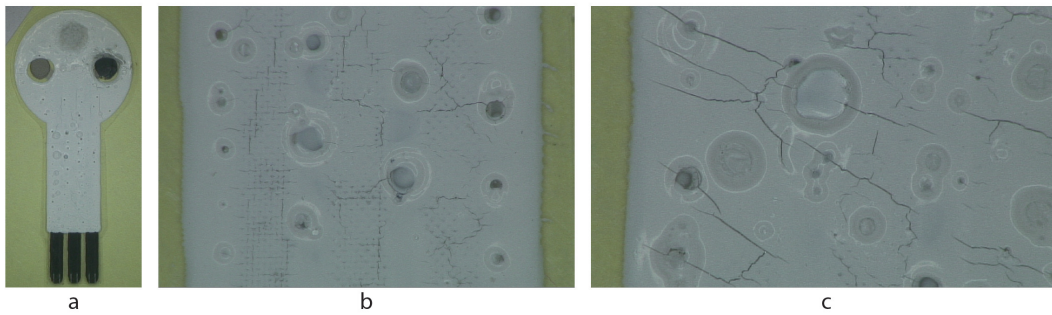


Figure 4.19: Sensor cracks, (a) total sensor, (b) & (c) zoomed in on the cracks.
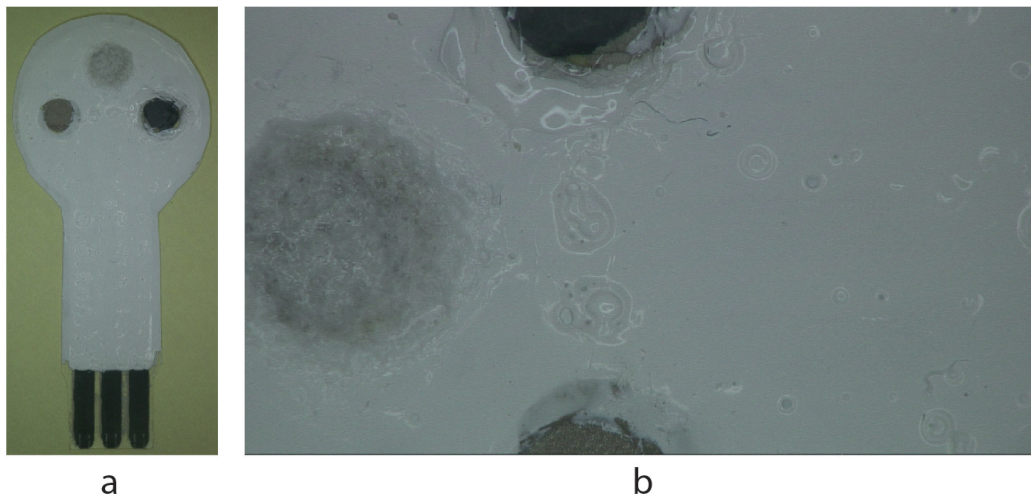


Figure 4.20: Repaired sensors, (a) total sensor, (b) zoomed in on previous cracks.

$5$

# Read-out circuit

The read-out circuit is a crucial part of the sensor system since it directly determines the accuracy of the sensor reading, the interference and the signal to noise ratio of the sensor system. To design an appropriate read-out circuit, it was first necessary to understand and model the electrical qualities of the sweat sensor. However, how the behaviour of the sensor can be modelled was not yet described in detail in literature. To create this model of the sweat sensor, a simple read-out circuit was built and sweat sensor V2 was tested with this circuit to determine the electrical qualities of the sensor. Based on these results, a computer model of the sensor behaviour was built and a circuit was designed to optimise the read-out of the sensor. Furthermore, the circuit was optimised to read-out multiple sweat sensors at the same time.

## 5.1. Design
A voltage measurement setup which only allows a very small current to flow between the reference electrode and the sensing electrode, should be sufficient to measure the potential difference between the reference electrode and the ion-selective electrode from the sweat sensor. To stabilise the output of the sensor and to suppress interference, a low pas filter can be added [50] [31].

The final product of the sweat sensor application should consist out of the parts mentioned in figure 5.1. However, this study focuses only on the parts related to the sensor and its read-out, e.g. the sensor, amplifiers, filter, analog-digital converter (ADC) and microcontroller (MCU). In this study, the data storage, the battery and power supply are not a priority.
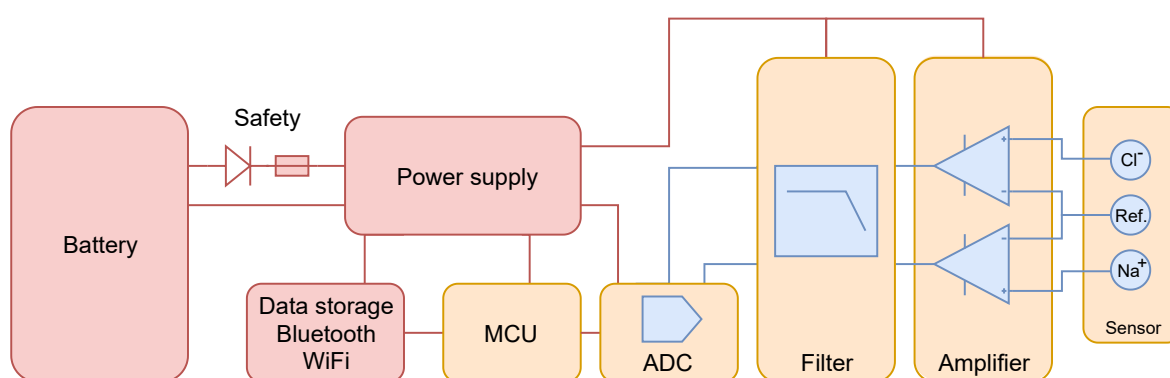


Figure 5.1: Circuit overview of final application.

## 5.2. Single channel circuit

The first designed read-out circuit consisted of a instrumentation amplifier, ADC and a microcontroller. This circuit was designed to read-out one sweat sensor, consisting of a chloride sensor and a sodium sensor. Both sensors share the same reference electrode. The circuit scheme is illustrated in figure 5.2.

The instrumentation amplifier was selected based on the following aspects:

- Variable gain set, 1x - 20x minimum preferred

- Supply voltage range, $5V$ preferred

- Low input voltage noise, below $100nV/\sqrt{Hz}$

- Offset voltage of maximum of $0.25mV$

The AD8422 instrumentation amplifier from Analog Devices meets all the requirements, as can be seen in table 5.1. Furthermore, the AD8422 is used in the read-out circuit from in a screen-printed sodium and chloride sensor designed by Emaminejad *et al.* where the read-out circuit worked successfully [31].

Table 5.1: Specifications AD8422 instrumentation amplifier.

| Specifications | AD8422 |
| --- | --- |
| Manufacturer | Analog Devices |
| Supply voltage min. | +/- 2.3 V |
| Supply voltage max. | +/- 18 V |
| Input voltage noise | 8nV/$\sqrt{\text{Hz}}$ |
| Gain set | Resistor |
| Gain range | 1x -1000x |
| Input bias current max. | 2 nA |
| Vos max. | 25 $\mu$V |
| Available at Farnell | Yes (few) |
| Price | €5.43 |

The ADC was selected on its sample frequency, range and its accuracy. The first read-out design was designed to have a relatively fast sampling frequency for detecting sensor behaviour. In theory, the sensor should almost behave as a dc signal. However, it could be expected that the sensor could have some interference problems around $50Hz$ due to long conducting paths. Therefore, the sample frequency for the first design was chosen to be at least $120Hz$. Since it was unknown in which voltage range the first sensor combinations would operate, an ADC with programmable gain amplifier was preferred since that would make the sensing range more adjustable. Furthermore, an ADC with a minimum accuracy of 12-bit was required. The Texas Instruments ADS1115 perfectly fitted for this application due to the following features:

- Wide range due to programmable gain amplifier (gain of: 2/3, 1, 2, 4, 8, 16)

- 16-bit, resulting in a least significant bit (LSB) between 187.5 $\mu V$ and 7.8125 $\mu V$

- Possibility for 2 differential channels and one Single-Ended channel

- (Easy) controllable via I$^2$C protocol

- Optimised library in Mbed for single differential read-out up to $1kHz$

- Already in house, no delivery delay

Since it was unknown in which range exactly the voltages of the sensor could be exactly expected, it was required to have the capability to read both positive as negative voltages. However, the ADS1115 is a single-supply device. Therefore, the output voltage of the instrumentation amplifier was lifted with a $2.5V$ offset. The $2.5V$ offset was created with a voltage follower after a voltage divider connected to the $5V$. The opamp used was the Microchip MCP6292.

The microcontroller was selected for its capability to read-out the ADC at the required frequency of a minimum of $120Hz$. Since the ADS1115 was selected, the microcontroller should have an I$^2$C bus. To store

the data, a serial connection with a computer was selected above the usage of a SD-card or wireless connection to a computer because of simplicity and speed. The data was sent via UART to the computer, where the incoming data was collected and stored with the usage of Putty.
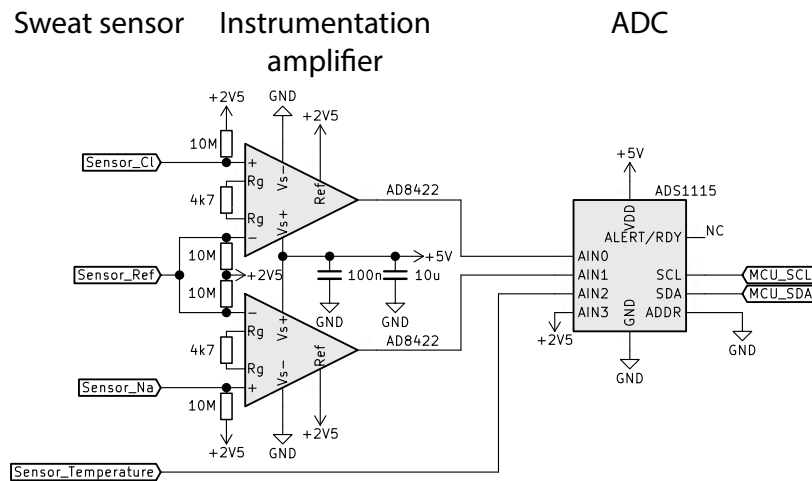


Figure 5.2: Read-out circuit for single sweat sensor.

## 5.3. Electrical sensor model

The single-channel circuit described in the previous section was designed to understand the basic behaviour of the sensor. However, to have a very accurate read-out of the sensor, it is necessary to understand the electrical behaviour of both the sensor as the read-out circuit. As mentioned before, an electrical model of the sweat sensor was needed for this purpose. Since this model of the sensor was not yet described in detail in literature, it was researched in this project.

As explained in previous chapters, the potentiometric sensor basically behaves as two half cells which can be modelled as a battery. In this model, the voltage of the battery depends on the difference in salt concentration between the reference and ion-selective electrode. Furthermore, the voltage of the sensor which can be measured is also dependent on impedance caused by the transition from one part or domain of the sensor to another. For example, the transition in the reference membrane from saturated salt to the Ag/AgCl ink can be modelled as resistance and capacitance in series with the battery. The same goes for the translation from the chemical domain to the electrical domain or the impedance in the wires. An example of this model is illustrated in figure 5.3.
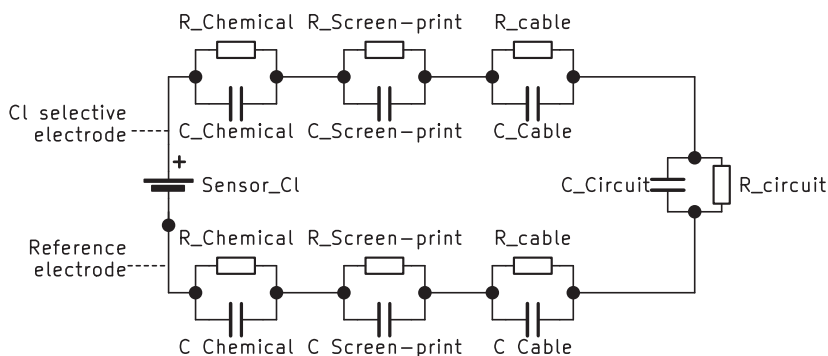


Figure 5.3: Sweat sensor model.

From literature and the first test with the single channel circuit, it was shown that the sensor does not contain high frequency components. In addition, the salt concentrations in sweat changes very slowly. Therefore, it can be concluded that the sweat sensor will have a near DC behaviour, making it not necessary to investigate the high frequency (>10$Hz$) components in this phase of the research. In conclusion, the model can be

simplified to a model with a resistance in series with each half cell. This is shown in the model in figure 5.4. However, reality is more complex since these resistors in series will not be constant and can be influenced by several factors such as:

- Temperature

- Water contact surface of the electrodes/membranes

- Gas bubbles at the interface

- Size of the reference membrane

- Consistency of the reference membrane

- Size of the electrodes

- Ratio of Ag:AgCl in the ink

- Ink thickness

- Conduction path length

Since these factors will differ between each sensor and application, it is not necessary to know their exact values but it would be useful to get an impression of the order of magnitude of the series resistance.
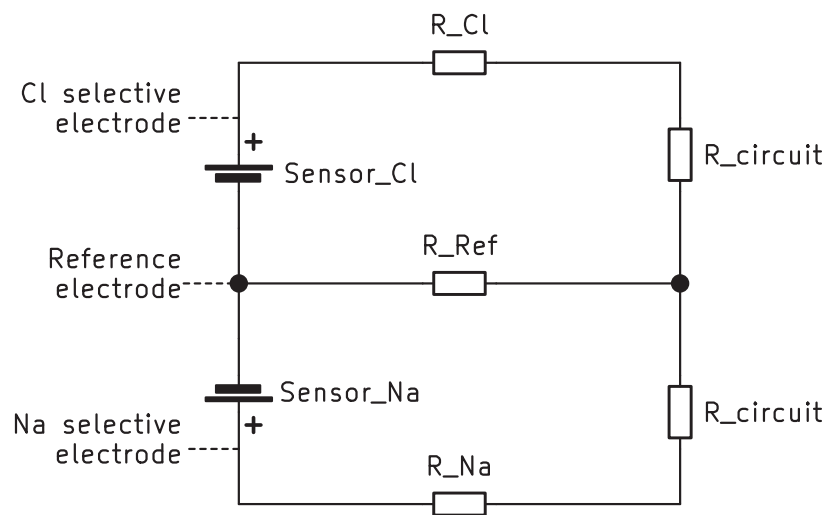


Figure 5.4: Sweat sensor model simplified.

The magnitude the series resistance can not be measured with a standard resistance measurement since the resistance is integrated in the battery. Therefore, a measurement setup was built in which resistances with different values are switched in series with the sensor, as illustrated in figure 5.5. Resistance $Rs$ isv ideally very low, resulting in a low voltage drop on the resistance. However, in case $Rs$ as large as $Rn$ or even larger, the voltage drop over $Rs$ will become significant.
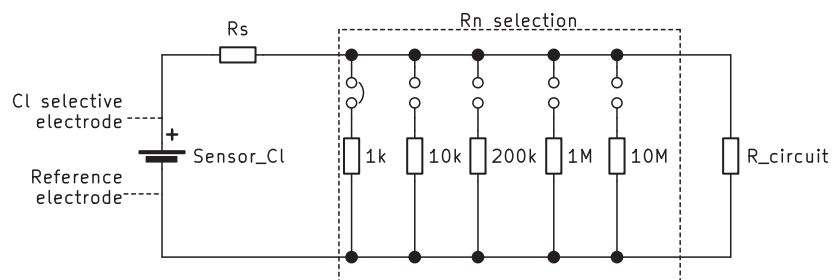


Figure 5.5: Sweat sensor circuit with Rn selection.

An example of the influence of $Rn$ on the output is shown in figure 5.6. As can be seen, the voltage is only severely influenced if $Rn$ is above 1 MΩ. However, for lower values of $Rn$, it is clear that the voltage drop over $Rs$ is large, indicating a $Rs$ value between 200 kΩ and 10 kΩ.
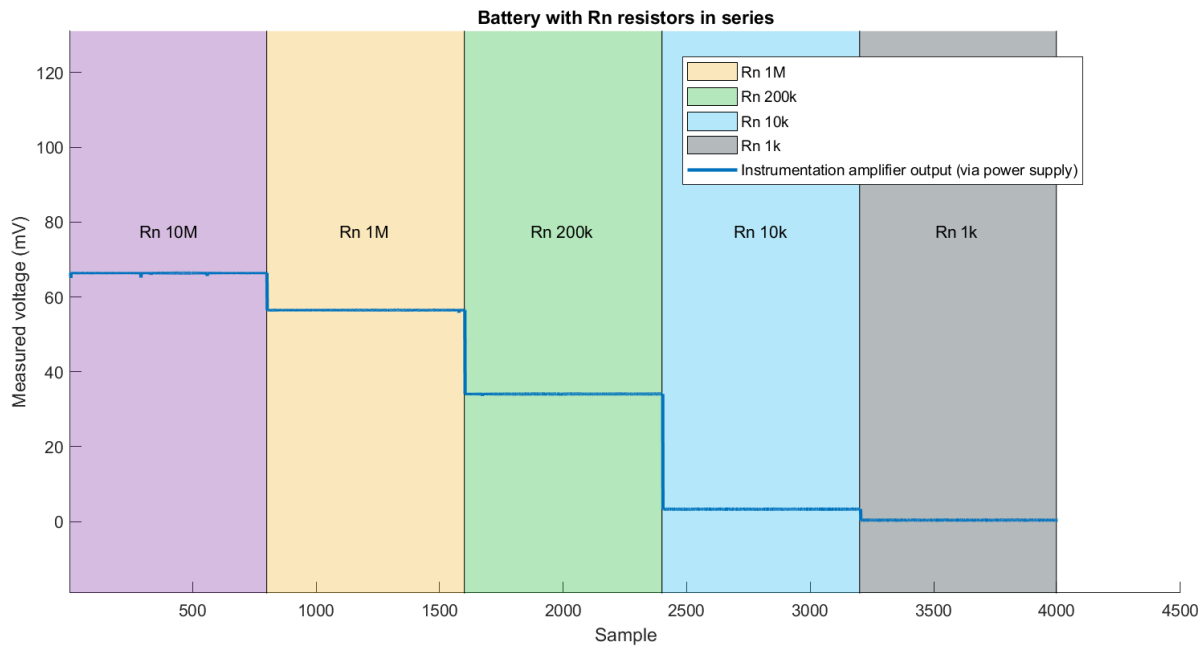


Figure 5.6: Output under different values of Rn in series with battery.

The influence of $Rs$ on the sensor read-out is strongly dependent on $R_{circuit}$. The value of $R_{circuit}$ is in the ideal situation infinitely large. However, in practice the value is not infinitely due to properties of the instrumentation amplifier. The DC error sources can influence the results significantly [75]. The DC error sources from the amplifier are shown in figure 5.7, input bias current $I_{bias1}$ and $I_{bias2}$ are not equal which results in an offset current. Especially, the input bias currents can influence the results, since this can form a voltage error in combination with the sensor resistance $Rs$ which can be large in this application.
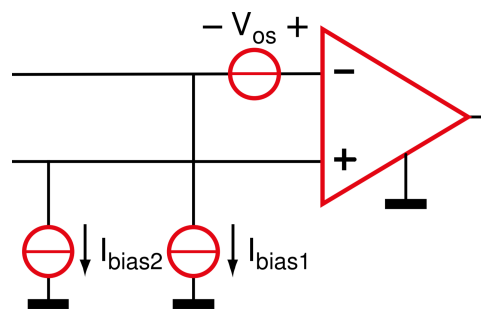


Figure 5.7: Modelling of DC Errors [75].

To increase the model accuracy, the model was extended with the influence of the bias currents and offset voltage. The bias current from the used instrumentation amplifier was measured, as shown in figure 5.8. The bias currents and offset voltage measured are presented in table 5.2.
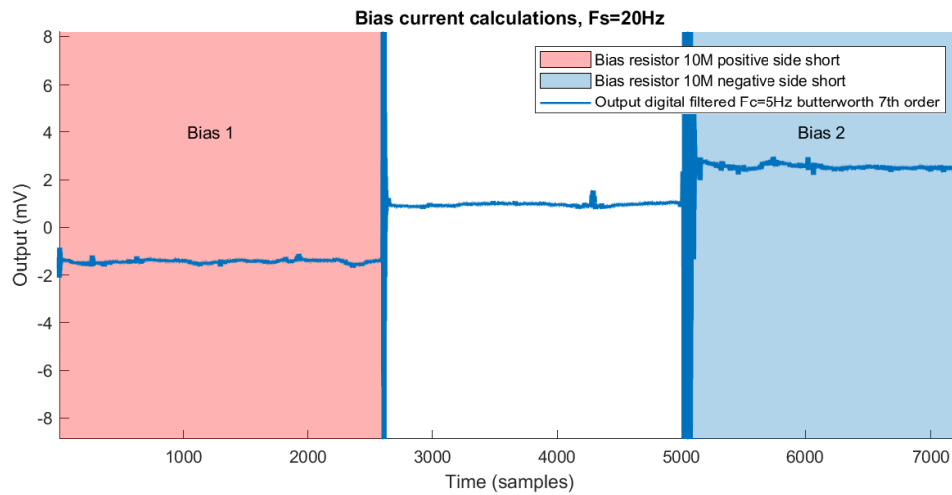
Figure 5.8: Read-out circuit calculated bias current.

Table 5.2: Input bias current and offset voltage of AD8422.

| Parameter | Value |
|---|---|
| Following datasheet $I_{bias}$ typ. | 0.5 nA |
| Following datasheet $I_{bias}$ max | 2 nA |
| $I_{bias_1}$ | -0.142 nA |
| $I_{bias_2}$ | 0.204 nA |
| $I_{bias_{offset}}$ | 0.162 nA |
| Following datasheet $V_{os}$ max | 70 $\mu$V |
| $V_{os}$ | 40 $\mu$V |

With the bias current known, it became possible to calculate the model values with different $Rs$ and $Rn$ values. To check whether the model is calculated correctly, a test setup with a battery was built and tested in the model. The test setup is shown in figure 5.9. The $Rn$ values were switched with the same values as the sweat sensor setup from figure 5.5. The results of the battery test setup and the sweat sensor were plotted against the model. The battery test setup matched indeed with the model. In figure 5.10, the model output for multiple values of $R_s$ is plotted against different $R_n$ values. As can be seen, the modelled output around $200k\Omega$ for $R_s$ match with the measurements from the battery circuit in which a $200k\Omega \pm 5\%$ resistor was used for $R_s$. The results of the sweat sensor compared to the model are shown in figure 5.11.
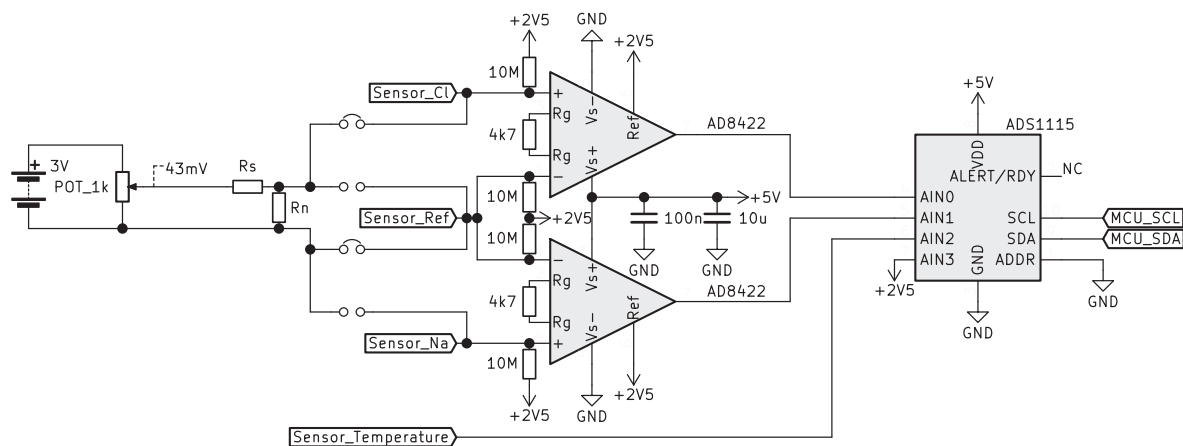


Figure 5.9: Battery circuit with Rn selection.
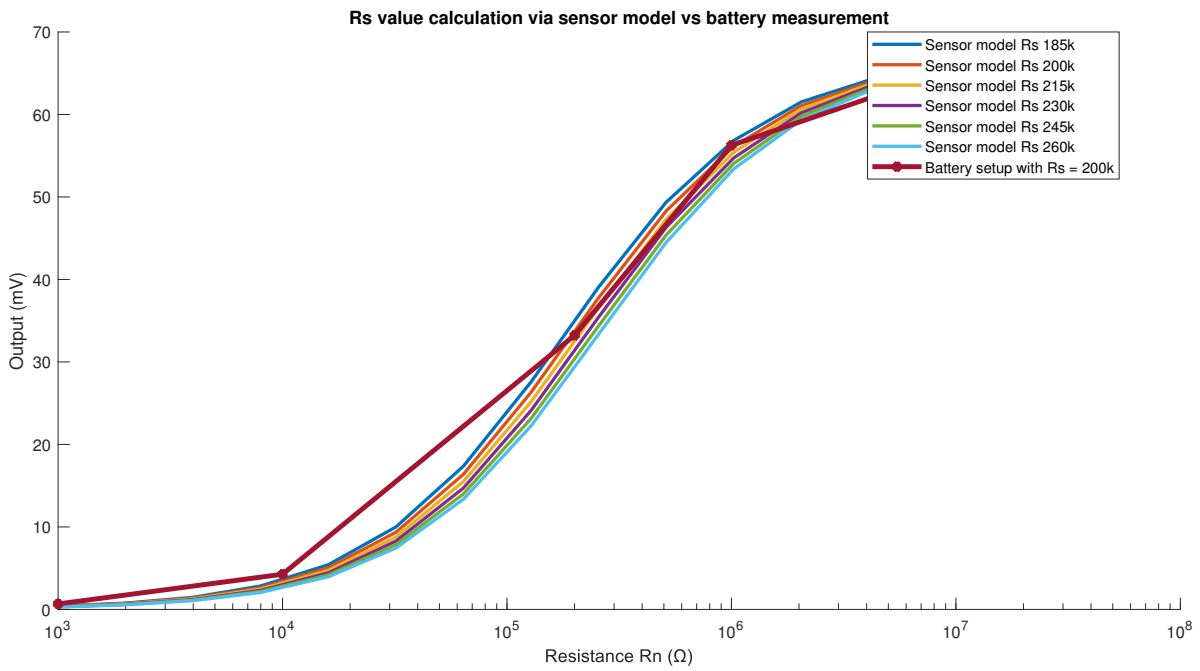
Figure 5.10: Rs value calculation of battery measurement via sensor model.
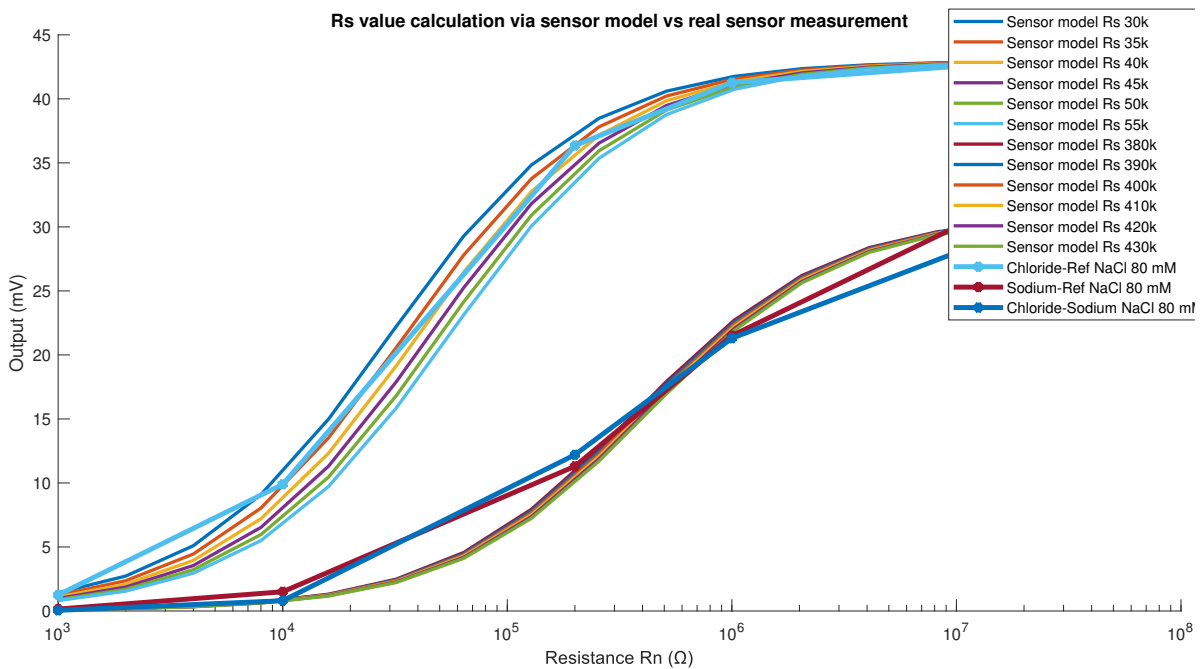


Figure 5.11: Rs value calculation of sensor via sensor model.

From the results shown in figure 5.11, it is concluded that the $Rs$ values for the chloride are around $35\,k\Omega$ and for the sodium sensor around $400\,k\Omega$. As mentioned before, it is not necessary to know the values exact, it is only necessary to know the order of magnitude. The error due to non ideal $Rs$ resistance is dependent on the bias current, or in the case of a system with a multiplexer on the leakage current of the multiplexer. The voltage error for the sweat sensor is illustrated in figure 5.12.
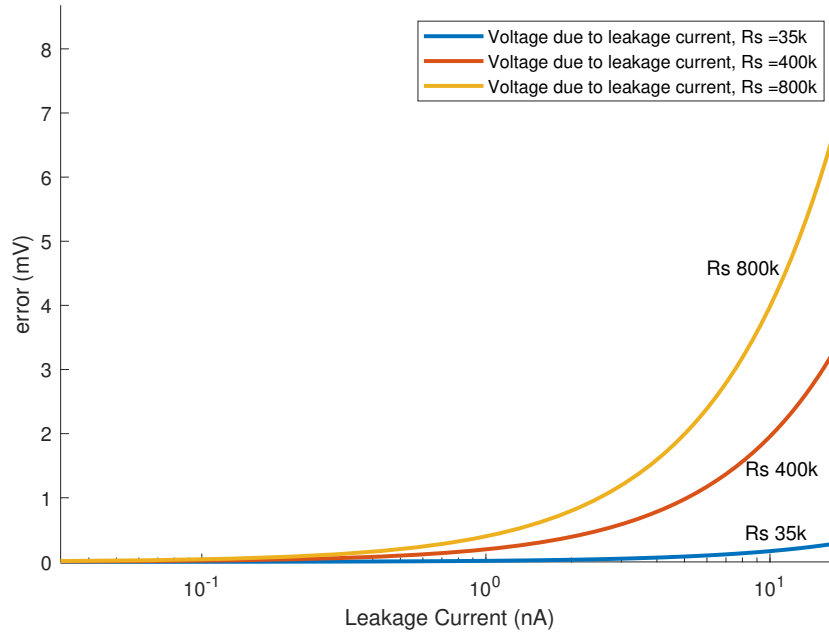
Figure 5.12: Measurement error due to leakage/bias currents through Rs.

In a worse case scenario, the value for $Rs$ is not expected to be more than doubled. Therefore, the measurement error calculation were based on a worse case scenario with $Rs$ was $800k\Omega$. A maximum bias and leakage current of $5nA$ in total in case $Rs$ was $800k\Omega$ is accepted to limit the measurement error to $2mV$ due the bias and leakage current. The AD8422 instrumentation amplifier was on itself accepted with a input bias current of $2nA$ maximum. However, in combination with other devices such as a multiplexer, the total current can be too high. Therefore, a read-out system with a different instrumentation amplifier has been designed as will be explained in the coming section.

## 5.4. Multi-channel circuit

The first circuit design was based on the read-out of a single sensor, the second read-out system was designed to read-out multiple sensors at the same time. The read-out of multiple sensors is more time efficient, as multiple sensors can be tested at the same time in one setup. In addition, it results also in a better comparison between the sensors since environmental conditions are the same for each sensor during testing. Besides the increase in channels, the performance in the second circuit design was also improved based on the sensor analysis from the previous section.

To increase the channels for the read-out, it was decided to use a multiplexer to connect multiple sensors to one instrumentation amplifier. Since bias currents can influence the performance of the sensor system significantly, the multiplexer and instrumentation amplifier were mainly selected on this criterium. As can be seen in figure 5.12, the total bias current had to be kept at a maximum of $2nA$. Commercial available multiplexers which were considered for this application are shown in table 5.3. The requirements for the selection of the multiplexer were defined as:

- Very low leakage current with typical $5pA$

- Supply voltage of $5V$, same as micro-controller and ADC

- 8 channels, 2 outputs making it possible to connect 2 chloride and 2 sodium sensors per multiplexer

Based on these requirements the ADG659 multiplexer from Analog Devices was selected.

Table 5.3: Overview of considered multiplexers for multi-channel circuit.

| Quality | ADG659 | ADG5209 | ADG759 | ADG604 | ADG739 | ADG709 | ADG1209 | ADG1204 | ADG707 | CD4052B | MAX389CPN+ | MAX4639ESE+ |
|---|---|---|---|---|---|---|---|---|---|---|---|---|
| Brand | AD | AD | AD | AD | AD | AD | AD | AD | AD | TI | MI | MI |
| Inputs | 8 | 8 | 8 | 4 | 8 | 8 | 8 | 4 | 16 | 8 | 8 | 8 |
| Outputs | 2 | 2 | 2 | 1 | 2 | 2 | 2 | 1 | 2 | 2 | 2 | 2 |
| Interface | Parallel | Parallel | Parallel | Parallel | SPI | Parallel | Parallel | Parallel | Parallel | Parallel | Parallel | Parallel |
| Supply span single max (V) | 5,5 | 40 | 5,5 | 5,5 | 5,5 | 5,5 | 16,5 | 13,2 | 5,5 | 20 | 22 | 5,5 |
| Supply span single min (V) | 2,7 | 9 | 1,8 | 2,7 | 2,7 | 1,8 | 5 | 10,8 | 1,8 | | 22 | 1,8 |
| Supply dual max (+/-V) | 6 | 22 | 2,5 | 5,5 | NA | 2,5 | 16,5 | 16,5 | 2,5 | 10 | 22 | 2,5 |
| Supply dual min (+/-V) | 2 | 9 | 2,5 | 2,7 | NA | 2,5 | 5 | 13,5 | 2,5 | | 22 | 2,5 |
| $I_{on}$ typ. (pA) | 5 | 10 | 10 | 10 | 10 | 10 | 20 | 20 | 10 | | | 10 |
| $I_{on}$ max. @25°C (pA) | 100 | 200 | 100 | 100 | 100 | 100 | 200 | 200 | 200 | 300000 | 2000 | 750 |
| Charge injection (pC) | 2 | 0,2 | 3 | -1 | 3 | 3 | 0,4 | -0,7 | 5 | Unkown | 55 | 13 |
| Farnell available | Yes | Yes | No | Yes | Yes | Yes | Few | Yes | Yes | Yes | Yes | Few |
| Price | €4,46 | €5,69 | - | €4,94 | €5,15 | €3,47 | €5,82 | €5,50 | €6,29 | €0,50 | €12,60 | €3,28 |

AD = Analog Devices, TI = Texas Instruments, MI = Maxim Integrated
Blue highlighted was used in this study

As mentioned before, the performance of the instrumentation amplifier is mainly based on bias current. Furthermore, other error sources such as noise and voltage offset were considered. The performance of the INA333 instrumentation amplifier from Texas Instruments performed better as or comparable to the AD8422 used in the first circuit. The INA333 fulfilled the requirement of a maximum of $2nA$ bias and leakage current, as can be seen in table 5.4. In combination with the multiplexer, the total bias and leakage current will be typically $75pA$ with a maximum of $400pA$.

Table 5.4: Specifications INA333 instrumentation amplifier.

| Specifications | INA333 |
|---|---|
| Manufacturer | Texas Instruments |
| Supply voltage min. | +/- 1.8 V |
| Supply voltage max. | +/- 5.5 V |
| Input voltage noise | $50nV/\sqrt{Hz}$ |
| Gain set | Resistor |
| Gain range | 1x - 1000x |
| Input bias current max. | 200 pA |
| Vos max. | 25 $\mu$V |
| Available at Farnell | Yes |
| Price | €4.09 |

The filter was designed to reduce the influence of noise and interference on the system while keeping the delay time low. The settling time of the filter has to be low to make it possible to keep the switching delay as low as possible. Therefore a Bessel filter architecture was chosen since this has a very flat phase and flatter group delay. The Microchip MCP607 was selected as operational amplifier for the filter circuit, its specifications meet the requirements for the second order Bessel filter.
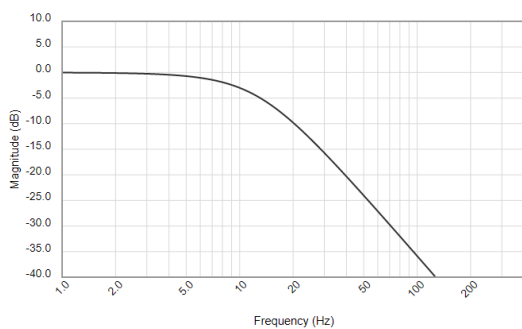


Figure 5.13: Magnitude frequency response second order Bessel filter, $f_c$=10Hz.
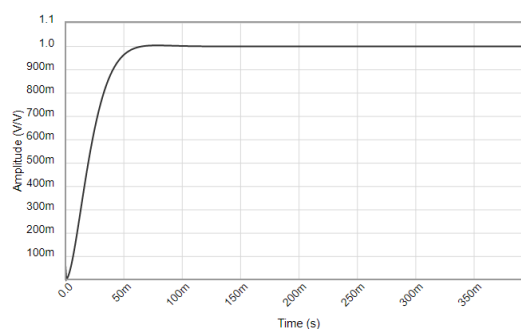


Figure 5.14: Step response of second order Bessel filter, $f_c$=10Hz.

The ADC and micro-controller were kept the same as in the single-channel circuit. This completes the circuit as illustrated in figure 5.19. The software and timing of the read-out had to be changed to make it possible to read-out all 4 sensors at a significant sample rate. The total circuit consists of 2 multiplexers with each 8 inputs and two outputs. The instrumentation amplifier and filter circuit can cause a delay in the signal

due to the settling time. Therefore, it is not possible to switch the first multiplexer at high speed. To make it still possible to switch between the sensors at higher frequencies, an optimised Mbed code was written in which the signal from channel 1 can be processed through the filter circuit while the other channel is being read. artefacts due to the settling time are in this way minimised. The process of sampling is presented in figure 5.15. As can be seen in the diagram, first circuit 1 is sampled while in the mean time circuit 2 can settle. After 20 samples, the ADC switches to circuit 2 and the next sensor from circuit 1 can settle.
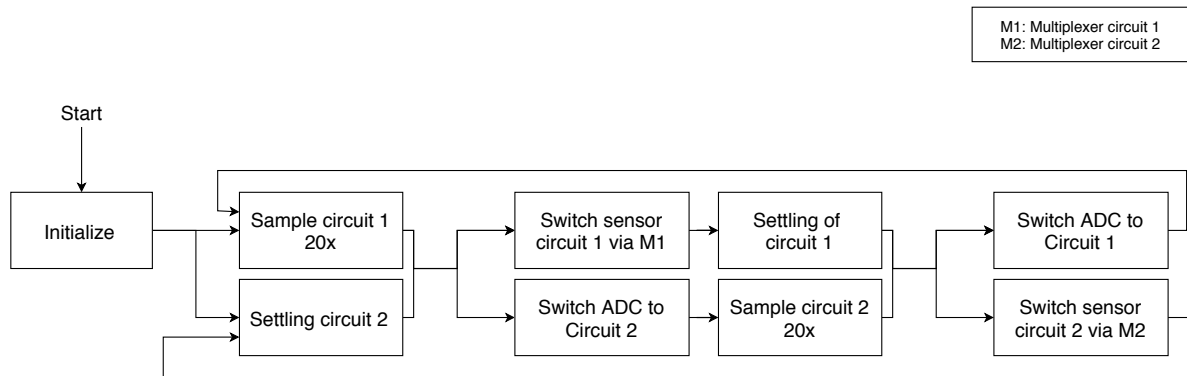
Figure 5.15: Functional diagram of sampling and switching process.

The hardware abstraction layer (HAL) of the read-out circuit is presented in figure 5.18. This used Mbed code is illustrated in the flowchart in figure 5.16 and can be found in appendix B. Implementing a settling time with a minimum of $50\,ms$ prevents artefacts as illustrated in figure 5.17. In this measurement, the settling time was to short. As a result, the signal of sensor S1 is still visible in the measurements of sensor S2 and were the signal of sensor S2 is visible in the measurement of sensor S3.
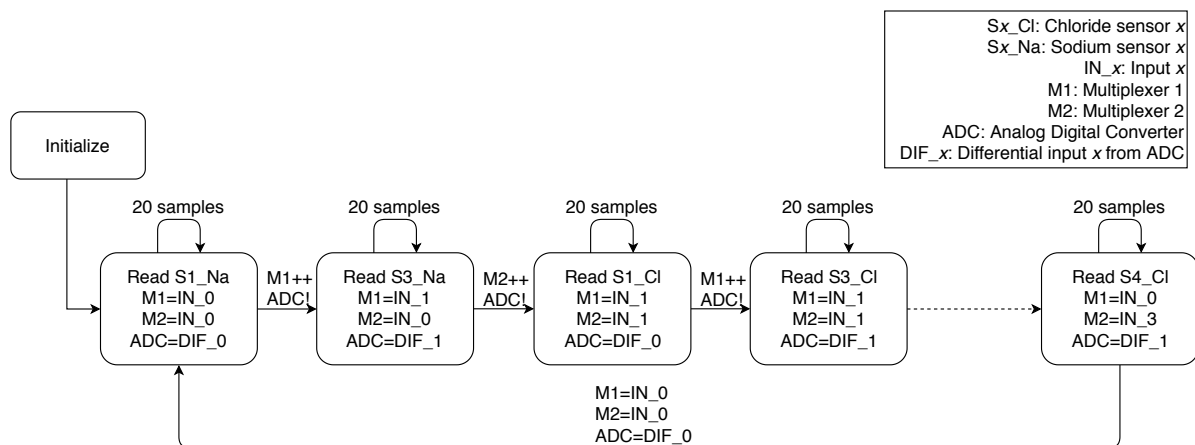
Figure 5.16: Software flowchart for multi-channel circuit.

**Sampling error, Fs=160 Hz, settling time = 31.25 ms**
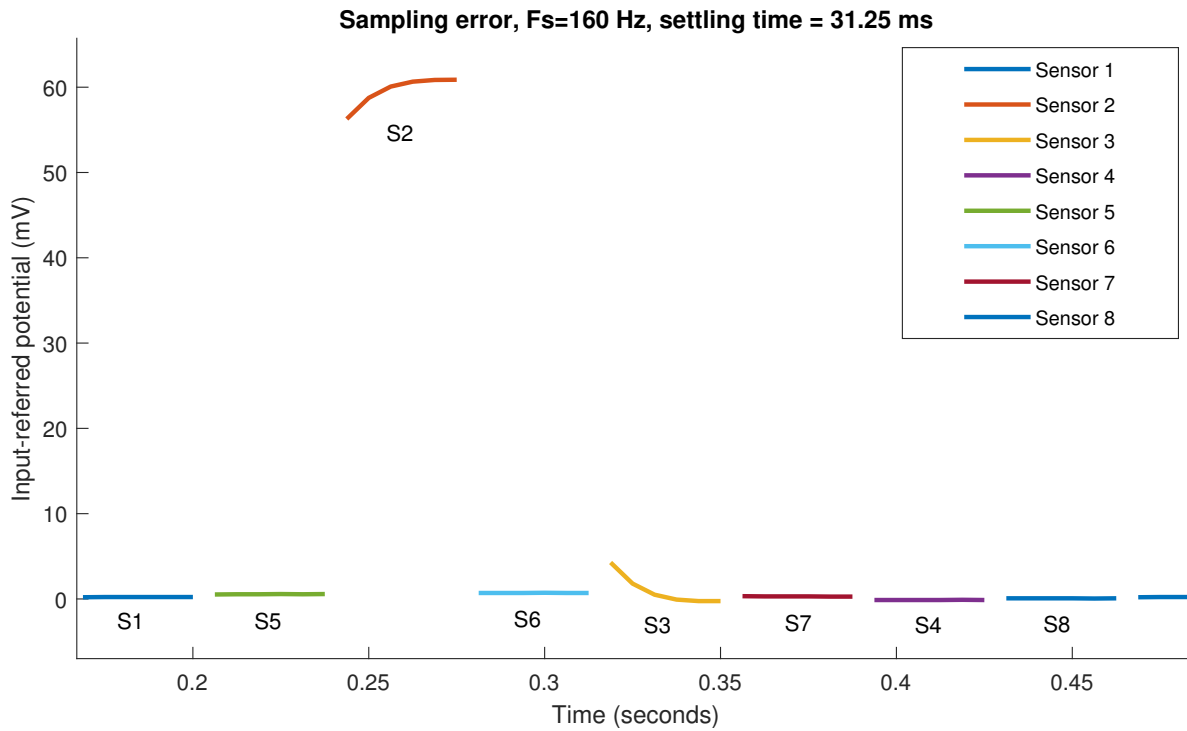


Figure 5.17: Settling time error, sensor 2 = 60.8mV while other sensors are around 0.2mV.


The library of the ADC was also optimised to increase the efficiency of the code. The standard library ask the ADC for a sample and will wait while the ADC is executing this process. In the optimised library, the ADC send its previous sampled value and start taking a new sample at a sample request. In this way, the sample wait time can be used by the micro-controller for processing and sending data while the timing of the samples is kept intact.

With the two optimisations, it is possible to increase the sample frequency from $60Hz$ to $400Hz$ without artefacts. During the test with the multi-channel circuit, 20 samples from each sensor (4x chloride and 4x sodium) were collected every second. This results in a sample frequency of $160Hz$ and a settling time of $125ms$.
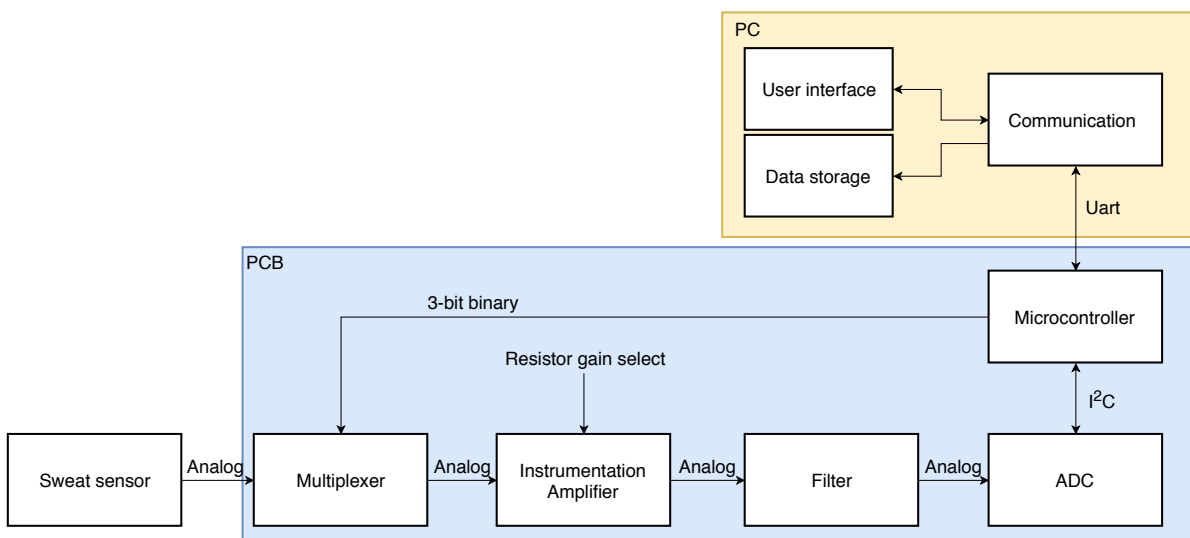


Figure 5.18: Hardware abstraction layer (HAL) of read-out circuit.
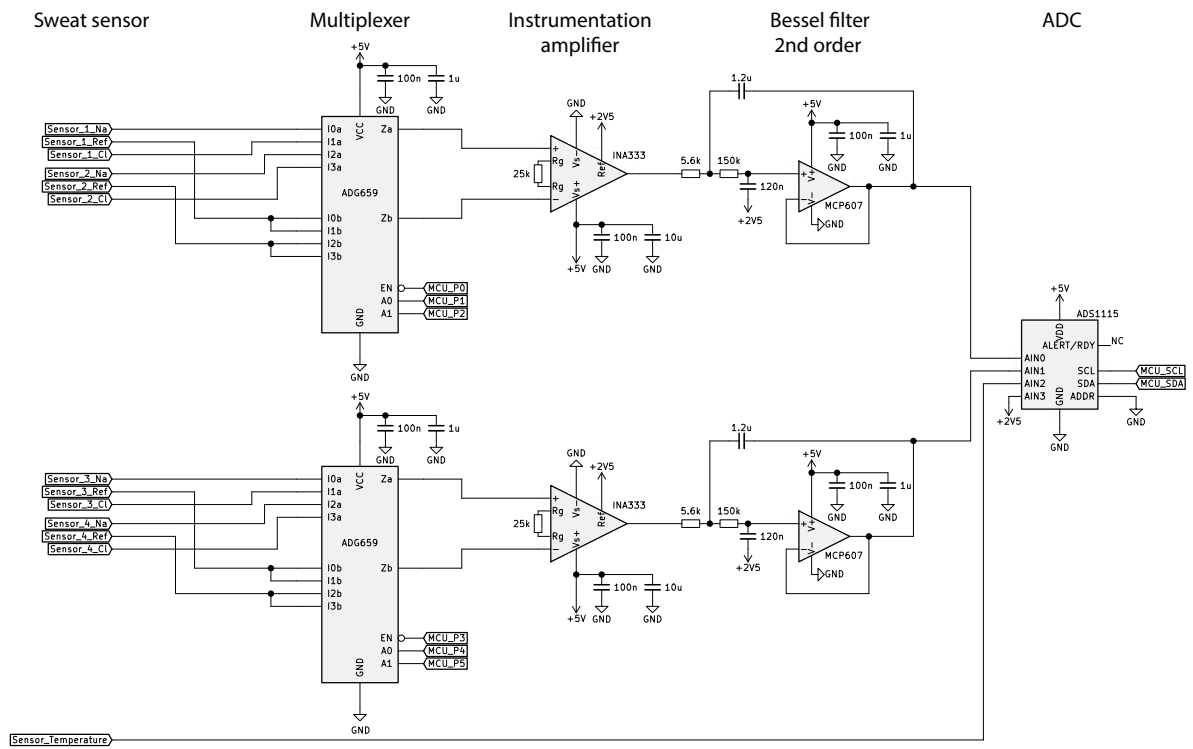
Figure 5.19: Read-out circuit for four sweat sensors.

## 5.5. Temperature sensor

As explained in chapter 4, the sensor output is temperature dependent. However, it is not expected to have a large temperature change in this application. Since the measurement setup is placed in a normal office room, temperature differences between the opening and closing hours of the office of maximum 10 °C can be expected. To monitor these differences, a temperature sensor was placed in the samples. The used temperature sensor, the NTC015WH01, is a Negative Temperature Coefficient (NTC) sensor and was selected on its temperature range and its availability. The circuit used for the read-out of the sensor is shown in figure 5.20. Following the datasheet of the NTC015WH01, the resistance was 10 $k\Omega$ ±1% maximum with a beta factor of 3435. Equation 5.1 show the formula to calculate the measured temperature.

$$\frac{1}{T} = \frac{1}{T_0} + \frac{1}{B} \ln \frac{R}{R_0} \tag{5.1}$$

$$R_0 = 10k\Omega \tag{5.2}$$

$$T_0 = 298.15k \tag{5.3}$$

$$B = 3435 \tag{5.4}$$
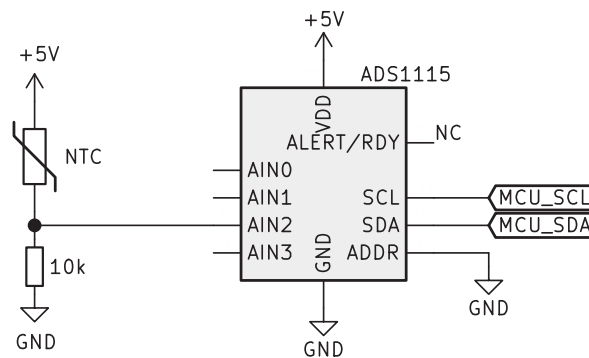


Figure 5.20: Temperature sensor circuit.

The NTC sensor was placed in a beaker with ice-water to calibrate the sensor. The temperature had a few degree offset as can be seen in figure 5.21. After 14 hours, an increase in temperature was monitored due to warming of the room by the morning sun. The offset was not compensated since only the temperature difference is important during the measurements and not the absolute temperature.
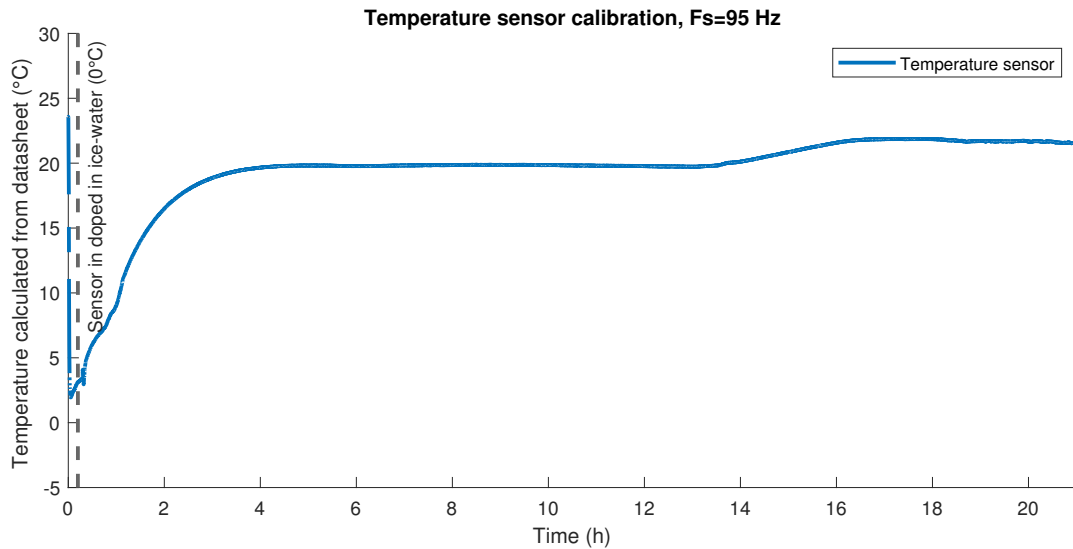


Figure 5.21: Temperature sensor calibration in ice-water.

# 6

# Sweat collector

As explained in chapter 2, sweat is a very useful body fluid for clinical analyses. However, the amount of sweat at the skin surface is limited, especially under non-exercise conditions. The overall sweat rates are mentioned in table 6.1. For example, the sweat rate at the forearm (ventral), a practical location for measurements, is on average 0.4 mg/cm$^2$/min during rest [21]. Since this is very limited, it is important to collect sweat from a bigger surface. Furthermore, the sweat rate can be so low that it is not possible to measure electrolytes in it. In that case, it is necessary to increase the sweat rate; this can be done artificially as will be explained in chapter 7. Using a good functional sweat collector, the need for artificially increasing sweat rate can be minimised. In addition, sweat can accumulate on the skin making real-time measurements unreliable. The sweat collector can have an important role in increasing the reliability of real-time measurements by avoiding sweat accumulation.

Table 6.1: Mean sweat-rates during rest and exercise conditions [21][76][77][78].

| Location | Mean at rest (mg/cm$^2$/min) | Mean at exercise (mg/cm$^2$/min) |
|---|---|---|
| Head (forehead) | 1.0 | 3.4 |
| Back (scapula) | 0.6 | 1.7 |
| Forearm (ventral) | 0.4 | 1.1 |
| Chest (upper) | 0.4 | 1.4 |
| Thigh (posterior: upper) | 0.2 | 0.8 |

Research in sweat rate and sweat composition changes during exercise is performed by the Electrical Instrumentation research group from the faculty of Electrical Engineering, Mathematics and Computer Science (EEMCS) of TU Delft. PhD candidate A.S.M. Steijlen is researching sweat rate and sweat composition changes during exercise in trials by collecting sweat samples during exercises such as spinning. During the first trial, the Macroduct Sweat Collector was used for collecting the sweat samples by Steijlen. This collector is illustrated in figure 6.1. The Macroduct Sweat Collector is an off the shelve product and also used in hospitals for obtaining sweat samples. However, this collector appeared to be unsuitable for this application for the following reasons:

- The collector must be worn tight on the skin to force the sweat to enter the collector

    – Uncomfortable for the participants

    – This limits the movements of the participants

- The collector stores the sweat in one compartment of 100$\mu l$

    – To see changes in sweat composition over time, it is necessary to replace the collector during the exercise

    – Takes a long time before the sweat collector is filled completely

- Due to movements the sweat collector can leak sweat out



Figure 6.1: Macroduct Sweat Collector [79].

To overcome the problems listed above, an optimised sweat collector has been developed by Steijlen. This collector is illustrated in figure 6.2. In this study, the screen-printed sweat sensor was integrated with the collector to test the concept of using the combination of the sweat collector and sweat sensor for measuring the sweat composition in CF patients. In the following sections, the design and the integration of the sweat collector and sweat sensor are discussed.
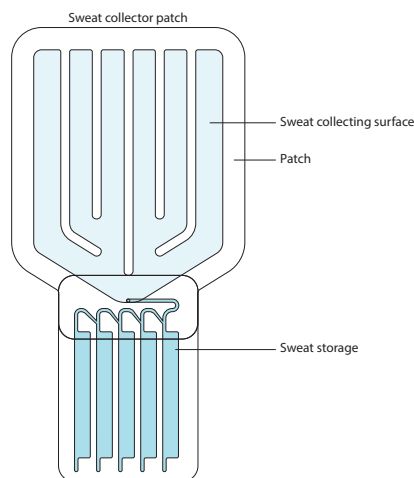


Figure 6.2: Optimised sweat collector designed by Steijlen.

## 6.1. Design

In this research, the main functionality of the sweat collector is to make it possible to measure sufficient sweat and prevent the accumulation of sweat on the sensor. Therefore, the following points concerning the sweat collector should be taken into account:

- There has to be a continuous flow of sweat over the sensors

- It should be possible to wear the collector for 24 hours at least

- The buffer for collecting old sweat should have sufficient capacity for 24 hours to avoid the accumulation of sweat

As mentioned before, an optimised sweat collector was developed to replace the Macroduct sweat collector. The collector is built as a patch that sticks to the skin and has some flexibility to bend with the movements of the participant. The collector consists out of multiple smaller compartments, that fill after each other. Therefore, it is possible to see the changes in the sweat over time afterwards.

## 6.2. Collector and sensor integration

The sweat collector is designed to be used by athletes and to store their sweat in the sweat reservoirs. With a few adjustments in the design, it became possible to integrate the sweat sensor in the sweat collector. However, the sweat production from athletes is much higher compared to a CF patient in rest. The reservoirs and channels are designed for athletes and as a consequence too large for the sweat measurements at CF patients. It will take too long to fill the reservoirs and channels with sweat from a person in rest. However, it is possible to test the concept of a sweat collector combined with a sweat sensor could be tested with this prototype. In further research, the size of the collector and sensor can be scaled down to the size needed for CF patients.

The first design of the combination between the sweat sensor en collector was based on the implementation of the complete sweat sensor in the channel from the sweat collector, as shown in figure 6.3.
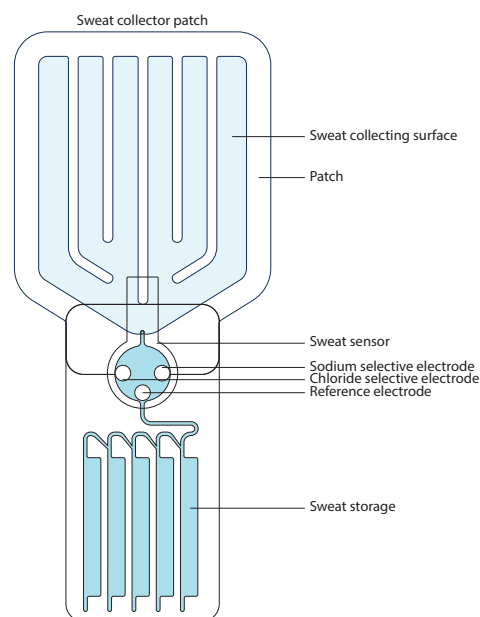


Figure 6.3: Integration of sweat sensor and sweat collector.

The sweat sensor requires complete coverage with sweat to work correctly, otherwise the chemical cell is not forming a complete electrical circuit. This prototype (figure 6.3) would require a large volume to provide a complete coverage. A better design would be to place the sensor electrodes in a line close to each-other. This is possible with the sensor from prototype V3 described in chapter 4, if only the chloride or sodium sensor is used in combination with the reference electrode, as shown in figure 6.4. This concept was used during the experiments.
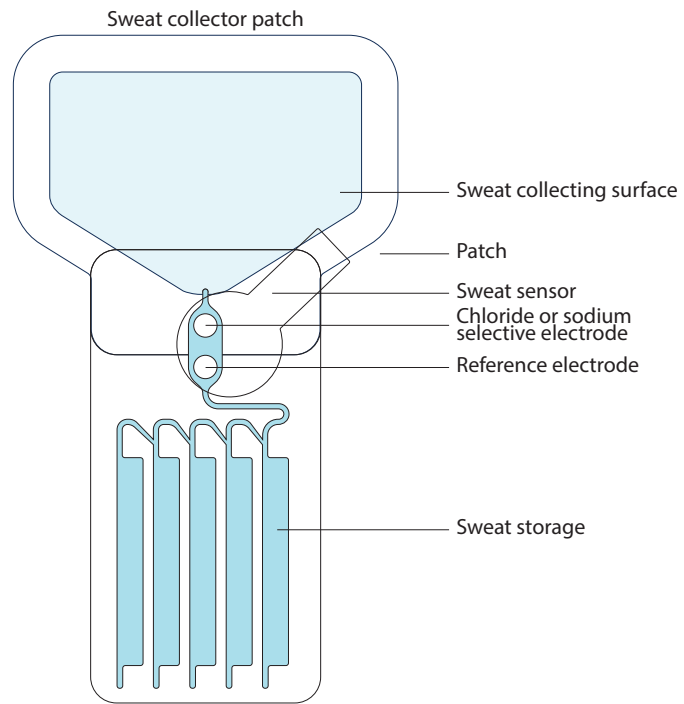
Figure 6.4: Integration of sweat sensor and sweat collector used in measurements.

# Sweat stimulator

The commercially available sweat stimulator Macroduct Sweat collection system Model 37700-SYS (illustrated in figure 7.1) costs €2500 (ELITechGroup B.V., December 2018). These costs are high compared to the components needed for the stimulation. Furthermore, the size of the stimulator ($9.2cm$ x $4.5cm$ x $15.5cm$ and $0.4kg$ [79]) is too large for a wearable device. For this study, building an own stimulator would therefore be interesting. In the following sections, the design, technique, safety and electrical circuit of the self-developed stimulator are discussed.



Figure 7.1: Webster Sweat Inducer Model 3700 [79].

## 7.1. Design
The design of the stimulator is in the basics straightforward; the components neede are an energy source, a voltage controller, a current controller and electrodes. The main challenge was to create a safe device since wrong stimulation could result into excessive skin irritation or burns. Due to some basic safety measures, the following design choices were made:

- Batteries as energy source to protect the participant from the mains to limit the electric shock risk
- A voltage limit, with a maximum voltage of $28V$
- A current limit, with a maximum current of $1.5mA$

- A on/off switch to stop the stimulation directly

- Usage of medically graded pilocarpine gel

- Usage of medically graded electrodes designed for pilocarpine iontophoresis

- Electronics placed in an isolated box to protect the operator

It was chosen to include the possibility of manipulating the shape of the stimulation current between a Constant Direct Current (CDC) or a Pulsed Direct Current (PDC). This concept will be explained in more detail in section 7.2. Adjustment of the settings (voltage, current, shape) had to be easy, for example with a switch or potentiometer.

## 7.2. Constant and pulsed direct current

As mentioned before, iontophoresis uses a small controlled current. Most of the commercially available iontophoresis equipment uses Direct Current (DC). DC allows the maximum ion transfer per unit of applied current, which makes it, therefore, the best parameter to control [27]. Electric current will flow through the path with the least resistance; this path depends on the distance between the electrodes, the positioning and location of the electrodes [57]. Since the skin does not have a constant impedance, also the voltage generated by the system is not constant following from Ohms law.

The pattern of the current application has an influence on the ion transfer, and therefore on the efficiency of the iontophoresis. The sweat stimulator used in the hospital is the Webster Sweat Inducer Model 3700. This stimulator has a profiled ramp up and ramp down, equivalent to $1.5mA$ for 5 minutes. The maximum current is limited to $1.5mA$ to limit the skin irritation. A gradual increase is often chosen to keep the possibility of skin irritation as low as possible. However, a gradual increase is less efficient than applying directly the full current [27]. As a result, the stimulation is less efficient, which requires a longer stimulation time, which can result in more patient discomfort. Therefore, an optimal current dosage and application procedure can be determined, taking efficiency and patient comfort into account. Besides methods in which a CDC or ramp CDC was applied, PDC also has been tested as an alternative. Examples of PDC waveforms are shown in figure 7.2. Patient discomfort is related to the amount of current applied, the wave shape, the frequency and the duty cycle. Most studies showed greater efficiency, less charge accumulation in the skin and less uncomfortable situations for the patients when monophasic PDC was applied compared to CDC [30].
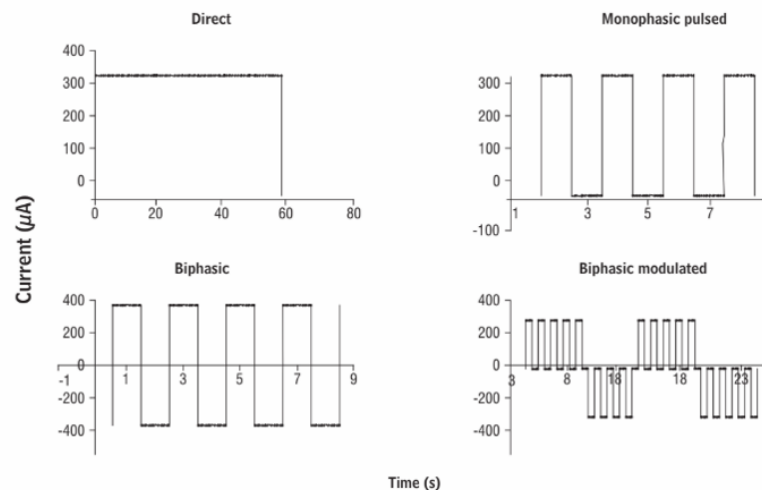


Figure 7.2: Types of quadratic waveform used in iontophoresis [34].

Biphasic PDC and modulated biphasic PDC is expected to be less effective in pilocarpine iontophoresis, since it will push the pilocarpine in the skin during the positive stimulation. However, it will pull the pilocarpine back during the negative stimulation. Therefore, only stimulation with effective a DC-current will be effective for sweat stimulation.

Unacceptable skin irritation or skin burns can occur when the current density applied is more than 0.5 $mA/cm^2$ [57] [15], so the ideal system would have a lower current density. Figure 7.3 illustrates the benefit of using monophasic PDC. In this test, the current density was between $0.07mA/cm^2$ and $0.21mA/cm^2$. As can be seen, the use of monophasic PDC at a frequency of 1 $kHz$ requires a smaller current for more or less the same sweat volume as could be obtained with CDC being below the threshold of skin irritation.
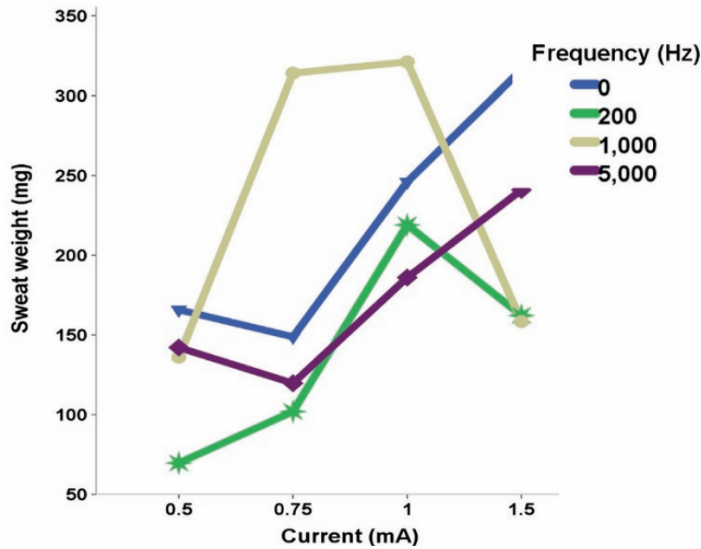


Figure 7.3: Interaction among current, frequency (triangular waveform) and sweat weight (p = 0.7488) [57].

## 7.3. Electrical circuits used in related research

Basically, a constant current of 1 $mA$ which can handle voltages up to $25V$ is necessary, since the resistance can go up to $20k\Omega$ or even higher [31]. An example of a circuit which can be used as a constant current source is illustrated in figure 7.4. However, this circuit does not have safety and control qualities. An example of a circuit used for iontophoresis by Emaminejad *et al.* has safety protections and the option to be used for PDC as illustrated in figure 7.5. This stimulator has two protection properties to prevent burns. Firstly, the current is used as negative feedback for the opamp and also monitored with an ADC. When the current measured via the ADC is too high, the microcontroller adapts the PWM signal to the input of the opamp. Secondly, a junction field-effect transistor is used to limit the current to $2mA$.
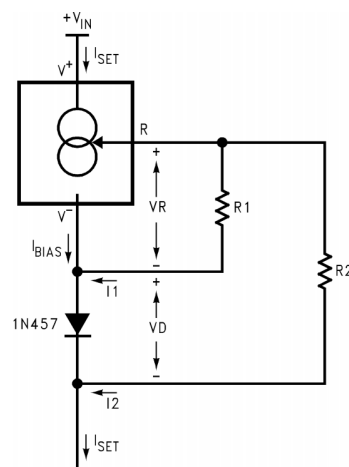


Figure 7.4: Typical application of LM234 as zero temperature coefficient current source [80].
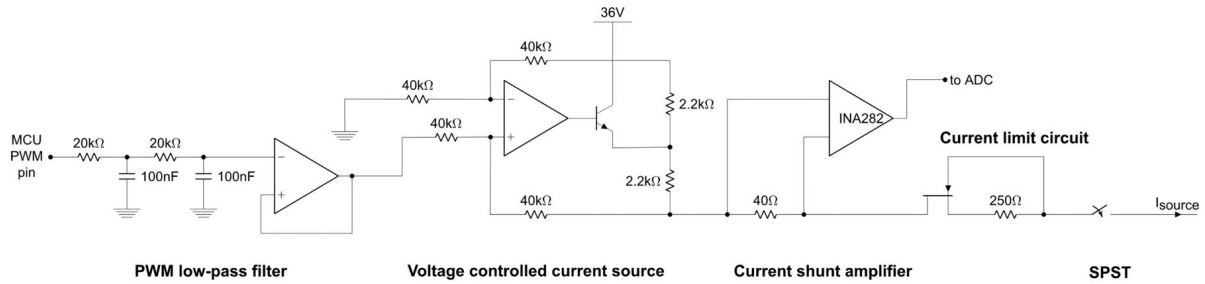
Figure 7.5: Schematic showing of a current delivery circuitry for iontophoresis [31].

## 7.4. Electrical device

The stimulator device (Pilogel stimulator) was used to provide a constant continuous/pulse current, with a typical current of $1mA$ and a max. current of $1.2mA$. The current flows through the positive electrode and the pilogel to the skin, where the current will flow through the skin to the negative electrode which also contains a conducting gel.

As mentioned before, it is necessary that the stimulator can handle voltages up to $25V$, since the skin resistance can go up to $20k\Omega$ or even higher. Furthermore, the skin resistance is not linear due to different skin layers and changes in the fluids in the skin. Using low voltages will only result in a current through the top skin layer while higher voltages can break through the different skin layers and reach the sweat glands.

Since pilocarpine is positively loaded, it will get pushed into the skin at the positive electrode side, this is illustrated in figure 1. The stimulation will typically take 5 minutes, with a maximum of 8 minutes (in accordance with the hospital protocol, see appendix F). The device consist of four main components: battery, voltage control, current control and the electrodes, as illustrated in figure 7.6 and will be discussed in more detail in this section.
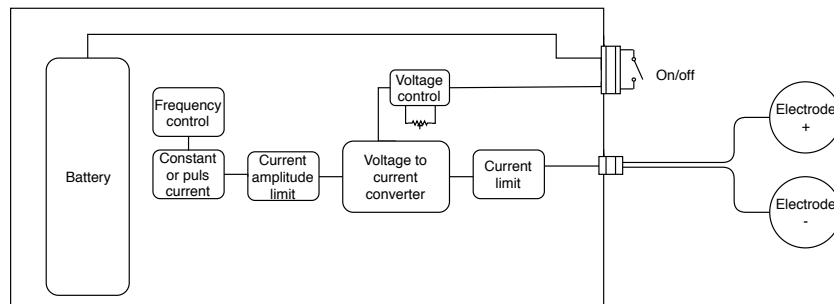


Figure 7.6: Pilogel sweat stimulator overview.

### Battery
The battery used was a block of 3 batteries of $9V$ in series. A switch at the outside of the device can be used to disconnect the batteries from the rest of the circuit.

### Voltage control
To have a constant limited voltage supply from the batteries, a LM317 voltage regulator was used. The regulator can be controlled with a potentiometer. The maximum voltage is $25V$. In case of a failure, the maximum voltage of the system is $27V$ (3x $9V$ battery in series).

### Current control
In the current control, a constant or pulsed current is produced with the usage of a current mirror with transistors that are matched, as shown in figure 7.7. The reference current is controlled with a NMOS transistor with a series resistance. This principal is also used in a design for a spinal cord stimulator [81]. The current can be assumed to follow equation 7.1 if $R_s$ is large enough. The equation for the reference current and output current resulted from the current mirror are shown in equation 7.2 and 7.3. To have an accurate current mirror, it is required to have two well matched PMOS transistors for M2 and M3. For $I_{out}$ to be an accurate representation of $I_{ref}$ the threshold voltages and the physical attributes of both devices have to be the same.

This can be partly achieved by using an off the shelf transistor array with two matched transistors on it. Or less accurate but simpler, by introducing matching resistors at the source of M2 and M3.

$$I_{ref} = I_{DS} = \frac{V_{G,M1} - V_{TH,M1}}{R_s} \tag{7.1}$$

$$I_{ref} = I_{SD2} = \frac{\kappa_{p2}}{2}(V_{SG2} - |V_{TH,P2}|)^2(1 + \lambda_2 V_{SD2})$$
$$I_{out} = I_{SD3} = \frac{\kappa_{p3}}{2}(V_{SG3} - |V_{TH,P3}|)^2(1 + \lambda_2 V_{SD3}) \tag{7.2}$$

$$\frac{I_{out}}{I_{Ref}} = \frac{1 + \lambda_3 V_{SD3}}{1 + \lambda_2 V_{SD2}} \tag{7.3}$$

Equations 7.2 and 7.3 show that even when the physical attributes of the transistors are perfectly matched the currents still differ based on the difference between $V_{SD}$ of the two transistors. This property could potentially introduce large inaccuracies in the output current [81]. To suppress the inaccuracies that occur from channel length modulation in the simple current mirror, a cascoded current mirror can be used instead. However, in this setup, the output current does not have to be that accurate since it can easily be measured and adjusted. The setup with a single current mirror with two input resistors is chosen to be sufficient. In the final design, two BJT transistors were used, in which the transistors are thermally coupled by putting them together with heat shrink to improve the matching.

The output current shape is controlled with an active feedback system operational amplifier circuitry, an Pulsed Direct Current (PDC) or Constant Direct Current (CDC) can be selected via a switch. The operational amplifier circuitry provides active feedback to the NMOS. The amplifier adjusts its output voltage in such a way that the voltage over resistor $R_s$ at the negative input terminal has the same potential as the voltage selected at the positive terminal. In this way, the reference current is no longer dependent on the nonlinear properties of the NMOS and the linearization of the configuration is not dependent on the size of the source resistor anymore [81]. The pulse input for the positive terminal of the operational amplifier was generated with the LM555 timer. The frequency range can be chosen between $0 Hz$ and $5 kHz$. The output current can be selected with a potentiometer, the maximum output current is $1.2 mA$. For extra safety, a zener-diode is added before the potentiometer. In case of a fault in the pulse generation, the zener-diode will limit the signal to the voltage-current converter and thus limit the output current.
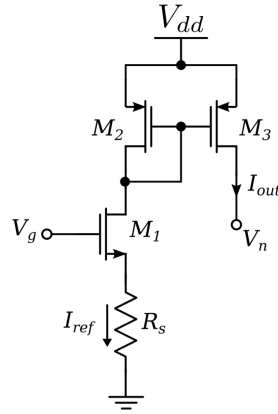


Figure 7.7: NMOS transistor with a single current mirror [81].

### Electrodes

The electrodes used were the official Macroduct electrodes with a surface of 7 $cm^2$. The system is based on two electrodes, positive (red) and negative (black). The surface of the electrodes is RVS. The electrodes are shaped to fit perfectly with the pilogel discs. Both the electrodes as pilogel are the same as used in hospitals in the Netherlands. Since the current is limited to $1.2 mA$, the current density is limited to $0.17 mA/cm^2$, which is much lower compared to the $0.5 mA/cm^2$ related with skin irritation and burns [15][57]. A picture of the used electrodes can be found in appendix D.

Figure 7.8 shows the schematic of the final design of the stimulator used in the experiments.
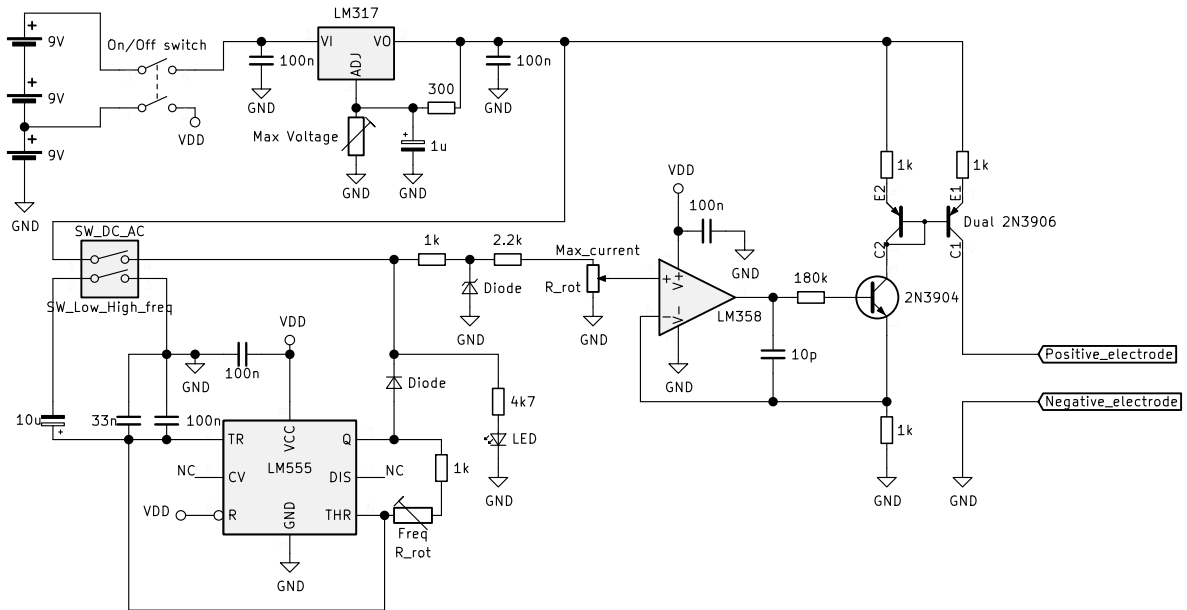
Figure 7.8: Electrical circuit for PDC and CDC stimulation with 1.2mA max stimulation current.

## 7.5. Safety

During this study, the sweat stimulator was validated on participants, healthy volunteers. For this clinical study, the sweat stimulator had to comply to safety requirements and had to be accepted by the Human Research Ethics Committee (HREC) of the TU Delft.

The HREC asked for multiple documents and a technical assessment to check the safety of the device. In conclusion, the following safety measures are taken to have a safe stimulator:

- Voltage limit, $25V$

- Current limit, $1.2mA$

- Stimulation time limit, 8 min

- Current density limited to $0.17mA/cm^2$

Pictures of the final device can be found in appendix D. A more detailed report of the safety measures can be found in appendix G.

The aim of the clinical study was to prove the working principle of the stimulator. Further clinical studies were out of the scope of this study. Future research should focus on proving the efficiency on both sweat production as physical discomfort.

<div style="text-align: right; font-size: 3em;">8</div>

# Experimental methods

In this chapter, the experimental setup for testing the three parts, the sweat sensor, the sweat collector and the sweat stimulator is discussed.

## 8.1. Sweat sensor validation

For determining the performance of the sweat sensor, it was tested for the following parameters:

- Sensitivity ($\Delta$ mV/concentration)

- Long-term stability (measurements for multiple hours)

- Selectivity for ion of interest (influences by ions other than $Cl^-$ and $Na^+$)

The sweat sensor was validated in a laboratory setting. The measurement setup consisted of:

- The sweat sensor, prototype V1, V2 or V3

- The NTC temperature sensor

- The read-out circuit, single or multiple channel

- A holder for the sensor

- Beakers with the samples

A picture of the setup with the single channel is presented in figure 8.1, a picture of the multi-channel is presented in figure 8.2.
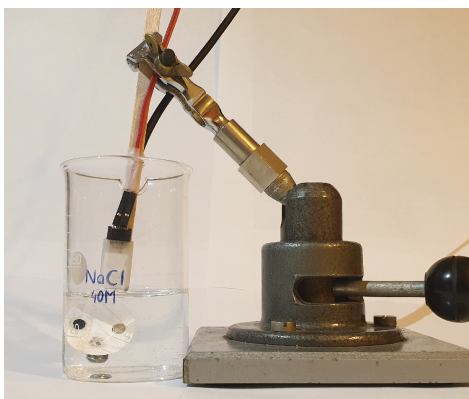




Figure 8.1: Measurement setup with a single sweat sensor.
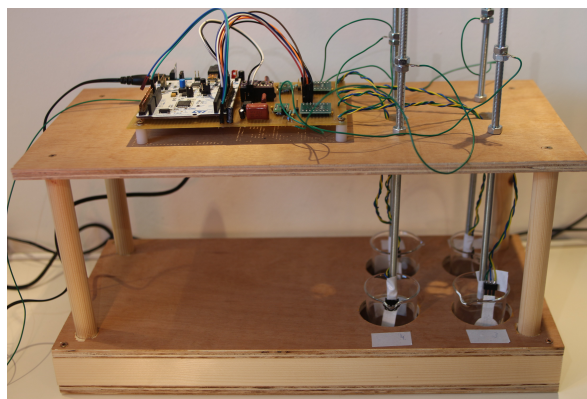
Figure 8.2: Multi-channel measurement setup running 4 experiments at the same time.

### 8.1.1. Sensitivity measurements

During the sensitivity measurements, the sensor was placed in solutions with different NaCl concentrations, typically in the range of 20 mmol/l up to 80 mmol/l. The measured potential was divided by the gain of amplifier circuit to determine the input referred potential which is the potential developed between the reference electrode and the sensing electrode from the sensor.

The results were compared with results reported for related studies in literature.

### 8.1.2. Long-term stability

During the long-term stability measurements, the sensor was placed in a sample beaker with a known NaCl concentration. Since the setup was not changed or moved during the measurements. Such a setup is also called static system stability measurement in literature. The measurements ran minimal a couple hours. From the moment the sensor results were stable, the measurements were extended with 24 hours. The final goal was measure for 3 days.

The results were compared with results reported for related studies in literature.

### 8.1.3. Selectivity for ion of interest

It was expected that the chloride sensor would behave the same in a KCl solution as in a NaCl solution, while the sodium sensor should have a negligible outcome for a KCl solution. It was not necessary to test the sensor extensively for the selectivity since the sweat composition mainly consists of NaCl, as mentioned in section 2.2. In this phase, it is expected that other factors such as temperature, sensitivity and long-term stability have the most influence on the measurements and not the selectivity. During this experiment, the sweat sensor was exposed to samples other than NaCl solutions. For example, a KCl solution was used.

## 8.2. Sweat collector validation

The sweat collector combined with the sensor was tested on its capability to have a constant sweat flow. It was also planned to run experiments with different NaCl concentrations to see if the results were comparable with those from the experiments with the sweat sensor alone (without sweat collector).

## 8.3. Sweat stimulator validation

During this study, the stimualtor had to be validated on a human volunteer. This required the approval of the HREC. Therefore, a protocol for the experiment was composed. In the next section, the main items of the protocol are described.

### 8.3.1. Participant selection

Participants with known health issues related to skin and or/sweating were excluded from the experiments. Participants under the age of 18 were also excluded from the experiments.

A participants had to give his/her written permission for the research by signing an 'Informed Consent' form stating the nature of the research, its duration, the risk, and any difficulties involved. The 'Informed Consent' form and 'Participant Information' sheet are attached in appendix H.

### 8.3.2. Preparation & setup

Before the experiment, the participant was informed orally and via the 'Participant Information' sheet explaining the procedure, goal and risk of the research. The experiment was only executed after the participant had signed the 'Informed Consent' form.

Before the start of the experiment, the skin of the volunteer was cleaned with alcohol at the sites where the stimulation and sweat collection were located. Furthermore, the stimulator was tested on its settings before the stimulation on the human volunteer. This was done by measuring the output current with a current meter and testing the frequency and shape with a signal analyser.

### 8.3.3. Experimental trial

The experiment consisted of two steps:

Step 1:  Stimulation with pilocarpine ionthoporesis.

Step 2:  Sweat collection and analyses.

The stimulations took around 5 minutes. During the stimulation, the participant was asked to indicate whether the stimulation caused pain. The stimulation was stopped if the participant felt any form of pain due to the stimulation.

After stimulation, the participant could do office work or relaxing while in between the sweat was collected. After 30 minutes, the collected sweat was weighed. The participant was asked to indicate the amount of skin irritation multiple times, this was continued till the skin irritation was completely gone.

Sweat was collected by using a gauze swab at the stimulation site after the stimulation. A gauze swab is an absorbent compress, by weighing before and after the sweat collection, the sweat weight can be determined. The gauze swab was covered with a hydrofilm. The hydrofilm cover was to prevent sweat evaporation while maintaining air flow. The sweat was collected at three places, one at the sweat stimulation area (L1) and two for reference purpose (L2 & L3). The sweat sampling locations are illustrated in figure 8.3. The sweat increase was determined by the difference between sweat weight at L1 and the average sweat weight of L2 and L3. The results were compared to the typical sweat increase obtained in sweat stimulation tests in hospitals. Pictures of the placement of the gauze swab during the experiment are presented in appendix C.
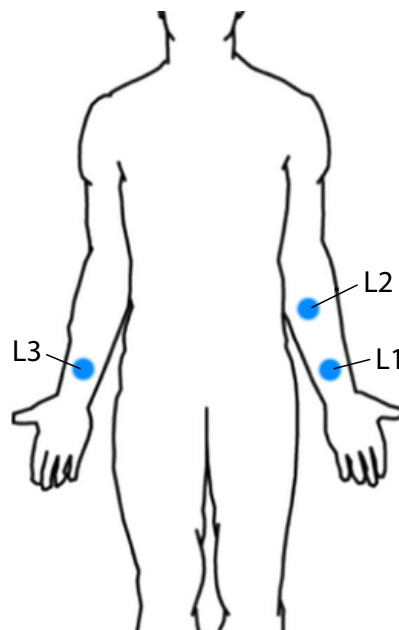


Figure 8.3: Location of sweat samples, anterior view.

# 9

# Results

In this chapter, the results from the experiments are presented. The results are divided in three sections, results from the sweat sensor, the sweat stimulator and the integration of the sweat sensor with the sweat collector.

## 9.1. Sweat sensor

In chapter 4, three prototypes of the sweat sensor have been described. These prototypes were tested on three characteristics in the usage in a sweat sensor application:

- Sensitivity for chloride or sodium

- Long-term stability

- Selectivity for ion of interest, e.g. chloride and sodium

In next section, the results for each sweat sensor prototypes are shown.

### 9.1.1. Sensor v1

Figure 9.1 shows the first results of the chloride sensor in prototype v1. A moving-average filter with a window size of 52 samples was applied on the raw data. The raw signal contained 50Hz interference of a couple millivolts, the moving-average filter neglected this interference. As can be seen in the results, a clear potential difference was measured under the different concentrations of NaCl. Especially the difference in potential is large in the region of interests, 30-60$mmol/l$.

Figure 9.2 presents the same data in a stair-way graphic. This stair-like presentation of the data is often used in literature, an example is shown in figure 9.3. In this presentation, the effect of different concentrations on the potential is easily visible. However, in real-life, the transition in the potential due to the different concentrations is not as steep as presented. The transition time is removed to have a more clear result.
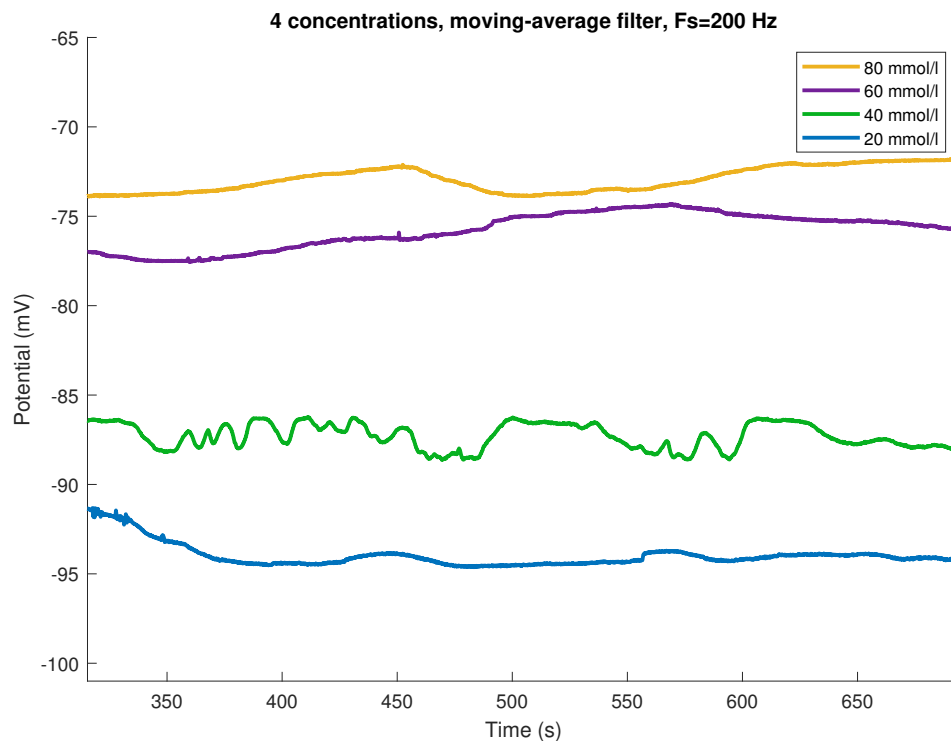
Figure 9.1: Open-circuit potential responses of the chloride sensors in NaCl solutions.
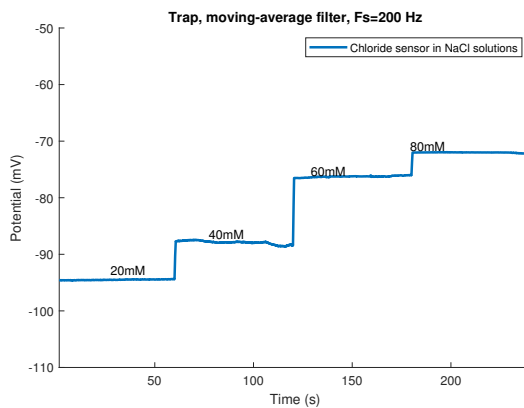


Figure 9.2: Open-circuit potential responses of chloride sensors V1 in NaCl solutions after each-other.
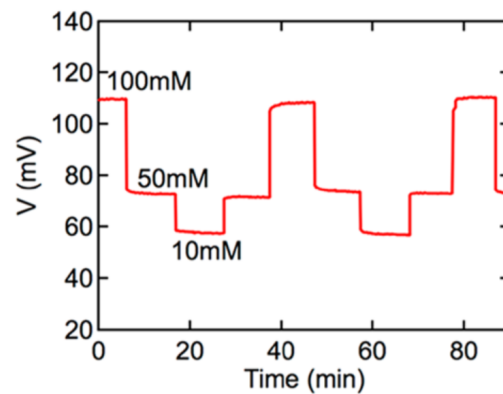
Figure 9.3: Literature example of open-circuit potential responses of chloride in NaCl solutions from Choi *et al.* [64].

As mentioned before, the system can be influenced by interference, especially the 50 Hz interference from the power-line. The interference was dependent on the power source used during the measurements, as can be seen in the raw data illustrated in figure 9.4. However, due to the high sample frequency it was possible to remove this interference digitally. During the setup for long time measurements, a lower sample frequency is storage wise preferred. Consequently, it would be necessary to minimise the interference in the analog domain, for example by using a battery power source or a low pass filter.
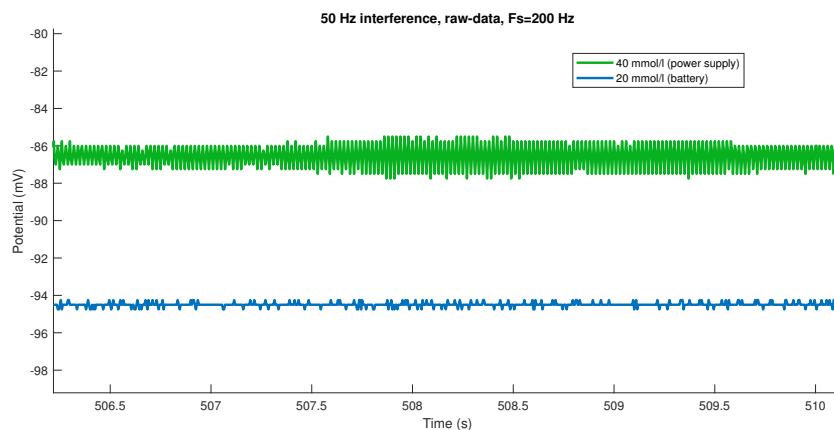
Figure 9.4: Raw data of open-circuit potential responses of the chloride sensors in 40mM NaCl at laptop power supply and 20mM NaCl on laptop battery.

The first prototype of the sweat sensor was tested for its stability for 2 hours as presented in figure 9.5. Over time, the sensor fluctuated around the average potential with ± 5mV. Although the stability over 2 hours was acceptable, it was unclear why the signal had fluctuations repeating every 5 to 10 minutes. This is discussed in more detail in chapter 10.
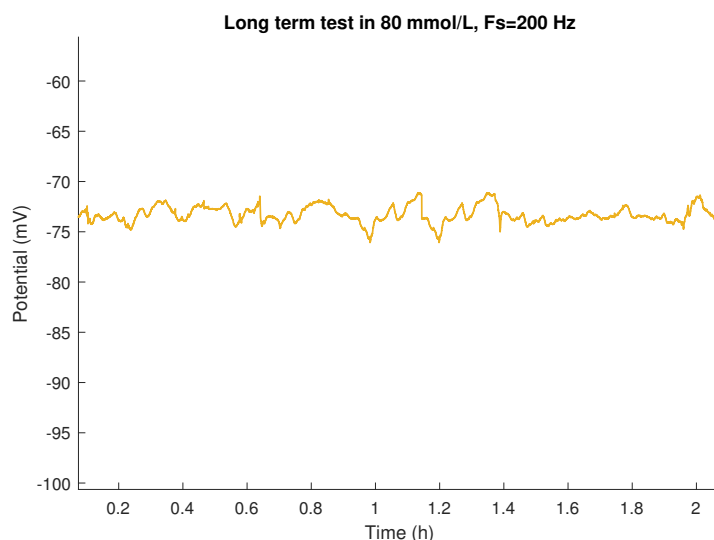


Figure 9.5: Open-circuit potential responses of the chloride sensors in 80M NaCl solution for 2 hours.

### 9.1.2. Sensor v2

Sensor prototype V2 was tested in more detail compared to prototype V1. For example, the sensor was tested in more concentrations of NaCl. Besides the chloride sensor, also the sodium sensor was tested. It should be noted that the chloride and sodium sensors have an offset difference and react in the opposite way for concentration differences. The behaviour of the sodium and chloride sensor was as expected, very similar when looking at the absolute potential differences for multiple concentrations of NaCl. This can be explained by the fact they share the same reference electrode, a change in the reference electrode will affect both the sodium as chloride sensor.

As was done for the results from prototype V1, the chloride sensor results from prototype V2 under different concentrations are plotted in a graph both beneath each-other (figure 9.6) and in stair-way plot (figure 9.7).
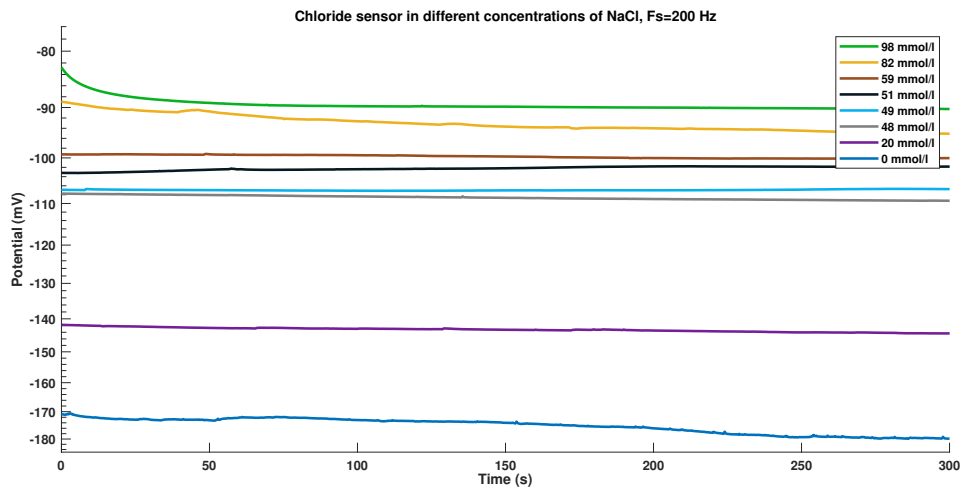
Figure 9.6: Open-circuit potential responses of chloride sensors V2 in NaCl solutions.

The response around $0 mmol/l$ was unstable, as can be seen in figure 9.7. However, since this is not in the region of interest, it is not a problem during this study.
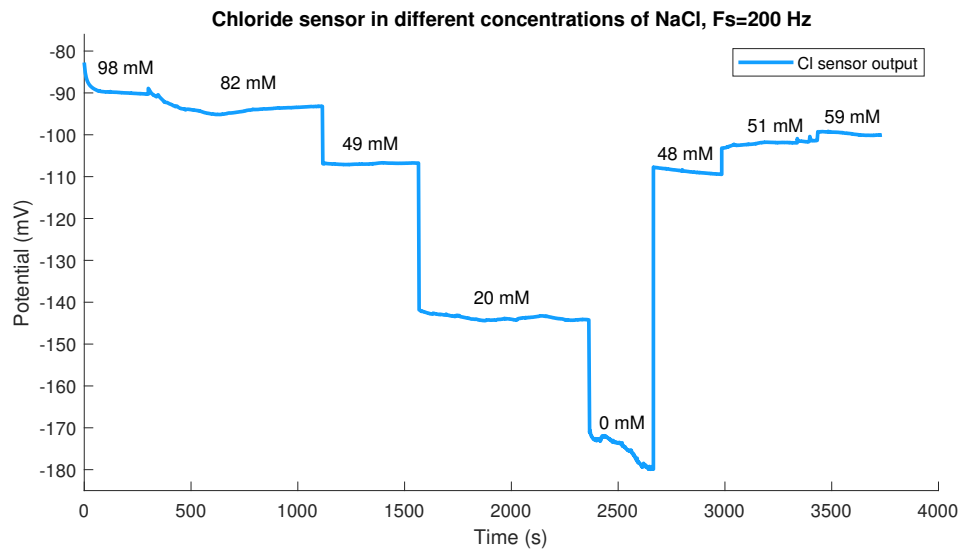


Figure 9.7: Open-circuit potential responses of chloride sensors V2 in NaCl solutions after each-other.

The chloride and sodium sensitivity against the concentration of NaCl are plotted in figure 9.8 and 9.9 respectively. The sensitivity in the region of interest, 30-60$mmol/l$, is around $1 mV$ per $mmol/l$. However, it should be mentioned that this figure is based on the stable values of one sensor. Unstable results due to the transitions time from one concentration to another are not taken into account. Furthermore, these graphs are based on data from a single test session. The offset due to the degradation over time of the reference potential are not taken into account.
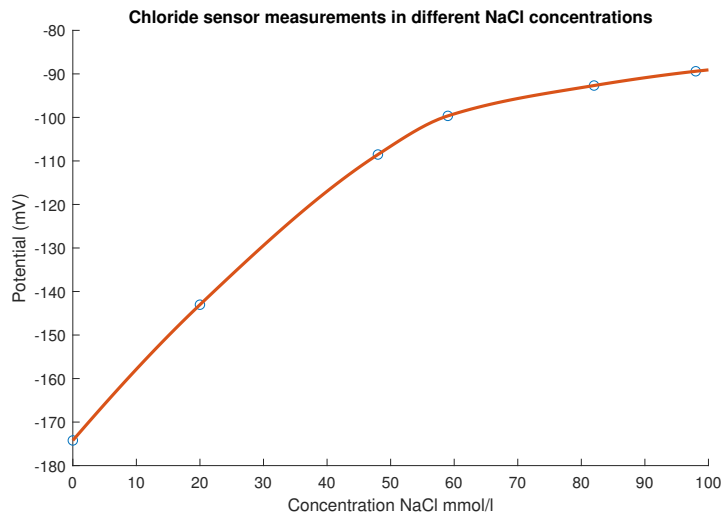
Figure 9.8: Best results of open-circuit potential responses of chloride sensors V2 in NaCl solutions.
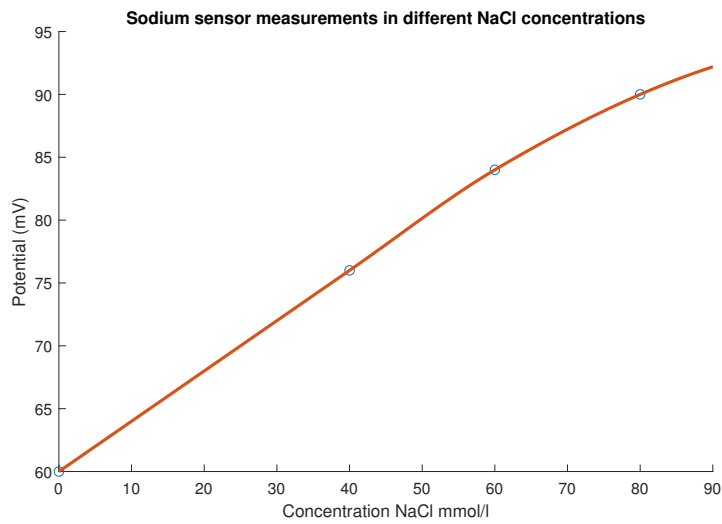


Figure 9.9: Best results of open-circuit potential responses of sodium sensors V2 in NaCl solutions.

During a measurement for more than 80 hours, a decrease in the potential was measured as can be seen in figure 9.10. In the first hours, a potential increase was measured in both sensors. This is followed by a gradual decrease with some small fluctuations This is discussed in more detail in chapter 10.
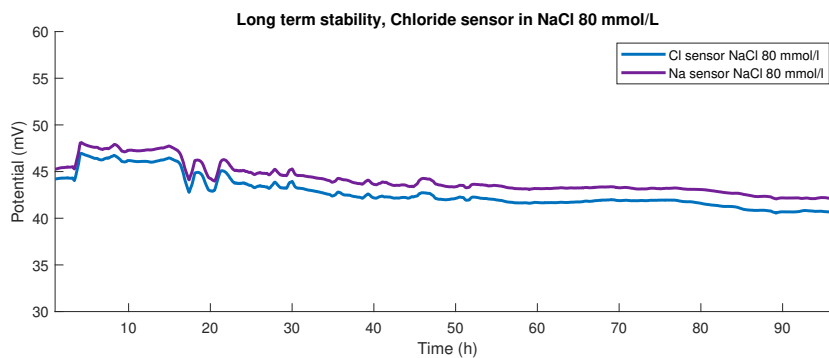


Figure 9.10: Open-circuit potential responses of chloride and sodium sensor in 80mM NaCl solution for 97 hours.
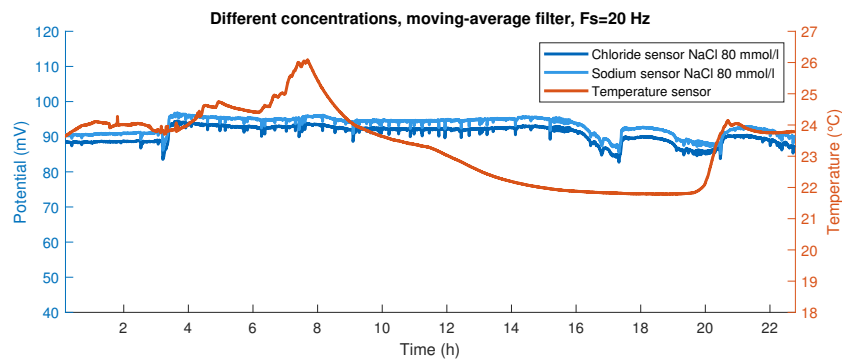
Figure 9.11: Open-circuit potential responses of chloride and sodium sensor V2.1 in 80mM solution vs temperature of solution.

### 9.1.3. Sensor v3

Section 4.3.3 mentioned difficulties in the stability of the dielectric layer of sensor V3 when immersed in water. As a result, the sensor started to bent and cracks were formed in the insulation layer. This effect is clearly visible in the measurement results shown in figure 9.12. During this measurement, the sensor was kept in a $60mM$ NaCl solution for 14.5 hours. During this time, low potentials and a potential decrease is visible. Due to the cracks, a electric path was created between the sensing electrode and reference electrode. Causing the sweat sensor, which is basically a chemical cell, to drain. This heavily damaged the sensor. Furthermore, the measured potentials were low since the emerged electric path was effecting the measurement, comparable to a low resistance of $Rn$ from the sensor model explained in section 5.3.
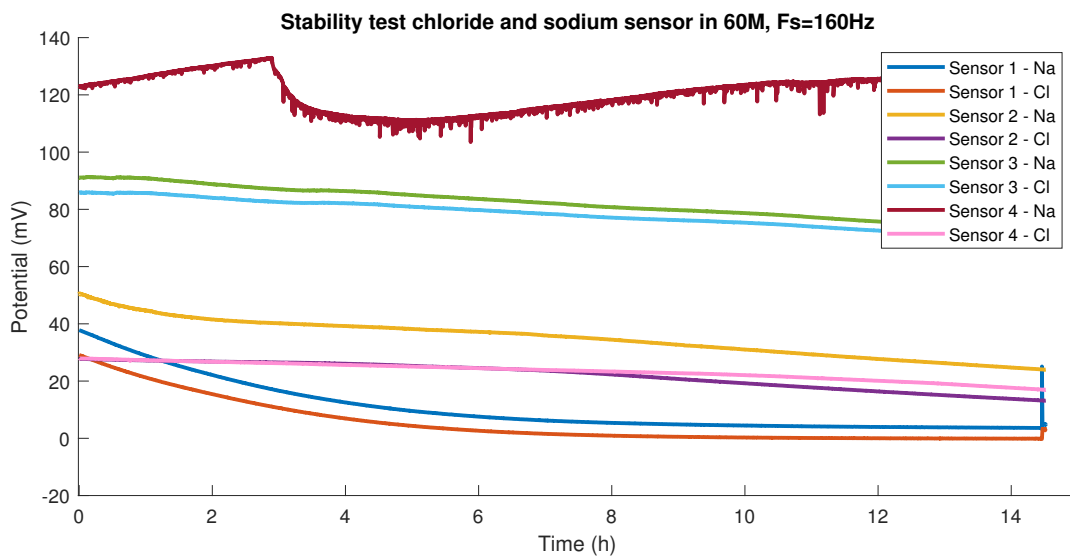


Figure 9.12: Open-circuit potential responses of chloride and sodium sensor V3 in 60mM solution for 14.5 hours.

The tear down in the dielectric was stopped by adding an layer of water resistant dielectric. It was tried to revive the potential of the reference electrode by applying the reversed effect, e.g. immersing the sensor in very high concentrations of salt while shorting the reference and ion-selective electrode. This effect increased the potential for a short period. However, the electrodes and membranes were damaged too much making it unable to maintain a stable potential. Figure 9.13 presents the sensitivity response to different NaCl concentrations. As can be seen, the sensitivity effect for NaCl is still visible and the potential was slightly recovered. However, the potential was draining making it unable to conduct further usefully measurements.
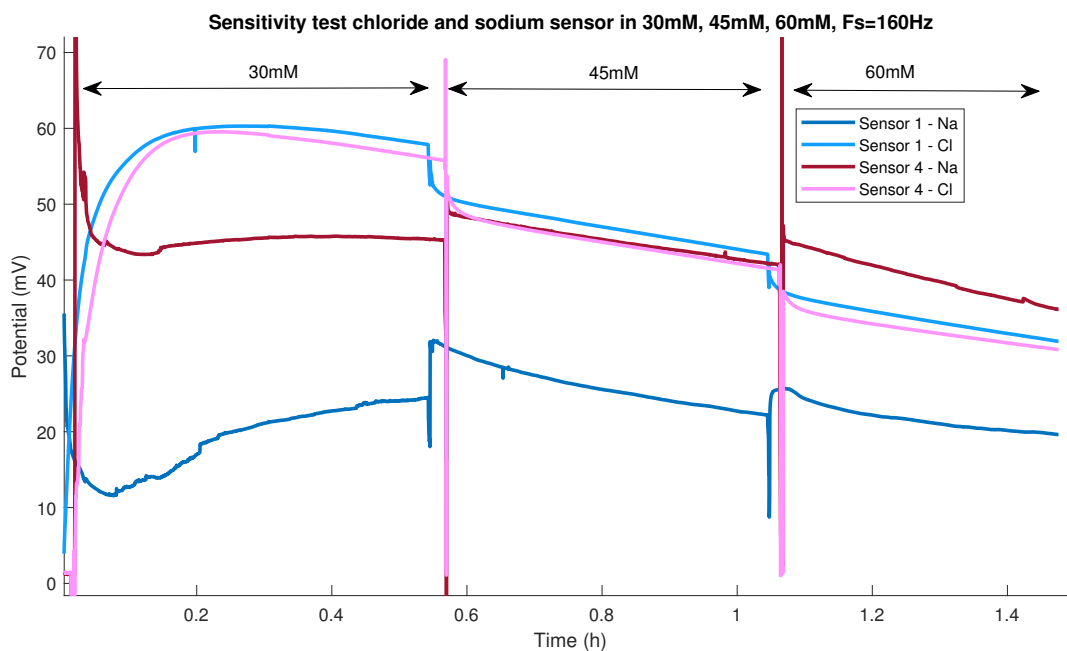
Figure 9.13: Open-circuit potential responses of chloride and sodium sensor V3 in 30mM, 45mM and 60mM NaCl solution.

## 9.2. Sweat collector

In this first experiment, the combination of the sweat sensor and sweat collector was tested with a sodium selective sensor. Unfortunately, the combination was not working sufficient for a reliable measurement. In figure 9.14 it is clear that no valuable data was obtained. The expected output for this sensor in a $30mM$ NaCl solution was expected to be around 80mV. However, the data was unstable, especially during the first minutes. The experiment was nevertheless useful since multiple recommendations were formed to make a future combination of the collector and sensor more successful. This is discussed in more detail in section 10.
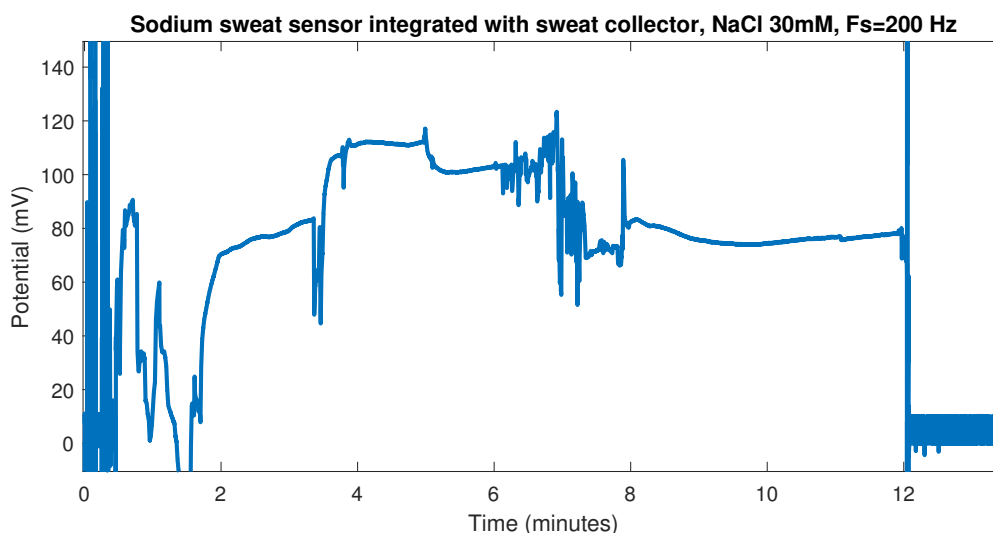
Figure 9.14: Open-circuit potential responses of sodium sensor in 30mM solution via sweat collector.

## 9.3. Sweat stimulator

The sweat stimulator is tested on one human volunteer following the protocol as mentioned in chapter 8. The sweat stimulator was used with the following settings:

- PDC at 1 KHz

- 1.2mA max current

- Voltage ramp up during the first minut

- 25V max voltage

- 6 minutes stimulation in total

The measurement results from the experiment are presented in table 9.1, the sweat collection sites are indicated in figure 8.3.

Table 9.1: Sweat weight increase in 30 minutes at stimulator area L1 and at control location L2 and L3.

| Weight | L1 (mg) | L2 (mg) | L3 (mg) |
|---|---|---|---|
| Mesh before | 528.24 | 492.87 | 480.15 |
| Mesh after | 641.98 | 533.64 | 515.38 |
| Sweat weight | 113.74 | 40.77 | 35.23 |

The sweat increase was determined by the difference between sweat weight at L1 and the average sweat weight of L2 and L3, as described in section 8.3.3.

$$m_{L_1} = 113.74 mg \tag{9.1}$$

$$m_{L_{2,3\_average}} = 38.00 mg \tag{9.2}$$

$$\Delta m_{L_1} = 113.74 - 38.00 = 75.74 mg \approx 75.74 \mu l \tag{9.3}$$

The sweat increase due to the sweat stimulation was calculated to be 75.74 $\mu l$, this result proofed the working principal of the sweat stimulator.

During the experiment, the skin irritation was also frequently monitored. The skin irritation did not exceeded the limit of unacceptable. The skin irritation was not sensible nor visible after 90 minutes. For the same participant, the skin irritation in the hospital sweat stimulation was visible for 180 minutes. Pictures of the visible skin irritation are illustrated in appendix C.

Since the experiment was classified as successful, it was decided not to test other participants. It will be more useful to test the sweat stimulator in a clinical trail in CF patients.

# 10

# Discussion

In this chapter, the design choices, production techniques and results are discussed. The main goal of the project was to perform research into the development of a sweat sensor and to provide a proof of principle for its use in real-time monitoring of medicine effectiveness in CF patients. Since this objective required a multidisciplinary approach, the discussion covers a range of topics from more theoretical to practical. Some of the discussion points result in recommendations for future research, the most important recommendations are concluded in chapter 11.

## 10.1. Production of sweat sensor

The production of the sweat sensor included screen-printing and the production of the membranes. In the following section, the design choices and the practical problems related to the production are discussed and theoretical solutions are proposed.

### 10.1.1. Screen-printing

Screen-printing is the first step in the production of the sweat sensor. Any form of an error in this phase influences the performance of the sensor. During the project, multiple issues concerning screen-printing had to be faced, as described in chapter 4.

Some of the issues could be solved by using a different design or another substrate. Several issues were related to the quality of available materials, such as, inks being expired or screens being contaminated. This demonstrated the importance of high quality materials. The usage of new materials of high professional quality will increase the screen-printing quality. During this study, it was explored whether it would be possible to produce a batch of sweat sensors in a professional screen-printing production hall. However, time constraints and financial constraints made this impossible during this study. Using a professional production hall in future research would improve the sensor on the following points:

- Improved consistency between sensors because of

    - Usage of new inks
    - More consistent ink thickness
    - Better alignment of different layers

- Less air bubbles due to a better drying method and usage of new screens

- Better adhesion due to cleaning facilities for the substrate

- Higher resolution in screen mask compared to vinyl plotter

To increase the quality of the screen-printing even more it would be interesting to add carbon fibers to the conducting inks. In the study from Bandodkar *et al.*, carbon fibers were added to the carbon and the Ag/AgCl inks, at 1.5%w/w and 1.2%w/w, respectively, to increase the tensile strength of the printed electrodes [49]. This could enhance the life-time in bending conditions.

In the screen-printing process, the formation of bubbles and cracks in the dielectric formed most of the problems. As explained in chapter 4, the bubbles were mainly caused due to the stickiness of the ink. The ink stuck to the screen when the screen was lifted, making it possible for air to get under the ink. The stickiness of the ink was partly solved by adding solvent to the ink to make it less sticky and by using a new, less contaminated screen. Furthermore, using a different dielectric with a better solvent could solve these problems. After the prototyping study, a dielectric ink from DuPont (Dielectric 8153) was tested and performed better with respect to not forming bubbles, as can be seen in figure 10.1. Although the DuPont 8153 ink was the oldest ink (2015) compared to the other tested dielectric inks (2016 and 2018), the solvent was more present in the ink. However, the DuPont 8153 is not yet tested by immersing in water, further research is needed to evaluate the performance in the sweat sensor application.
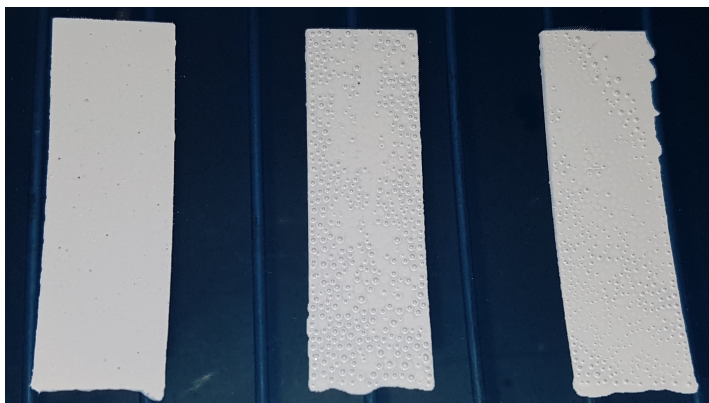


Figure 10.1: Different dielectric inks tested on PET, from left to right, Dupont 8153 (2015), SunChemical D2080121P12 (2016), SunChemical D2080121P12 (2018).

The cracks in the dielectric were formed due to stresses between the dielectric and substrate. Probably, this occurred due to the hygroscopic qualities of the PET substrate, making the PET substrate extend in water while the ink site was not hygroscopic. This could be solved by limiting the hygroscopic qualities of the substrate, for example by adding an extra dielectric layer at the other site of the PET substrate. Another solution is preventing the dielectric from forming cracks by using more flexible and stretchable ink.

In the final product, the sensor system should be save to use by operators and patients. The read-out circuit for the sweat sensor works on low voltages ($<12V$) and can be isolated from the patient which minimises the hazard of a electric shock. The sensor itself is not expected as high risk for humans since most of the materials are not a hazard to humans. However, some of the solvents used in production can be classified as hazardous. Future research should prove whether traces of these solvents used are not a hazard during the application on patients.

Screen-printing was chosen as production technique, being one of the reasons the possibility to create multiple prototypes during this project. Other techniques such as ISE-FETs were not chosen since these techniques did not allowe for prototyping in a short time. However, using ISE-FETs in this application could be beneficial since the sensor can become much smaller compared to screen-printing and is directly integrated with the electronic circuit. In theory, the technique behind the reference membrane and ion-selective electrodes used in this study can also be applied to ISE-FETs. However, future research should investigate whether these techniques indeed can be applied and whether it is cost efficient compared to the usage of (disposable) screen-printed sensors.

### 10.1.2. Reference membrane composition

The salt used in the reference membrane was sodium chloride (NaCl). This was used since this was also used in the PVB membrane of a sodium sensor with an application similar to this study. However, also other salts are commonly used in references membranes, especially potassium chloride (KCl) is often used. The mobility difference of $K^+$ and $Cl^-$ in KCl is the least among chlorides, which creates smaller liquid junction potential and a minor correction to the standard potential. Therefore, KCl would be a better salt to use in theory. It must be investigated whether this also applies for the PVB membrane.

Multiple problems were faced when creating a uniform mixed membrane which is easy to drop-cast. Therefore, the membranes could differ between sensors resulting in non-comparable results. In literature,

none of these practical problems are mentioned. However, also none of the papers included clear pictures of the reference membranes. This may indicate that they also had problems producing a uniform mixed membrane. During this study, the PVB and NaCl were not solved completely in both ethanol as methanol. This problem was partly solved by reducing the NaCl particle size and using an ultrasonic bath for mixing. However, wetting techniques of PEDOT:PSS in inkjet print of uniform PEDOT:PSS layers could possibly also be applied to the PVB membrane [82]. Exploring the effect of adding a co-solvent such as isopropanol during the membrane composition is therefore interesting for future research.

The membrane was drop-casted with a spoon during this study. Using a piston-driven microliter pipette would have been beneficial to make more uniform membrane volumes between sensors. Furthermore, the pressure applied during the drop-casting with these pipette could possibly reduce the bubble formation in the membrane. In any case, future research is necessary to improve the process to decrease the bubble formation.

### 10.1.3. Sodium ionophore X membrane
During this study, Sodium ionophore X was used for the sodium selective membrane. As mentioned in chapter 4, for the composition of one membrane, $0.3mg$ of KtCB and $1mg$ of Sodium Ionophore X was necessary. However, the weight scale available in the lab was only capable of measuring with $0.1mg$ accuracy. To minimise the measurement error, the membranes were produced in larger batches. However, a more accurate weight scale will be beneficial to minimise these errors further.

### 10.1.4. Sensor stability
To make the sensor more stable, a technique used in a study from Ghosh, Chung, and Rieger in the development of a more stable sodium sensor [83] could be considered in future research. Ghosh, Chung, and Rieger used chitosan/Prussian blue nanocomposite (ChPBN) as the solid contact layer for an all-solid-state sodium ion-selective electrode in a potentiometric sodium ion sensor. The ChPBN layer exhibited high redox capacitance and fast charge transfer capability, which significantly enhanced the performance of the sodium ion-selective electrode [83].

Another technique for the reference membrane composition used in a study from Wang *et al.* was the usage of Polyvinyl Acetate (PVA) instead of Polyvinyl Butyral (PVB) [84]. They reported a highly stable potential even after 3 months' storage. However, their potential decrease was large during usage in experiments. Using an electrode surface of $0.10\ cm^2$ resulted in $50mV$ decrease in 14 hours, while a electrode surface of $7.23\ cm^2$ had only a negligible potential decrease. During this study, it is not explicitly researched what the influence of the electrode surface is on the long-term stability. This should be investigated in future research.

## 10.2. Sweat collector
During sweat collection in hospitals, a sweat collector which thightly attaches to the skin is currently used. This results in patient discomfort. The sweat collector used during this study was based on a flexible substrate with hydrophilic qualities to collect sweat. As a benefit, it does not result in patient discomfort. Therefore, this technique could also be interesting to replace currently used sweat collectors in hospitals as orally suggested by H. Panhuis, research assistant from WKZ Utrecht, The Netherlands.

The design of the sweat collector was based on a design for the collection of sweat from athletes. Creating an adequate connection between the sensor and the collector turned out to be difficult for the following reasons:

- Attaching the sensor to the surface of the collector was difficult due to the irregularities of the sweat sensor surface.

- The size of the sweat sensor combined with the sweat sensor appeared to be too large for use in a minimal sweat flow.

Nevertheless, the experiences obtained helped to create new design suggestions for future research.

The pilocarpine gel disks used during the experiment was designed for the RVS electrodes used in the experiment. In a future wearable application, these disk should be adjusted to fit in a wearable device and should be optimised for easy application. This objective was not yet in the scope of this project.

## 10.3. Sweat stimulator

The stimulator built was based on the working principle of a current mirror. In this study it was only aimed to proof the principle of sweat stimulation with CDC and PDC. Therefore, a circuit optimised on aspects such as power efficiency, digital control and production has not been designed yet. For example, to match the transistors a simple series resistance has been used. Furthermore, opportunities exist to improve the suppression of inaccuracies. A more accurate way to suppress the inaccuracies that occur from channel length modulation would be the usage of a cascode current mirror [81].

## 10.4. Results

In the following section, the results obtained from this study are discussed.

### 10.4.1. Sweat sensor

The difference in potential is large in the region of interests, 30-60$mmol/l$, which is a promising signal. The sweat sensor sensitivity was approximately 1$mV$ per $mmol/l$, which is comparable with the results from Bandodkar *et al.* [49].

Possible explanations for the fluctuations repeating every 5 to 10 minutes during the long-term measurements with sweat sensor v1 are:

- Little movement of the sensor in the sample causing a change in contact surface with the membrane or electrode

- Insufficient isolation of the tracks causing a small leakage current

- Small temperature differences which can influence the potential

The sensors showed unstable behaviour in demi-water (NaCl concentrations around 0$mmol/l$). An explanation for this is that low concentrations can damage the membrane easily since the strength to withdraw the salt from the membrane is large. The chemical transition is taking longer, resulting in an unstable potential. Possible reasons for these instabilities are listed below:

- Change in the temperature from the sample under test

- Movements causing a change in contact surface between the sample and membrane

- Leakage in the isolation layers, can lead to a run out of the chemical cell

The sweat sensor has not yet extensively been tested for its specificity for chloride and sodium. As explained in chapter 8, it can be expected that other factors such as temperature, sensitivity and long-term stability have the most influence on the measurement results and not the selectivity of the sensor. However, in this study, the sweat sensors has not yet been tested in real sweat or artificial sweat. To determine the uncertainties related to the selectivity, it would be beneficial to test the sensor in solutions other than NaCl solutions. An example used in literature is the usage of artificial sweat comprising various potential interfering electrolytes, including NaCl, $Na_2SO_4$, $NaHCO_3$, KCl, $MgCl_2$ $6H_2O$, $NaH_2PO_4$, $CaCO_3$ and $NH_4OH$.

### 10.4.2. Sweat collector

During the experiments, it was not possible to obtain reliable measurement. This was caused by the problems described below:

- Hydrophobic behaviour of the membrane compared to the hydrophilic qualities of the sweat collector, causing the sample to flow sideways of the membrane instead of on top of it.

- Width of the collecting channel too large causing the sample going in too fast. Which results in the sample went in as parts instead of in a consistent flow.

- Distance between reference electrode and sensing electrode too large, because of this it was possible to have air bubbles in between resulting in an open circuit.

- Inconsistent surface of reference membrane, this caused a blockade for the sample and forced the sample to flow sideways of the membrane instead of on top of it.

### 10.4.3. Sweat stimulator

The aim was to collect $60\mu l$ comparable to the sweat stimulation tests in hospitals. During this study, an increase of $75.74\mu l$ and a total of $113.7\mu l$ of sweat was collect. However, the collecting system in the hospital is less efficient compared to using an absorbing mesh as used in this experiment. The experiment from this study is comparable with sweat collected in hospitals in the case the collector in the hospital has 55% efficiency compared to the absorbing mesh. Since the efficiency of the collectors in the hospital compared to this study is expected to be more than 55%, it is concluded that the experiment was successful.

The skin irritation after the sweat stimulation experiment was less and disappeared in 90 minutes instead of 180 minutes during a comparable experiment with the same participant in the current hospital test. However, this could also be due to other factors than the stimulating signal, for example, temperature, cleaning and condition of the participant.

For safety and ethical reasons, the stimulator has only been tested on one human volunteer until now. Although this single test provided proof of principle, from a scientifically point of view, more clinical evidence on the consistency and efficiency is needed. To collect more evidence for this stimulator, a clinical trial with much more participants is necessary. For these trials a medically approved device is necessary, which requires extra safety measures and detailed documentation.

# 11

# Conclusion and recommendations

During this study, a sweat sensor system has built for a proof of principle for real-time monitoring of medicine effectiveness in CF trough sweat. For this proof of principle, the following sub-parts of the sensor system have been made and tested:

- Three sweat sensor prototypes

- A single channel read-out circuit

- A multi channel read-out circuit

- A sweat stimulator

- A sweat collector for the combination with the sweat sensor

During the project, multiple successful experiments were conducted. However, also multiple issues were faced which resulted in multiple design iterations and recommendations for further work. At the start of the project, system requirements were formulated. In the following section, it is concluded which system requirements can now be met and what is recommended to meet the remaining requirements.

*R1. The system should be capable of reliably monitoring a patient for 24 hours.*
The sensitivity range for the region of interest, $30 mmol/l$ - $60 mmol/l$, is for both the chloride as sodium sensor obtained with a potential change of $35 mV$ and $30 mV$ respectively. Therefore, it can be concluded that the system has a sweat sensor sensitivity of approximately $1 mV$ per $mmol/l$ for sodium and chloride in the region of interest which is comparable with the results from Bandodkar *et al.* [49].

From the long-term tests with sweat sensor V3, it is concluded that it is possible to build a potentiometric screen-printed sweat sensor with a stability for up to 90 hours in a 7mV range (input referred). This will translate to a concentration range of $\pm 4 mmol/l$. However, in a shorter time period of 24 hours, this range can be below $\pm 2 mmol/l$.

A discussion point is the reproducibility between sensors. Sensor V3 was designed to improve the reproducibility between sensors. However, a complete production batch with reliable sensors could not be built yet, mainly due to the problems faced in prototype v3 with the screen-printing inks.

With the following recommendations, the stability and reproducibility of the sweat sensor could be improved:

- Exclusively use new inks to avoid problems related to the ink life-time.

- Use a professional screen-printing production hall to avoid problems related to contaminated materials and for better screen-printing resolution, reliability, consistency and alignment.

- Improve the reference membrane structure by creating a more gel-like structure for better drop-casting to avoid bubble forming and inconsistencies.

85

To enhance real-time sweat monitoring, the sweat flow and volume have to be large enough. During measurement with patients in rest, an enlarged sweat sample surface is necessary to obtain enough sweat for the sweat sensor. The usage of a sweat collector is suggested to solve this problem. However, the following is recommended to combine successfully the sweat sensor and sweat collector:

- Scale down scaling the sensor size to reduce the sweat volume needed for complete coverage of the sensor.

- Develope a membrane structure which has a flat surface and hydrophilic behaviour for better sample flow.

- Improve the sweat collector design by reducing the sample flow speed to increase the time for sampling.

Besides obtaining the sample surface to increase the sweat collection also a sweat stimulater has been developed during this study. The stimulator can artificially increase the local sweat rate. During an experiment, the sweat stimulation was successful with a local sweat rate increase of $75.74 \mu l$. The stimulator is based on the principle of the sweat stimulator used in hospitals. In addition, the possibility for a PDC stimulating signal has been added. Literature showed that more efficient sweat stimulation can be obtained while using small currents for PDC which results in less skin irritation. PDC can enhance the usage of the sweat stimulator for 24 hours. In future research, the following recommendations should be considered:

- A clinical trial is necessary to obtain clinical evidence for the efficiency of the stimulator.

- From a electronic point of view, the electronic circuit could be improved on its accuracy by using a cascoded current mirror.

- By extending the electric circuit with a microcontroller and digital-analog converter, the stimulation signal can be manipulated to create other shapes than constant or pulsed signals.

In conclusion, a proof of principle for the four sub-parts is delivered for use in a system that is able to monitor reliably a patient for 24 hours. Future research is necessary to combine the sub-parts and to improve the consistency between the sensor systems to make a reliable final product.

*R2. The materials and techniques used for the system should enable the end product to become a wearable device*
Screen-printing has been used as production technique for the sweat sensor. This enables the usage of a flexible substrate which enhances the wearability on the skin of the patient. Also the sweat collector was built from a flexible substrate to enhance the wearability.

The read-out system was built with standard components which could be placed on a small wearable PCB. Future research should focus on the remaining part of the read-out system to create a complete wearable system, e.g. the energy storage, power supply control and data storage or transmission.

The components used in the sweat stimulator circuit can be minimised to fit on a small wearable pcb. Future research should focus on the energy storage. In this study, three 9V batteries are used to supply the circuit. In a wearable device, a smaller and lower voltage battery system is desirable. Therefore, it is recommended to add a power supply with voltage booster circuit to the circuit to maintain a stimulation voltage of $25V$.

The pilocarpine gel disks used during the experiment was designed for the RVS electrodes used in the experiment. In a future wearable application, these disk should be adjusted to fit in a wearable device and should be optimised for easy application. This objective was not yet in the scope of this project.

In conclusion, the device is built from materials and components which can be implemented in a wearable device. However, integration and minimisation has to be accomplished by future research to make a complete wearable device out of it.

*R3. The system should be safe for the operator and patient.*
In the presented sweat sensor system, the sweat collector and sweat stimulator are the only parts of the system in direct contact with the patient, e.g. the sweat sensor is not in direct contact with the patient. Therefore, the risk of patient contact with the electronics from the read-out system is minimalised. Furthermore, the read-out circuit for the sweat sensor works on low voltages (<12V) which minimises the hazard of a electric shock. Direct patient contact with the sensor is unlikely. The sensor itself is not expected as high risk since

most of the materials are not a hazard to humans. However, some of the solvents used in production can be classified as hazardous. Future research should prove whether traces of these solvents used are not a hazard during the application on patients.

The sweat stimulator transfers energy into the patient's body, due to the following measures, the risk has been minimised:

- Using of same medical protocol as used in hospitals

- Voltage limit, $25V$

- Current limit, $1.2mA$

- Stimulation time limit, 8 min

- Current density limited to $0.17mA/cm^2$

- Batteries as energy source to protect the participant from the mains to limit the electric shock risk

- A on/off switch to stop the stimulation directly

- Usage of medically graded pilocarpine gel and electroced

- Electronics placed in an isolated box to protect the operator

- Usage of PDC in addition to CDC to potentially reduce the skin irritation.

In conclusion, the risks of the sweat sensor, read-out circuit and sweat collector are limited to make the system safe for the operator and patient. Furthermore, the sweat stimulator can also be safely used under the mentioned limitations.

## Final conclusion

A proof of concept for a sweat sensor system for real-time patient monitoring is provided. The system consist out of four sub-parts which are individually validated. The sweat sensor is successful validated based on its sensitivity, selectivity and long-term stability. Future research should improve the reproducibility. Especially, the production of screen-printing and making more uniform membranes has to be improved.

The sweat sensor parts are built from materials and components which can be implemented in a wearable device. However, integration and minimisation has to be accomplished by future research to make a complete wearable device out of it. The safety risks of the sweat stimulator are minimised by not exceeding limits mentioned in protocols from hospitals, a clinical trial is necessary to prove if the safety measures are usefully in decreasing skin irritation after stimulation.
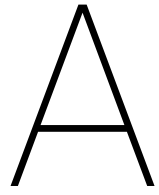
# Bibliography

[1]    J. Noordhoek, "Nederlandse cystic fibrosis registratie 2017", *Nederlandse Cystic Fibrosis Stichting*, Sep. 2018.

[2]    R. Morello *et al.*, "Design of a wearable sweat sensor for diagnosing cystic fibrosis in children", in *2013 IEEE International Symposium on Medical Measurements and Applications (MeMeA)*, May 2013, pp. 268–273. DOI: 10.1109/MeMeA.2013.6549750.

[3]    F. Bono-Neri, C. Romano, and A. Isedeh, "Cystic fibrosis: Advancing along the continuum", *Journal of Pediatric Health Care*, 2018, ISSN: 0891-5245. DOI: https://doi.org/10.1016/j.pedhc.2018.08.008.

[4]    M. C. Hagemeijer *et al.*, "Translational research to enable personalized treatment of cystic fibrosis", *Journal of Cystic Fibrosis*, vol. 17, no. 2, Supplement, S46–S51, 2018, Cystic Fibrosis Research Topics Featured at the 14th ECFS Basic Science Conference, Albufeira, Portugal, 29 March to 1 April, 2017, ISSN: 1569-1993. DOI: https://doi.org/10.1016/j.jcf.2017.10.017.

[5]    C. Woolston, *Moving forward with cystic fibrosis*, https://www.knowablemagazine.org/article/health-disease/2018/moving-forward-cystic-fibrosis, (Accessed on 02/20/2019), May 2018.

[6]    *Types of cftr mutations*, https://www.cff.org/What-is-CF/Genetics/Types-of-CFTR-Mutations/, (Accessed on 01/07/2019), 2018.

[7]    M. Ikuma and M. J. Welsh, "Regulation of cftr cl- channel gating by atp binding and hydrolysis", *Proceedings of the National Academy of Sciences*, vol. 97, no. 15, pp. 8675–8680, 2000, ISSN: 0027-8424. DOI: 10.1073/pnas.140220597.

[8]    V. Saint-Criq and M. A. Gray, "Role of cftr in epithelial physiology", *Cellular and Molecular Life Sciences*, vol. 74, no. 1, pp. 93–115, Jan. 2017, ISSN: 1420-9071. DOI: 10.1007/s00018-016-2391-y.

[9]    J. B Lyczak, C. Cannon, and G. Pier, "Lung infections associated with cystic fibrosis", *Clinical microbiology reviews*, vol. 15, pp. 194–222, May 2002. DOI: 10.1128/CMR.15.2.194-222.2002.

[10]   L. Singer and S. Keshavjee, "Lung transplantation and cystic fibrosis", *Cystic Fibrosis Canada*, Aug. 2014.

[11]   F. R. Adler *et al.*, "Lung transplantation for cystic fibrosis", *Proc Am Thorac Soc*, vol. 6, no. 8, pp. 619–633, Dec. 2009.

[12]   J. M. Beekman, "Individualized medicine using intestinal responses to CFTR potentiators and correctors", *Pediatr. Pulmonol.*, vol. 51, no. S44, S23–S34, Oct. 2016.

[13]   M. C. Fidler *et al.*, "Correlation of sweat chloride and percent predicted FEV1 in cystic fibrosis patients treated with ivacaftor", *Journal of Cystic Fibrosis*, vol. 16, no. 1, pp. 41–44, Jan. 2017.

[14]   M. J. Rock, L. Makholm, and J. Eickhoff, "A new method of sweat testing: The cf quantum sweat test", *Journal of Cystic Fibrosis*, vol. 13, no. 5, pp. 520–527, 2014, ISSN: 1569-1993. DOI: https://doi.org/10.1016/j.jcf.2014.05.001.

[15]   M. F. Servidoni *et al.*, "Sweat test and cystic fibrosis: overview of test performance at public and private centers in the state of São Paulo, Brazil", *J Bras Pneumol*, vol. 43, no. 2, pp. 121–128, 2017.

[16]   N. Traeger, Q. Shi, and A. J. Dozor, "Relationship between sweat chloride, sodium, and age in clinically obtained samples", *Journal of Cystic Fibrosis*, vol. 13, no. 1, pp. 10–14, 2014, ISSN: 1569-1993. DOI: https://doi.org/10.1016/j.jcf.2013.07.003.

[17]   Clinical and Laboratory Standards Institute (CLSI), "Sweat testing: Sample collection and quantitative chloride analysis approved guideline - third edition", *CLSI document C34-A3*, Dec. 2009.

[18]   A. Mena-Bravo and M. L. de Castro, "Sweat: A sample with limited present applications and promising future in metabolomics", *Journal of Pharmaceutical and Biomedical Analysis*, vol. 90, pp. 139–147, 2014, ISSN: 0731-7085. DOI: https://doi.org/10.1016/j.jpba.2013.10.048.

[19]    S. Jadoon *et al.*, "Recent developments in sweat analysis and its applications", *International Journal of Analytical Chemistry*, vol. 2015, pp. 1–7, Apr. 2015. DOI: `10.1155/2015/164974`.

[20]    C. Taylor, J. Hardcastle, and K. Southern, "Physiological measurements confirming the diagnosis of cystic fibrosis: The sweat test and measurements of transepithelial potential difference", *Paediatric Respiratory Reviews*, vol. 10, no. 4, pp. 220–226, 2009, ISSN: 1526-0542. DOI: `https://doi.org/10.1016/j.prrv.2009.05.002`.

[21]    N. A. Taylor and C. A. Machado-Moreira, "Regional variations in transepidermal water loss, eccrine sweat gland density, sweat secretion rates and electrolyte composition in resting and exercising humans", *Extrem Physiol Med*, vol. 2, no. 1, p. 4, Feb. 2013.

[22]    R. Baxter, F. Druggan, and A. Rad, "Histology of Sweat Glands", *Kenhub GmbH*, 2019.

[23]    C. Y. Cui and D. Schlessinger, "Eccrine sweat gland development and sweat secretion", *Exp. Dermatol.*, vol. 24, no. 9, pp. 644–650, Sep. 2015.

[24]    Pointhealth, "The Sweat Gland, How Does It Work and What Factors Affect Sweat Rate and Composition", *Pointhealth*, vol. 10, p. 14, 2006.

[25]    Y. Hu *et al.*, "Neural control of sweat secretion: A review.", *The British journal of dermatology*, vol. 178 6, pp. 1246–1256, 2018.

[26]    M. M. Reddy and P. M. Quinton, "Functional interaction of CFTR and ENaC in sweat glands", *Pflugers Arch.*, vol. 445, no. 4, pp. 499–503, Jan. 2003.

[27]    L. C. Li and R. A. Scudds, "Iontophoresis: an overview of the mechanisms and clinical application", *Arthritis Care Res*, vol. 8, no. 1, pp. 51–61, Mar. 1995.

[28]    Z. Sonner *et al.*, "The microfluidics of the eccrine sweat gland, including biomarker partitioning, transport, and biosensing implications", *Biomicrofluidics*, vol. 9, no. 3, p. 031 301, May 2015.

[29]    M. Parrilla, M. Cuartero, and G. A. Crespo, "Wearable potentiometric ion sensors", *TrAC Trends in Analytical Chemistry*, vol. 110, pp. 303–320, 2019, ISSN: 0165-9936. DOI: `https://doi.org/10.1016/j.trac.2018.11.024`.

[30]    M. Birlea, S. I. Barlea, and E. Culea, "Controlled iontophoresis for medical applications", Jan. 2007.

[31]    S. Emaminejad *et al.*, "Autonomous sweat extraction and analysis applied to cystic fibrosis and glucose monitoring using a fully integrated wearable platform", *Proceedings of the National Academy of Sciences*, 2017, ISSN: 0027-8424. DOI: `10.1073/pnas.1701740114`.

[32]    S. L. Souza, G. Graca, and A. Oliva, "Characterization of sweat induced with pilocarpine, physical exercise, and collected passively by metabolomic analysis", *Skin Res Technol*, vol. 24, no. 2, pp. 187–195, May 2018.

[33]    S. Basu, M. Mitra, and A. Ghosh, "Evaluation of sweat production by pilocarpine iontophoresis: a non-invasive screening tool for hypohidrosis in ectodermal dysplasia", *Indian J Clin Biochem*, vol. 28, no. 4, pp. 433–435, Oct. 2013.

[34]    E. Krueger *et al.*, "Iontophoresis: Principles and applications", en, *Fisioterapia em Movimento*, vol. 27, pp. 469–481, Sep. 2014, ISSN: 0103-5150.

[35]    M. Bariya, H. Yin Yin Nyein, and A. Javey, "Wearable sweat sensors", *Nature Electronics*, vol. 1, Mar. 2018. DOI: `10.1038/s41928-018-0043-y`.

[36]    R. C. Gupta, *Cystic fibrosis (cf) chloride sweat test (for parents) - kidshealth*, `https://kidshealth.org/en/parents/sweat-test.html`, (Accessed on 02/20/2019), Aug. 2015.

[37]    *11.1: Overview of Electrochemistry - Chemistry LibreTexts*. [Online]. Available: `https://chem.libretexts.org/LibreTexts/Northeastern/11%5C%3A_Electrochemical_Methods/11.1%5C%3A_Overview_of_Electrochemistry` (visited on 12/13/2018).

[38]    J. Robinson, E. Frame, and G. Frame, *Undergraduate Instrumental Analysis, Sixth Edition*. Taylor & Francis, 2005, ISBN: 9780849306501.

[39]    M. P. Mousavi *et al.*, "Avoiding Errors in Electrochemical Measurements: Effect of Frit Material on the Performance of Reference Electrodes with Porous Frit Junctions", *Analytical Chemistry*, vol. 88, no. 17, pp. 8706–8713, Sep. 2016.

[40]  Y. Segui Femenias *et al.*, "Ag/agcl ion-selective electrodes in neutral and alkaline environments containing interfering ions", *Materials and Structures*, vol. 49, no. 7, pp. 2637–2651, Jul. 2016, ISSN: 1871-6873. DOI: `10.1617/s11527-015-0673-8`. [Online]. Available: `https://doi.org/10.1617/s11527-015-0673-8`.

[41]  S. Komaba *et al.*, "All-solid-state ion-selective electrodes with redox-active lithium, sodium, and potassium insertion materials as the inner solid-contact layer", *Analyst*, vol. 142, no. 20, pp. 3857–3866, Oct. 2017.

[42]  Y. Yang and W. Gao, "Wearable and flexible electronics for continuous molecular monitoring", *Chemical Society Reviews*, Apr. 2018. DOI: `10.1039/C7CS00730B`.

[43]  W. Gao *et al.*, "Fully integrated wearable sensor arrays for multiplexed in situ perspiration analysis", *Nature*, vol. 529, no. 7587, pp. 509–514, Jan. 2016.

[44]  S. Søpstad *et al.*, "Long-term stability of screen-printed pseudo-reference electrodes for electrochemical biosensors", *Electrochimica Acta*, vol. 287, pp. 29–36, 2018, ISSN: 0013-4686. DOI: `https://doi.org/10.1016/j.electacta.2018.08.045`.

[45]  A. C. V. Mattar *et al.*, "Sweat conductivity: An accurate diagnostic test for cystic fibrosis?", *Journal of Cystic Fibrosis*, vol. 13, no. 5, pp. 528–533, 2014, ISSN: 1569-1993. DOI: `https://doi.org/10.1016/j.jcf.2014.01.002`.

[46]  V. Dam, M. Zevenbergen, and R. van Schaijk, "Toward wearable patch for sweat analysis", *Sensors and Actuators B: Chemical*, vol. 236, pp. 834–838, 2016, ISSN: 0925-4005. DOI: `https://doi.org/10.1016/j.snb.2016.01.143`.

[47]  T. Guinovart *et al.*, "A potentiometric tattoo sensor for monitoring ammonium in sweat", *Analyst*, vol. 138, pp. 7031–7038, 22 2013. DOI: `10.1039/C3AN01672B`.

[48]  T. Guinovart *et al.*, "A reference electrode based on polyvinyl butyral (pvb) polymer for decentralized chemical measurements", *Analytica Chimica Acta*, vol. 821, pp. 72–80, 2014, ISSN: 0003-2670. DOI: `https://doi.org/10.1016/j.aca.2014.02.028`.

[49]  A. J. Bandodkar *et al.*, "Epidermal tattoo potentiometric sodium sensors with wireless signal transduction for continuous non-invasive sweat monitoring", *Biosensors and Bioelectronics*, vol. 54, pp. 603–609, 2014, ISSN: 0956-5663. DOI: `https://doi.org/10.1016/j.bios.2013.11.039`.

[50]  D. P. Rose *et al.*, "Adhesive RFID Sensor Patch for Monitoring of Sweat Electrolytes", *IEEE Trans Biomed Eng*, vol. 62, no. 6, pp. 1457–1465, Jun. 2015.

[51]  F. Cao *et al.*, "Microscale chloride sensor", *Carnegie Mellon University*, 2006.

[52]  L. Trnkova *et al.*, "Amperometric Sensor for Detection of Chloride Ions", *Sensors (Basel)*, vol. 8, no. 9, pp. 5619–5636, Sep. 2008.

[53]  J. Huang *et al.*, "Fully organic graphene oxide-based sensor with integrated pump for sodium detection", *icSPORTS 2013 - Proceedings of the International Congress on Sports Science Research and Technology Support*, pp. 83–88, Jan. 2013.

[54]  G. Liu *et al.*, "A wearable conductivity sensor for wireless real-time sweat monitoring", *Sensors and Actuators B: Chemical*, vol. 227, pp. 35–42, 2016, ISSN: 0925-4005. DOI: `https://doi.org/10.1016/j.snb.2015.12.034`. [Online]. Available: `http://www.sciencedirect.com/science/article/pii/S0925400515307516`.

[55]  D.-H. Choi *et al.*, "A wearable potentiometric sensor with integrated salt bridge for sweat chloride measurement", *Sensors and Actuators B: Chemical*, vol. 250, pp. 673–678, 2017, ISSN: 0925-4005. DOI: `https://doi.org/10.1016/j.snb.2017.04.129`.

[56]  J. R. Sempionatto *et al.*, "Skin-worn soft microfluidic potentiometric detection system", *Electroanalysis*, vol. 31, no. 2, pp. 239–245, 2019. DOI: `10.1002/elan.201800414`.

[57]  C. C. Gomez *et al.*, "Pulsed direct and constant direct currents in the pilocarpine iontophoresis sweat chloride test", *BMC Pulm Med*, vol. 14, p. 198, Dec. 2014.

[58]  S. Claus, "Designing with transparent lighting: A Do-It-Yourself approach", May 2016.

[59]  R. Mikkonen, "Evaluation of commerically available silver inks screen printed on a PPE based substrate", Apr. 2017.
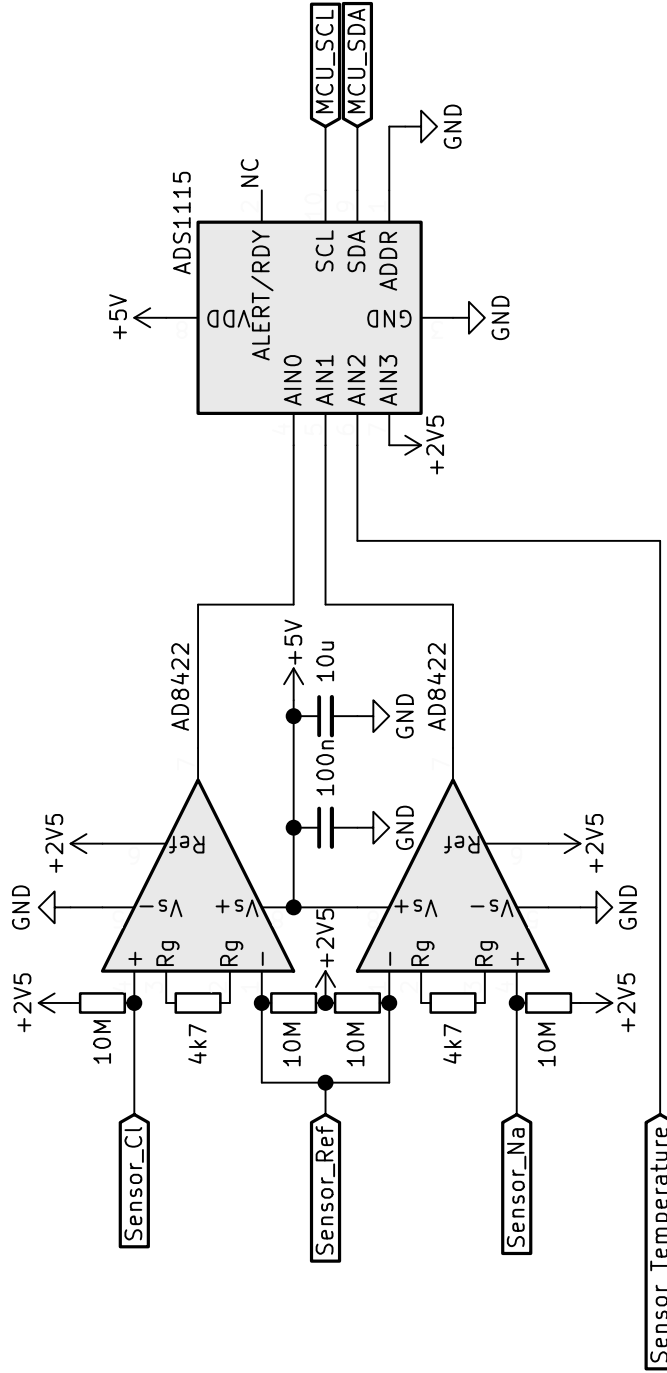
[60]  M. Sophocleous and J. K. Atkinson, "A review of screen-printed silver/silver chloride (ag/agcl) reference electrodes potentially suitable for environmental potentiometric sensors", *Sensors and Actuators A: Physical*, vol. 267, pp. 106–120, Nov. 2017, ISSN: 0924-4247. DOI: `https://doi.org/10.1016/j.sna.2017.10.013`.

[61]  *Metrohm reference electrodes*, (Accessed on 01/07/2019). [Online]. Available: `https://www.metrohm-autolab.com/Products/Echem/Accessories/ReferenceElectrodes`.

[62]  S. Roy, M. David-Pur, and Y. Hanein, "Carbon nanotube-based ion selective sensors for wearable applications", *ACS Applied Materials & Interfaces*, vol. 9, no. 40, pp. 35 169–35 177, 2017, PMID: 28925684. DOI: `10.1021/acsami.7b07346`. [Online]. Available: `https://doi.org/10.1021/acsami.7b07346`.

[63]  M. McCaul *et al.*, "Wearable platform for real-time monitoring of sodium in sweat", *ChemPhysChem*, vol. 19, no. 12, pp. 1531–1536, 2018. DOI: `10.1002/cphc.201701312`. [Online]. Available: `https://onlinelibrary.wiley.com/doi/abs/10.1002/cphc.201701312`.

[64]  D. H. Choi *et al.*, "Wearable potentiometric chloride sweat sensor: The critical role of the salt bridge", *Analytical Chemistry*, vol. 88, no. 24, pp. 12 241–12 247, 2016, PMID: 28193033. DOI: `10.1021/acs.analchem.6b03391`.

[65]  S. Anastasova *et al.*, "A wearable multisensing patch for continuous sweat monitoring", *Biosensors and Bioelectronics*, vol. 93, pp. 139–145, 2017, Special Issue Selected papers from the 26th Anniversary World Congress on Biosensors (Part II), ISSN: 0956-5663. DOI: `https://doi.org/10.1016/j.bios.2016.09.038`.

[66]  A. M. Cadogan *et al.*, "Sodium-selective polymeric membrane electrodes based on calix[4]arene ionophores", *Analyst*, vol. 114, pp. 1551–1554, 12 1989. DOI: `10.1039/AN9891401551`. [Online]. Available: `http://dx.doi.org/10.1039/AN9891401551`.

[67]  D. H. Choi *et al.*, "Sweat test for cystic fibrosis: Wearable sweat sensor vs. standard laboratory test", *Journal of Cystic Fibrosis*, vol. 17, no. 4, e35–e38, Jul. 2018.

[68]  V. D. Matteis *et al.*, "Chromogenic device for cystic fibrosis precocious diagnosis: A "point of care" tool for sweat test", *Sensors and Actuators B: Chemical*, vol. 225, pp. 474–480, 2016, ISSN: 0925-4005. DOI: `https://doi.org/10.1016/j.snb.2015.11.080`.

[69]  C. Nie *et al.*, "Bio-inspired microfluidics for wearable sensors", *Proceedings*, vol. 1, p. 824, Nov. 2017. DOI: `10.3390/proceedings1080824`.

[70]  M. A. G. Zevenbergen *et al.*, "Solid state ph and chloride sensor with microfluidic reference electrode", in *2016 IEEE International Electron Devices Meeting (IEDM)*, Dec. 2016, pp. 26.1.1–26.1.4. DOI: `10.1109/IEDM.2016.7838482`.

[71]  V. Dam, M. Zevenbergen, and R. van Schaijk, "Flexible ion sensors for bodily fluids", *Procedia Engineering*, vol. 168, pp. 93–96, 2016, Proceedings of the 30th anniversary Eurosensors Conference – Eurosensors 2016, 4-7. September 2016, Budapest, Hungary, ISSN: 1877-7058. DOI: `https://doi.org/10.1016/j.proeng.2016.11.155`.

[72]  J. Gonzalo-Ruiz *et al.*, "Early determination of cystic fibrosis by electrochemical chloride quantification in sweat", *Biosensors and Bioelectronics*, vol. 24, no. 6, pp. 1788–1791, 2009, ISSN: 0956-5663. DOI: `https://doi.org/10.1016/j.bios.2008.07.051`.

[73]  L. Tymecki, S. Glab, and R. Koncki, "Miniaturized, planar ionselective electrodes fabricated by means of thick-film technology", *Sensors*, vol. 6, pp. 390–396, Apr. 2006. DOI: `10.3390/s6040390`.

[74]  B. Schazmann *et al.*, "A wearable electrochemical sensor for the real-time measurement of sweat sodium concentration", *Analytical Methods*, vol. 2, Apr. 2010. DOI: `10.1039/B9AY00184K`.

[75]  P. P. L. Regtien, *Electronic Instrumentation*, English. VSSD, 2005, p. 387, ISBN: 9071301435.

[76]  C. Smith *et al.*, "Design data for footwear: Sweating distribution on the human foot", *International Journal of Clothing Science and Technology*, vol. 25, Feb. 2013. DOI: `10.1108/09556221311292200`.

[77]  C. A Machado-Moreira *et al.*, "Sweat secretion from the torso during passively-induced and exercise-related hyperthermia", *European journal of applied physiology*, vol. 104, pp. 265–70, Sep. 2008. DOI: `10.1007/s00421-007-0646-x`.
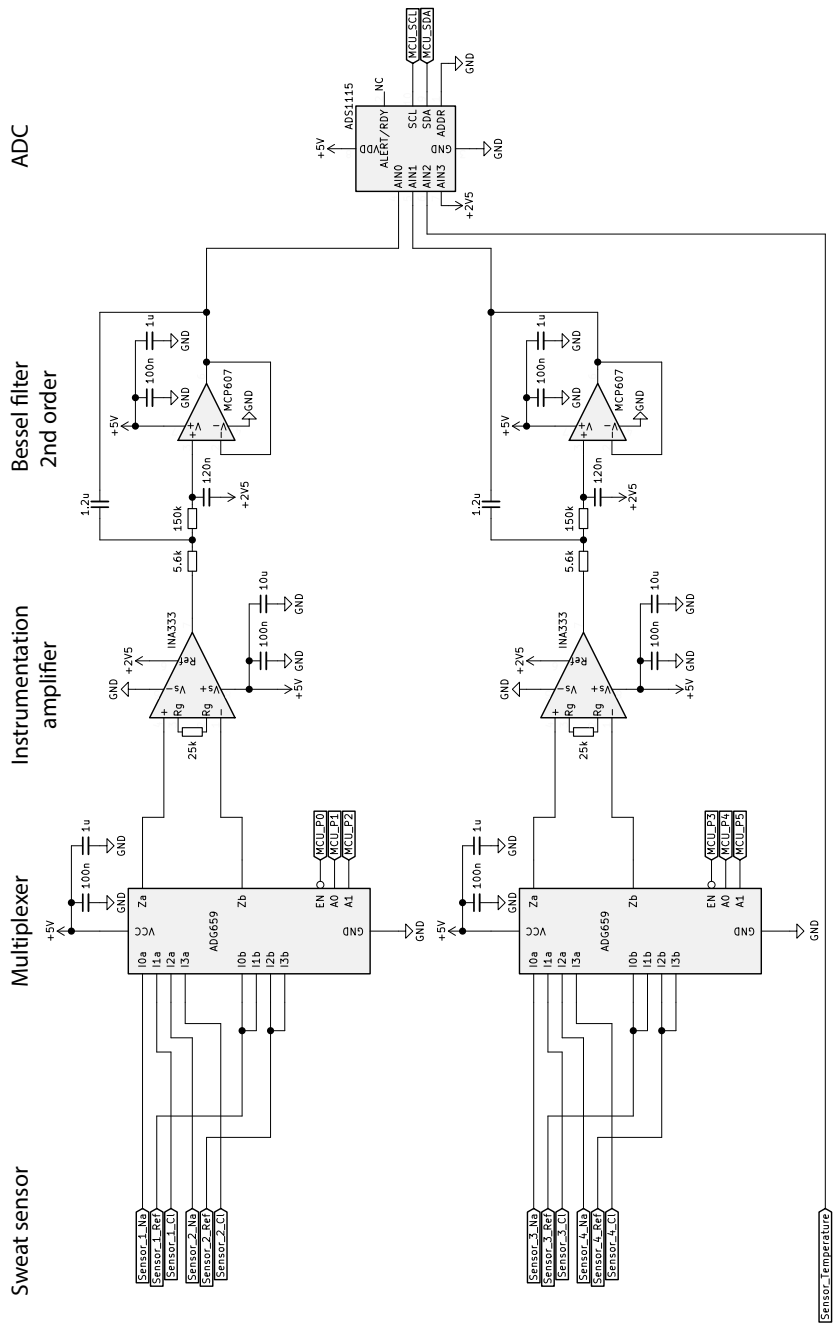
[78]   C. A Machado-Moreira *et al.*, "Local differences in sweat secretion from the head during rest and exercise in the heat", *European journal of applied physiology*, vol. 104, pp. 257–64, Sep. 2008. DOI: 10.1007/s00421-007-0645-y.

[79]   ELITechGroup, "Macroduct/sweat chek - sweat testing system", *Elitech Biomedical Systems - Laboratory CF Diagnosis*, May 2014.

[80]   *Lm134/lm234/lm334 3-terminal adjustable current sources*, LM234, Rev. 4, Texas Instruments, May 2013.

[81]   G. E. Ólafsdóttir, "An Implantable Spinal Cord Stimulator with Adaptive Voltage Compliance for Freely Moving Rats", Sep. 2017.

[82]   S. Kommeren *et al.*, "Combining solvents and surfactants for inkjet printing pedot:pss on p3ht/pcbm in organic solar cells", *Organic Electronics*, vol. 61, pp. 282–288, 2018, ISSN: 1566-1199. DOI: https://doi.org/10.1016/j.orgel.2018.06.004. [Online]. Available: http://www.sciencedirect.com/science/article/pii/S1566119918302957.

[83]   T. Ghosh, H. J. Chung, and J. Rieger, "All-Solid-State Sodium-Selective Electrode with a Solid Contact of Chitosan/Prussian Blue Nanocomposite", *Sensors (Basel)*, vol. 17, no. 11, Nov. 2017.

[84]   S. Wang *et al.*, "Wearable sweatband sensor platform based on gold nanodendrite array as efficient solid contact of ion-selective electrode", *Analytical Chemistry*, vol. 89, no. 19, pp. 10 224–10 231, 2017, PMID: 28862001. DOI: 10.1021/acs.analchem.7b01560.

[85]   WESCOR INC, "Macroduct sweat collection system - model 3700 sys", *instruction/service manual*, 2004.

# A

# Schematics

Sweat sensor    Instrumentation    ADC
                amplifier

Positive_electrode

Negative_electrode

GND

Dual 2N3906

E1 1k

E2 1k

C1

C2

2N3904

1k

GND

180k

10p

GND

LM358

100n

VDD

GND

Max_current

R_rot

GND

2.2k

Diode

GND

4k7

LED

GND

1k

Diode

1k

Freq
R_rot

LM317

VO

VI

ADJ

300

1u

GND

GND

Max Voltage

100n

GND

100n

GND

On/Off switch

VDD

9V

9V

9V

GND

SW_DC_AC

SW_Low_High_freq

VDD

100n

GND

LM555

VCC

Q

DIS

THR

GND

GND

TR

CV

R

NC

NC

VDD

100n

33n

10u
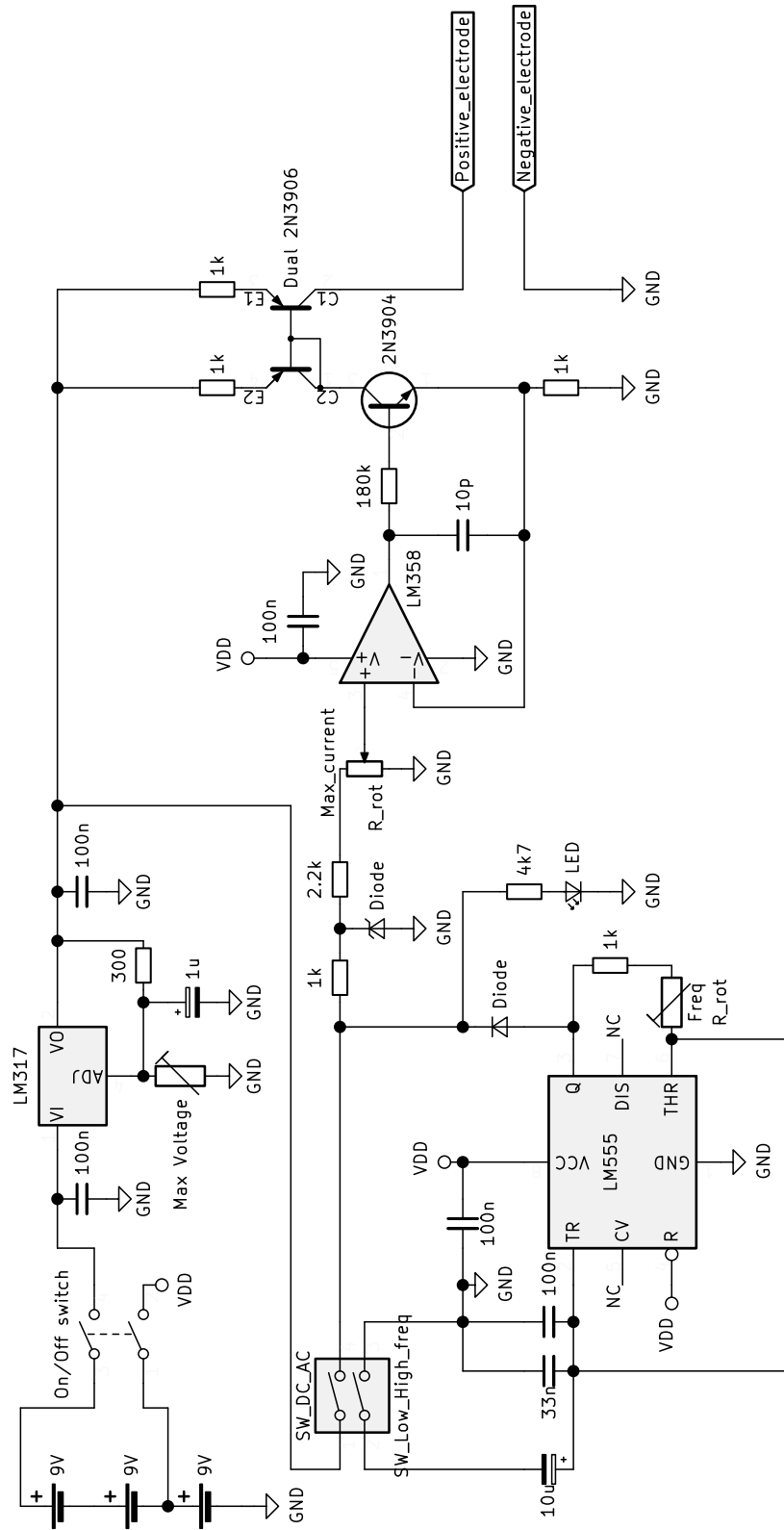
# B

## Read-out software code

```cpp
#include "mbed.h"
#include "Adafruit_ADS1015.h"
#define SERIAL_BAUD_RATE     115200

I2C i2c(PB_9, PB_8);                    // I2C pins
Adafruit_ADS1115 adc(&i2c, 0x48);       // Library optimised for more efficient sampling
Serial pc(SERIAL_TX, SERIAL_RX);        // debug tx, rx
Ticker sample;                          // Interrupt
Timer timer;                            // Timer for samples
int32_t sensor[8] = {0,0,0,0,0,0,0,0};  // Sweat sensors
int16_t single_temp = 0;                // Temperature sensor
bool channel=0;                         // Read-out channel (0 or 1)
bool read_e=0;                          // If read_e=1, start of collecting data
unsigned int sensor_count=0;            // Sensor sampled
unsigned int next_sensor=0;             // Sensor next sample
unsigned int sample_count=0;            // Numbers of samples in a row from the same sensor

DigitalOut a1(LED1);                    // Indication light
BusOut C_a(D3, D4, D5);                 // Databus to select channel Multiplexer 1
BusOut C_b(D7, D9, D11);                // Databus to select channel Multiplexer 2

void get_data()
{
    read_e = 0;
    if(sample_count<19) {
        sensor[sensor_count] = sensor[sensor_count]+adc.readADC_Differential(channel); // Load sampled data,
                                                                                        //   ask for next sample

        sample_count++;/
        return;
    }
    sample_count=0; //After 20 samples, a new sensor has to be selected
    channel=0;
    next_sensor = (sensor_count+4)%8;
    if(next_sensor<4) { Switch from multiplexer and sensor
        next_sensor++;
        channel=1;
        if(next_sensor>3) {
            next_sensor=0;
        }
    }

    sensor[sensor_count] = sensor[sensor_count]+adc.readADC_Differential(channel); // Load sampled data, ask for
                                                                                   // next sample at other channel
    if(next_sensor>3) {
        C_a = (sensor_count+1)%4; //Select channel of multiplexer 1
    }
    if(next_sensor<4) {
        C_b = (sensor_count+1)%4; //Select channel of multiplexer 2
    }
    int mseconds = timer.read_ms();
```

```
    pc.printf("%6d,%6u,%6d", sensor_count,mseconds,sensor[sensor_count]);      // Send through Uart the sensor number,
                                                                               // time of the sample and sensor values
                                                                               // of 20 samples
    pc.printf("\r");
    pc.printf("\n");
    sensor[sensor_count]=0;        // Reset sensor value
    sensor_count = next_sensor;  // This is the sample that is know being sampled due to the optimised library
}


void time_read()
{
    read_e = 1; // Start sampling
}


int main()
{
    i2c.frequency(800000);
    pc.baud(SERIAL_BAUD_RATE);
    adc.setGain(GAIN_ONE);
    sample.attach_us(time_read, 6250); // Specifying the repeat interval of the sampling
    timer.start();
    while(1) {
        if(read_e>0) {
            get_data(); // After interrupt, load data and start new sampling
            a1 = channel; // Indicate via led after successfully run through get_data()
        }
    }
}
```
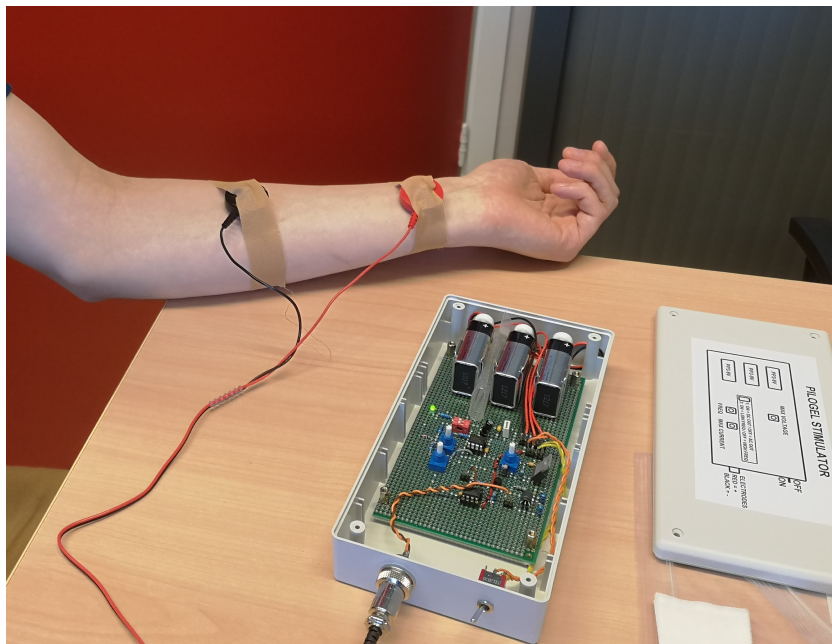
# C

## Pictures of experiments



Figure C.1: Experimental setup of sweat stimulation

Figure C.2: Experimental setup of sweat collection after sweat stimulation



Figure C.3: Visible skin irritation 50 minutes after stimulation

# D
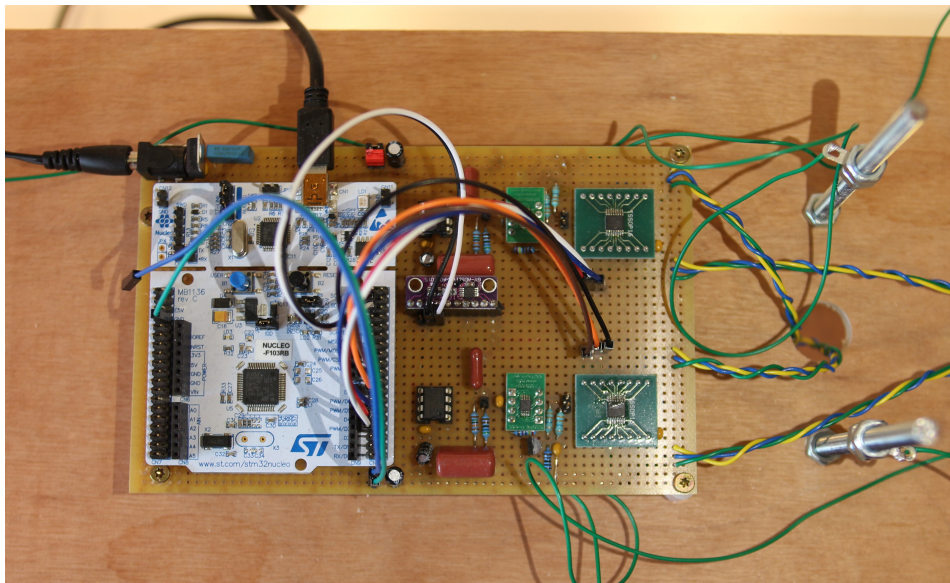
# Pictures read-out circuit and sweat stimulator



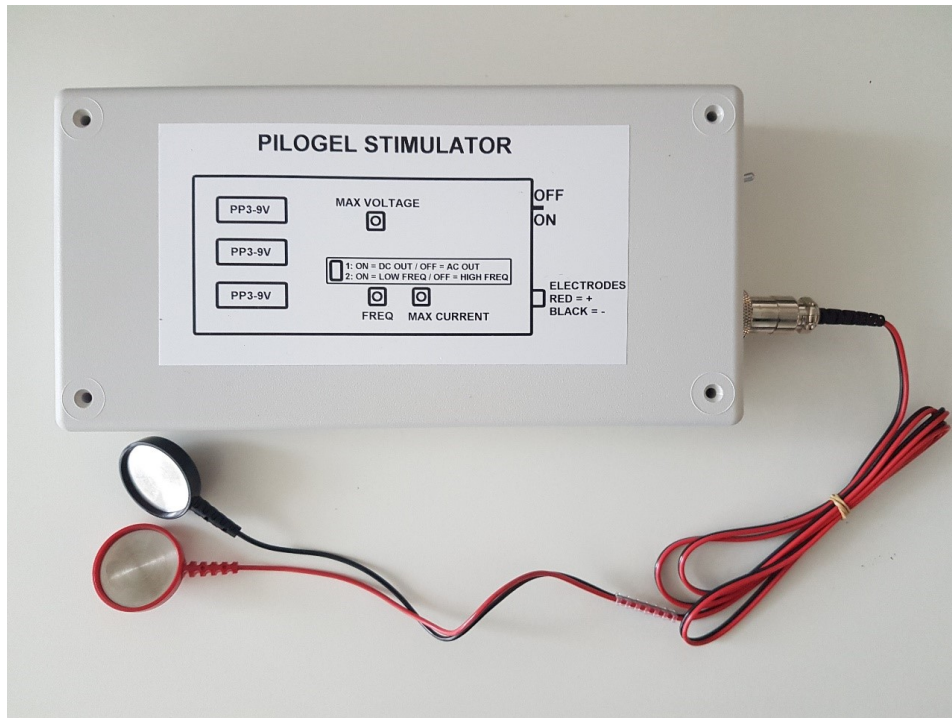Figure D.1: Picture of read-out circuit mounted on experimental setup
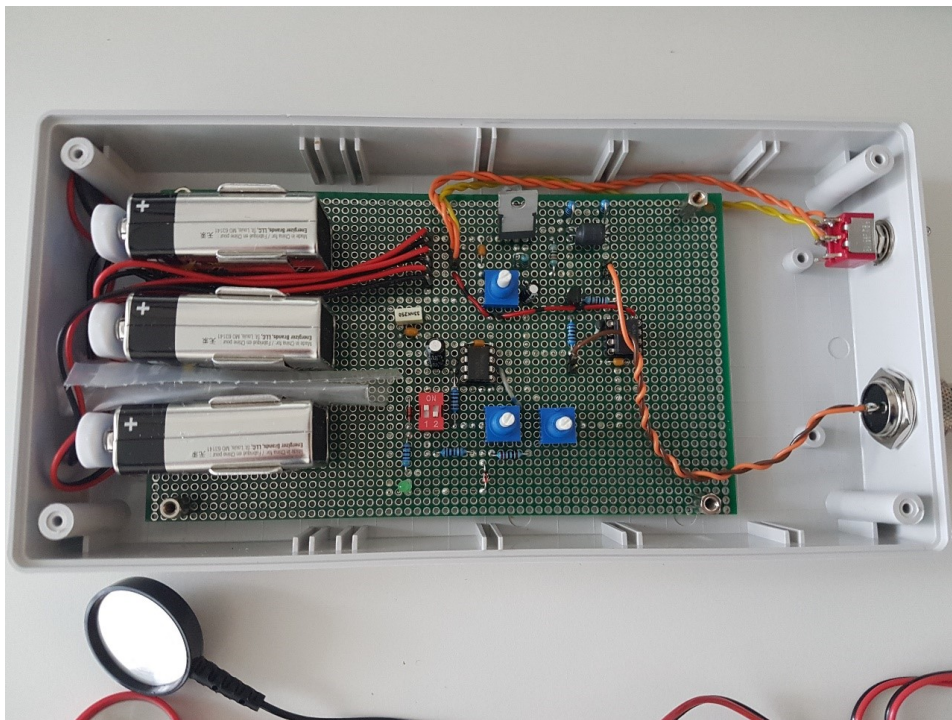
Figure D.2: Picture of stimulator with closed box



Figure D.3: Picture of stimulator with open box

# E

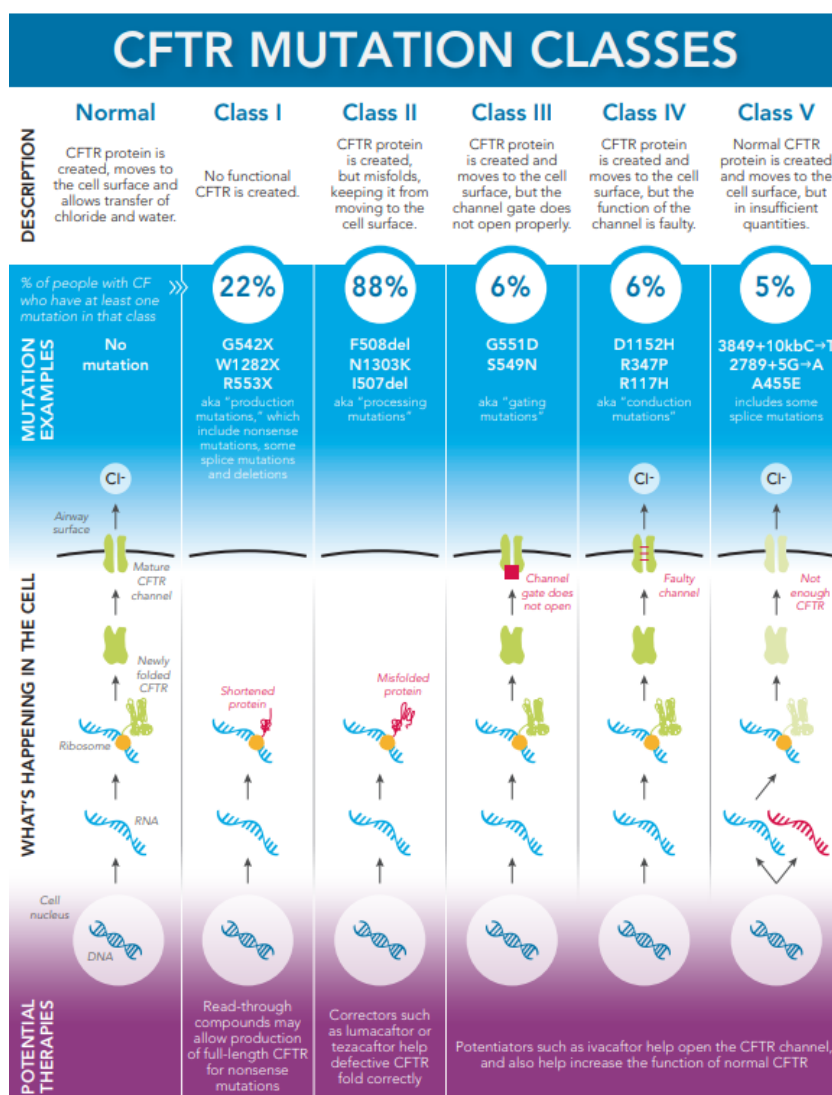## Infographic of mutation classes



Figure E.1: CFTR mutation classes [6]

# F

# Procedure for Sweat Induction and Collection

The following document with the procedure for sweat induction and collection originates from the the Model 3700 SYS instruction/service manual of Wescor, the manufacturer of sweat stimulator [85].

**2.1 Inducing Sweat**

**WARNING!**
Due to the possibility of an explosion, never attempt iontophoresis on a patient receiving oxygen-enriched respiratory therapy in an enclosed space. With medical approval, remove the patient from that environment during iontophoresis.

1 **ASSEMBLE EQUIPMENT AND SUPPLIES**
Make certain everything is on hand for the complete procedure. In addition to the complete Macroduct Sweat Collection System you will need a supply of pure water, alcohol, and cotton balls or gauze pads.
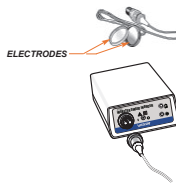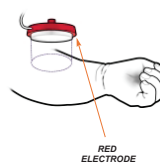
ELECTRODES

2 **INSPECT ELECTRODES AND CONNECT TO INDUCER**
Clean the electrodes if necessary (see Section 5.2). Check wires and insulation for cracks or fraying. **Replace electrodes if wires, insulation, or plastic housing are cracked or frayed.**

Press the electrode plug into the jack on the sweat inducer panel. You must engage the positive/negative alignment pins correctly to do so. Tighten the locking ring to secure the connection.

21

**2.1 Inducing Sweat**

3 **CLEAN THE SELECTED SKIN AREAS**
The positive (RED) electrode must be placed correctly for successful sweat collection. Locate it on an area of skin with a high density of sweat glands for optimum sweat yield. The preferred site is the lower portion of the flexor aspect of the forearm. This generally has a very high density of sweat glands, provided the limb is not so small as to prevent proper attachment of the Macroduct collector.

RED ELECTRODE

NOTE:
*Do not place the electrode so close to the wrist that tendons or bone are palpable just beneath the skin. Reasonably thick musculature is necessary for a proper interface with the Macroduct collector.*

If the limb is tiny, place the red electrode on the upper portion of the flexor aspect of the forearm (nearer the elbow) or even the upper arm. If the entire arm is too small to attach the collector (such as a premature infant), use the inner thigh. In this case, constrain the infant from flexing the knee during collection to avoid a loss of interface between the skin and the collector.

TINY INFANT PLACEMENT

RED ELECTRODE

Attach the negative (BLACK) electrode at any other convenient position on the arm, or to the leg **(on the same side of the body).**

22

107

## 2.1 Inducing Sweat

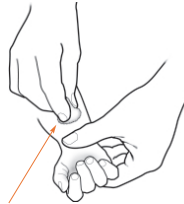The selected site must be free of breaks, fissures, or observable abnormality in the skin. There should be no sign of inflammation. Apart from exacerbating the complaint, there is the possibility of contamination of the sweat by serous exudates. The area must be as wrinkle-free and hairless as possible.

Clean the skin at the selected sites to remove dirt, fatty material and loose dead cells, to minimize the electrical impedance of the skin. To do this:

a Swab the area vigorously with alcohol, then with plenty of purified water.

b Leave the skin wet where the Pilogel disc is to be attached (**OR**):

Place a drop of water on the skin or on the surface of the Pilogel disc just before attachment.

This will ensure uniform contact over the area and reduce the possibility of a burn.

NOTE:
*Be sure that you are familiar with the precautions found in Section 1.6.*

**1 SWAB WITH ALCOHOL**
**2 SWAB WITH PURIFIED WATER**

23

## 2.1 Inducing Sweat

**4** INSTALL PILOGEL DISCS ON BOTH ELEC-TRODES

Pilogel discs have a diameter slightly larger than the inside diameter of the electrode skirt to provide a tight fit. Be sure to press firmly all around the outer perimeter of the disc to achieve uniform, air-free contact with the electrode. This may shave small slivers of gel from the outside of the disc as it is seated against the electrode. This is normal.

Do not be concerned if the Pilogel disc has a tendency to bulge away from the stainless steel electrode at the center. Attachment to the limb will flatten it against the electrode.

**WARNING!**
**Pilogel discs should be refrigerated at 2 to 8 °C. DO NOT FREEZE. Never use discs that have been frozen or that are cracked.**

**WARNING!**
**Never attach an electrode to the skin without Pilogel. Direct skin-to-metal contact will burn the patient. Refer to Section 1.6 for additional information.**

24

## 2.1 Inducing Sweat

**5** ATTACH THE ELECTRODES TO LIMB

Place each strap so that the stud of the electrode protrudes through the rivet of the strap, with the "hook" portion of the short tab facing upward, away from the skin. Secure the electrode firmly so that the gel surface is pressed flat against the skin. There should be moderate pressure to minimize discomfort, but do not tighten enough to crush the gel disc.

**ELECTRODE STUD**
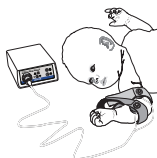
NOTE:
*Individuals vary in their sensitivity to iontophoretic current. Most subjects feel nothing more than a slight prickling sensation during iontophoresis. If a child complains or if an infant shows signs of distress, tighten the strap to increase pressure against the skin.*

25

## 2.1 Inducing Sweat

**6** ACTIVATE IONTOPHORESIS
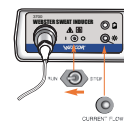
Push the control switch to the RUN (**I**) position and hold momentarily until you hear a short "beep." A steady tone indicates excessive external circuit resistance, a break in the line, or weak batteries. If this occurs, move the control switch to STOP (**0**) and correct the fault condition before proceeding (Section 4).

If everything is normal, the CURRENT FLOW indicator reaches full brightness in approximately 20 seconds, and diminishes in brightness during the last 5 seconds of iontophoresis as the current is reduced to zero.

If the circuit is broken even briefly during iontophoresis, current flow ceases and the alarm sounds. If this occurs, switch the inducer to STOP (**0**). Check leads and electrodes for fissures, breaks, etc. See Section 4 for complete information.

26

## 2.2 Collecting Sweat

**1** PREPARE MACRODUCT SWEAT COLLECTOR DURING IONTOPHORESIS

Open one end of the plastic wrapper and slide the Macroduct sweat collector slightly out of the package and thread a Macroduct strap of suitable size through one slot so that the "hook" side of the strap faces away from the Macroduct collection surface. DO NOT TOUCH THE COLLECTION SURFACE.

*GRASP MACRODUCT WITH PLASTIC WRAPPER*

**2** REMOVE ELECTRODES AT COMPLETION OF IONTOPHORESIS

Iontophoresis proceeds automatically for approximately 51/2 minutes after RUN is activated. At completion, an audible tone sounds briefly and the instrument turns itself off.

Remove the negative (black) electrode first and then clean the exposed area of skin. Before removing the positive (red) electrode, mark around the stimulated area with an alcohol-based felt marker to ensure proper placement of the Macroduct sweat collector.

Remove the positive (red) electrode.
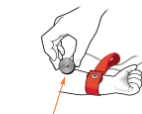
*REMOVE THE BLACK ELECTRODE FIRST*

## 2.2 Collecting Sweat

**3** CLEAN THE SKIN UNDER THE POSITIVE (RED) ELECTRODE

Clean the stimulated skin and the surrounding area thoroughly with purified water to remove salt, then blot dry. There should be a distinct redness under the red electrode. Proceed to Step 4 **immediately**.

**4** ATTACH MACRODUCT SWEAT COLLECTOR FIRMLY TO LIMB

Apply the concave surface of the Macroduct collector precisely over the area of skin contacted by the Pilogel disc. (The reddened area of skin will generally be larger than the sweat-stimulated area.)

Thread the free end of the strap around the limb and through the opening. Then tighten the strap until the collector is very firmly attached, with strap pressure pulling as evenly as possible from each end of the collector.

Check for collector displacement during attachment, and adjust if necessary.

## 2.2 Collecting Sweat

If a child attempts to disturb the collector, overwrap the device with an elastic bandage.

For neonate sweat collections, where the limbs are extremely small, overwrap the collector firmly with a 2 or 3 inch-wide elastic bandage. This ensures a continuous and firm contact between the collector and the skin, and greatly improves the probability of a successful collection.
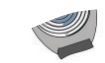
Macroduct allows you to visually assess sweat production at any time by reference to the spiral tube calibration diagram. A 30 minute collection time usually yields 50-60 microliters of sweat, although variance among individuals is extremely wide. You can vary collection time to maximize the sweat yield, but with most individuals, very little additional sweat can be collected after 45 to 60 minutes.

*BLUE COLORED SWEAT*

*SPIRAL TUBE CALIBRATION DIAGRAM*

## 2.2 Collecting Sweat

NOTE:
*Inadequately tightened collector straps can be detected simply by pressing the collector very firmly against the skin. If the advancing meniscus of sweat in the spiral tube moves by more than 2-3 millimeters, attach the strap more firmly.*

**5** REMOVE AND STORE SWEAT SAMPLE

NOTE:
*The following procedure must be done while the Macroduct collector is still firmly strapped to the limb. Removing the complete device before detaching the tubing may create a vacuum that will draw the collected sweat from the tubing and seriously reduce sample volume.*

**FOLLOW THESE INSTRUCTIONS CLOSELY:**

**a** Remove the protective transparent cover by inserting a pointed tool into one of the cut-out sections and prying upward. (The nippers supplied with the Macroduct system will work well.)

**b** Insert the blunt needle approximately 5 mm into the open end of the Macroduct microbore tubing using a twisting motion (see illustration). Alternatively, lift the open outer end of the micro-bore tubing and pull one or two inches of the tube free from the adhesive base before attaching the tube to the blunt needle of the syringe. **Position the plunger at mid point before inserting it into the tubing.**

Do not squeeze the dispenser or syringe body or move the syringe plunger at any time during attachment or during the following procedure.

*USE TWISTING MOTION WHILE INSERTING BLUNT NEEDLE INTO THE END OF THE MICRO-BORE TUBING.*

**2.2 Collecting Sweat**

c Grasp the tubing where it is attached to the needle and pull the tubing away from the collector body until the tubing is completely uncoiled and extending outward from the point of attachment. Use the provided nippers to sever the tube as close as possible to the collector surface.

*HOLD THE TUBING WHERE IT ATTACHES TO THE SYRINGE NEEDLE*



d Immediately after severing the tubing, carefully draw the sweat into the tube one or two inches. This is to prevent any loss of sweat from the cut end due to expansion of air in the syringe body. It also allows you to cut-off the tightly coiled end of the microbore tubing for easier handling.

**OR**

If using the Sweat Check™ Analyzer, attach the end of the tube to the Sweat Chek intake for analysis. Refer to instructions in the Sweat-Chek instruction manual.

e Expel the sweat specimen into the cup and immediately install the cover to protect the specimen.

31

**2.2 Collecting Sweat**

6 REMOVE AND DISCARD COLLECTOR BODY

Detach the collector body from the patient's limb. Retain the strap, and discard the collector body.



7 CLEAN THE ELECTRODES

Remove and discard the Pilogel discs. Clean the electrodes with purified water and wipe dry. See Section 4.2.

32

# G

# Safety measures sweat stimulator

Table G.1: Medical hazards and mitigations of sweat stimulator

| Hazard type | Present | Hazard source | Mitigation measures |
|---|---|---|---|
| Medical | Unlikely | Allergic reaction | |
| Medical | Likely | Skin irritation can occur due to the stimulation with a constant continuous/pulsed current. It is likely that minor skin irritation occurs. Skin irritation does also occur during pilocarpine ionthoporesis in the hospital. The skin irritation will typically have an duration of 4 hours. | The device works on a battery to limited the energy supply, a current limiter (max 1.2mA, max 0.17mA/cm2) and voltage limiter (max 25V) are implemented to ensure safe stimulation levels. Furthermore, the same electrodes, pilocarpine gel, stimulation current and procedures as used in the hospital for pilocarpine iontophoresis will be used during the experiment. A person with a BHV certificate will be close by during the experiments to provide first aid in case of an emergency. |
| Medical | Unlikely | Burning wounds due to the exceeding the maximum current density during stimulation (more than 0.5mA/cm2). | The device works on a battery to limited the energy supply, a current limiter (max 1.2mA, max 0.17mA/cm2) and voltage limiter (max 25V) are implemented to ensure safe stimulation levels. Furthermore, the same electrodes, pilocarpine gel, stimulation current and procedures as used in the hospital for pilocarpine iontophoresis will be used during the experiment. A person with BHV will be close by during the experiments to provide first aid in case of an emergency. A burnshield will be available to cool the wound in case water is not available (for example, during transport). In case of a burning wound, the BHV and/or medic will be asked for assistance. |

Table G.2: Hazards and mitigations of sweat stimulator

| Hazard type | Present | Hazard source | Mitigation measures |
|---|---|---|---|
| Mechanical (sharp edges, moving equipment, etc.) | Unlikely | A sharp edge causing a skin wound. | The box has curved shapes in will not come in contact with the participant. The electrodes are medical approved and does not have sharp edges. |
| Electrical | Unlikely | Component failure which is undetected causing failure of the system. | The device can easily be checked with a handheld multimeter to test functionality. |
| Structural failure | Unlikely | Failure in production causing problems during stimulation or measurements. | The device is tested and analysed by an experienced electrical engineer before usage. The device will be controlled by someone with knowledge in electrical engineering. The device works on a battery to limited the energy supply, a current limiter (max 1.2mA, max 0.17mA/cm2) and voltage limiter (max 25V) are implemented to ensure safe stimulation levels. Furthermore, the same electrodes, pilocarpine gel, stimulation current and procedures as used in the hospital for pilocarpine iontophoresis will be used during the experiment. |
| Touch Temperature | Unlikely | Short circuit causing excessive heat production. | The device works on a battery to limited the energy supply. The box will not come in contact with the participant. The electrodes are medical graded and does not have sharp edges. The max fault current is 20mA. |
| Electromagnetic radiation | Unlikely | Emission from other devices, influence on reliability of the system | |
| Ionizing radiation | N/A | | |
| (Near-)optical radiation (lasers, IR-, UV-, bright visible light sources) | N/A | | |
| Noise exposure | Unlikely | Noise exposure causing influences on the pulse current stimulation | The device is voltage and current limited to avoid safety risks due to pulse shape malformation. |
| Materials (flammability, offgassing, etc.) | Unlikely | Short circuit causing excessive heat production causing fire | The device works on a battery to limited the energy supply. |
| Chemical processes | N/A | | |
| Fall risk | Unlikely | Device falls causing components to come lose which results in defects of the device | Screws used to secure the electronics. The device will be controlled by someone with knowledge in the electrical field. |

# H
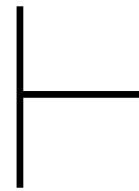
# Informed consent form and study information

**Consent Form for [*sweat stimulation and measuring experiments*]**

*Please tick the appropriate boxes*                                                  Yes   No

**Taking part in the study**

I have read and understood the study information dated [12/04/2019], or it has been read to me.     ○    ○
I have been able to ask questions about the study and my questions have been answered to my
satisfaction.

I consent voluntarily to be a participant in this study and understand that I can refuse to answer     ○    ○
questions and I can withdraw from the study at any time, without having to give a reason.

I understand that taking part in the study involves a stimulation for the sweat production with        ○    ○
the usage of pilocarpine gel, sweat will be collected and analysed on volume, chloride
concentration and sodium concentration. The information is recorded by making notes and
taking sweat samples.

**Risks associated with participating in the study**

I understand that taking part in the study involves the following risks: skin irritation which can     ○    ○
lead to physical discomfort for multiple hours.

**Use of the information in the study**

I understand that information I provide will be used for reports and publications                      ○    ○

I understand that personal information collected about me that can identify me, such as [e.g. my       ○    ○
name or where I live], will be anonymized.

**Future use and reuse of the information by others**

I give permission for the anonymized personal data, sweat volume, sweat chloride concentration         ○    ○
and sweat sodium concentration that I provide to be archived in TU Delft repository so it can be
used for future research and learning.

**Signatures**

_____          _____  _____
Name of participant             Signature             Date

I have accurately read out the information sheet to the potential participant and, to the best of
my ability, ensured that the participant understands to what they are freely consenting.

_____         _____       _____
Researcher name [printed]        Signature              Date

*Study contact details for further information*:
Thomas Bakker
T: --------
E: --------

113

**12-04-2019**

## Participant information sheet
### [*sweat stimulation and measuring experiments*]

**Experiment background information and socially importance**
Cystic Fibrosis (CF) is an autosomal recessive genetic disorder affecting mostly the respiratory, digestive and perspiration system. Patients with CF have dysfunctional chloride channels in their cells, due to mutations in both copies of the gene for the CFTR protein. The CFTR proteins are necessary for the production of mucus, a malfunction of the CFTR protein will result in tough mucus. This causes different, severe pathologies, of which inflammation and chronic airway obstruction are the most important. Therefore, patients suffering from CF have a limited life expectancy. The CFTR protein is also necessary for the reabsorption of salts from sweat to prevent a high loss of salt. As a consequence, CF patients have raised chloride and sodium concentrations in their sweat due to the malfunctioning CFTR protein.

New personalized medicines, able to repair the CFTR-protein, hold much promise for patients. However, monitoring the effectiveness of these medicines using traditional monitoring systems is difficult, due to lack of data points and the need to conduct measurements in a hospital setting, resulting in unreliable measurements. Research is in progress on wearable real-time sweat monitoring systems using screen-printed potentiometric sensors which are flexible, small and easy to use. Currently, these sensors are mainly used for the diagnosis of CF or monitoring of athletes. This is a different region of interest than monitoring CF medicines effectiveness.

For using these sensors to monitor the effectiveness of medicines, two technical hurdles have to be taken. Firstly, the amount of sweat produced under normal circumstances is often too low for conducting reliable measurements. For monitoring effectiveness of medicines, artificially generated sweat is needed, which is often not taken into account in ongoing research, compromising the reliability and usefulness of these studies. Secondly, the sensors have often only be tested for a few hours in a row, which is too short for monitoring medical effectiveness.

Real-time monitoring of medicines effectiveness can be beneficial for:
1. Improving patient treatment
2. Validating the use of intestinal stem cell cultures for selecting and composing personalized medicines treatment
3. Obtaining reimbursement for Cystic Fibrosis medicines from health insurers.

The goal of the research is to provide a proof of concept for such a real-time monitoring device. The end goal of the overarching project is to develop a real-time monitoring device which firstly can measure accurately and reliably, secondly is user friendly, and finally can be approved for clinical usage (CE-marked).

The nature of the experiment is to applying artificial sweat stimulation to obtain sweat for the analysis of chloride and sodium concentrations in sweat.

**Exclusion from experiments**
Participants with known health issues related to skin and or/sweat will be excluded from the experiments. Participants under the age of 18 will also be excluded from the experiments.

**Duration of experiment**
The duration can differ per experiment, the minimal time for the experiments will be 2 hours the maximum time will be 9 hours. To check consistency over time, it can be asked to take part in multiple sessions. Participants can withdraw their cooperation at any time. The participants can withdraw by mentioning the researcher who conduct the experiment. In case of a withdraw due to physical discomfort, the participant will be assisted in consulting the BHV or a medic.

**Data collection**
The data collected in this research will contain: age, gender and the data analyses of the sweat samples (volume, chloride concentration, sodium concentration). The data will be stored and possibly be published. All personal data will be anonymized. The participant have the right to request access to the data and erasure of personal data.

**Experiment setup**
The experiment will consists of 2 phases. Firstly, stimulation with pilocarpine ionthoporesis. Secondly, sweat collection and analyses. The stimulation phase of the experiment will take around 5 minutes. After the stimulation, participant can do office work or relaxing, in between the analysis will be conducted. It is not possible to do sport exercises or staying in high environmental circumstances during the experiments, since that will influence the results.

**Reasonably foreseeable risks for participants**
1. Skin irritation, it is likely that minor skin irritation occurs. Skin irritation does also occur during pilocarpine ionthoporesis in the hospital. The skin irritation will typically have an duration of 4 hours.
2. Burning wounds, it is unlikely that burning wounds appear due to the mitigation steps as will be explained in section PA.10. A burnshield will be available to cool the wound in case water is not available (for example, during transport). In case of a burning wound, the BHV and/or medic will be asked for assistance.
3. Electric shock, it is unlikely that an electric shock will occur since the device is placed in a shielded box. The electrodes have an current limit and voltage limit. Furthermore, the device is battery powered (3x 9V battery), so a risk of a shock from the mains is not applicable.
4. Allergic reaction, it is unlikely that an allergic reaction will take place. Participants with known health issues related to the skin are excluded. In case of an allergic reaction, the BHV and/or medic will be contacted.

If there are any questions related to the experiment, Thomas Bakker can be contacted via the contact details mentioned below.

*Study contact details for further information*:
Thomas Bakker
T: +31 (0)6 24246790
E: t.d.bakker@student.tudelft.nl